THE FOLIAR MICROMORPHOLOGY AND MEDICINAL PHYTOCHEMICAL PROPERTIES OF *Heteropyxis natalensis* (MYRTACEAE)

SAIYURI DAYINEE CHETTY

210524100

A research dissertation submitted in fulfilment of the academic requirements for the degree of

Master of Science in Biological Sciences

School of Life Sciences

College of Agriculture, Engineering and Science

University of KwaZulu-Natal

Westville

South Africa

November 2018

As the candidate's supervisor(s) I have approved this dissertation for submission.

Signed: _____

Prof. Y. Naidoo

Supervisor

30 November 2018

Signed: _____ 30/11/2018

Prof. Y.H. Dewir

Co-supervisor

30 November 2018

PREFACE

The research contained in this dissertation was completed by the candidate while based in the Discipline of Biological Sciences, School of Life Sciences of the College of Agriculture, Engineering and Science, University of KwaZulu-Natal, Westville, South Africa. The research was financially supported by the National Research Foundation.

The contents of this work have not been submitted in any form to another university and, except where the work of others is acknowledged in the text, the results reported are due to investigations by the candidate.

_____

Signed: Prof. Y. Naidoo

Supervisor

Date: 30 November 2018

_____

Prof. Y.H. Dewir

Co-supervisor

Date: 30 November 2018

DECLARATION: PLAGIARISM

I, **Saiyuri Dayinee Chetty**, declare that:

(i) the research reported in this dissertation, except where otherwise indicated or acknowledged, is my original work;

(ii) this dissertation has not been submitted in full or in part for any degree or examination to any other university;

(iii) this dissertation does not contain other persons' data, pictures, graphs or other information, unless specifically acknowledged as being sourced from other persons;

(iv) this dissertation does not contain another persons' writing, unless specifically acknowledged as being sourced from other researchers. Where other written sources have been quoted, then:

  a) their words have been re-written, but the general information attributed to them has been referenced;

  b) where their exact words have been used, their writing has been placed inside quotation marks, and referenced;

(v) this dissertation does not contain text, graphics or tables copied and pasted from the Internet, unless specifically acknowledged, and the source being detailed in the dissertation and in the References sections.

_____

Signed: Saiyuri Dayinee Chetty

Date: 30 November 2018

ABSTRACT

The use of medicinal plants as a form of therapeutic healing is an ancient tradition in various regions of the world. As a result, there is a dire need to screen medicinal plants for their unrevealed pharmacological potential. The foliar micromorphology of plants enables researchers to investigate the synthesis and location of medicinal phytocompounds. *Heteropyxis natalensis* is a South African medicinal plant and is traditionally used in Venda and Zulu communities to treat several illnesses. This study aimed to characterise the foliar structures of *H. natalensis* leaves, locate the site of secondary metabolites, determine the phytochemical composition of the leaves, and investigate the antibacterial efficacies and silver nanoparticles (AgNPs) of the methanolic extract. Emergent, young and mature leaves were examined using various microscopy techniques which confirmed the presence of non-glandular trichomes as the main external appendages of the leaves. Micrographs also revealed internal secretory cavities and crystal idioblasts. Secretory cavities were observed accumulating amorphous secretions and histochemical tests detected alkaloids, phenolics, essential oils and lipids. Qualitative phytochemical analyses were conducted on hexane, chloroform and methanol leaf extracts, and detected phenolics, alkaloids, saponins, sterols and terpenes. Crude methanolic extract was further examined using gas chromatography-mass spectrometry and identified several important bioactive compounds of pharmacological value. A "green approach" was used to synthesise AgNPs using the methanolic leaf extract. Characterisation studies identified spherical particles below 100 nm in size, as well as the functional groups responsible for the capping of silver ions (Ag+). The crude methanolic extract and AgNPs were screened for their antibacterial efficacy and showed inhibition of five pathogenic bacterial strains. The results obtained in this study revealed that the phytochemical compounds present in *H. natalensis* leaves justify the use of this species in traditional medicine.

DEDICATION

To my parents Ravi and Malini, and my partner Ché, thank you for being at my beck and call, tolerating my ever-changing mood and spoiling me with copious amounts of love and nourishment. This dissertation is dedicated to you.

ACKNOWLEDGEMENTS

First and foremost, I would like to express my gratitude and appreciation to the National Research Foundation for the financial support throughout this dissertation.

To my supervisor, Prof. Yougasphree Naidoo: thank you for granting me the opportunity to further my studies in academia. Your open-door-policy, unwavering support and indispensable wisdom never went unnoticed, for which I am truly thankful.

To my co-supervisor, Prof. Yaser Hassan Dewir: thank you for accepting me as your student. Your time, constructive suggestions and guidance during the compilation of my dissertation has been extremely appreciated throughout this year.

Microscopy assistance provided by the Microscopy and Microanalysis Unit, in particular Mr. Subashen Naidu, was greatly appreciated. In addition, I would also like to express my sincere thanks to Prof. Johnson Lin and his student Mr. Abdullahi Jimoh for their guidance and resources for the antibacterial component of my research.

I would like to extend my thanks to Mr. Vishal Bharuth for always encouraging me to do great things and inspiring me throughout the duration of this degree.

My dear friends in Office 05-074, we've had some trying times, but I am immensely appreciative for the assistance, inspiration and reassurance throughout this journey. Thank you for being the sunshine when skies were grey.

A special mention needs to be made to my grandfather, Mr. Subramoney Perumal Moodley, for taking his time to proof-read and help me edit my dissertation.

Lastly, a heartfelt thank you to the friends and family that support me irrespective of understanding what I study.

TABLE OF CONTENTS

LIST OF FIGURES

LIST OF TABLES

LIST OF ABBREVIATIONS

Ag^+	Silver ions
$AgNO_3$	Silver nitrate
AgNP(s)	Silver nanoparticle(s)
Bc	Basal cell
CC	Cap cells
CW	Cell wall
D	Domatium
DC	Druse crystal
$_dH_2O$	Distilled water
$_{di}H_2O$	Deionised water
Ec	Secretory epithelial cells
EDX	Energy dispersive X-ray spectroscopy
EO	Essential oils
ER	Endoplasmic reticulum
FTIR	Fourier transform infrared spectroscopy
GB	Golgi body
GC-MS	Gas chromatography-mass spectrometry
H_2SO_4	Sulphuric acid
HRTEM	High resolution transmission electron microscopy
L	Lumen
Li	Lipid bodies
M	Mitochondrion
MHA	Mueller Hinton agar
Mi	Mite
MRSA	Methicillin resistant *Staphylococcus aureus*
N	Nucleus
NG	Non-glandular trichomes
OsO_4	Osmium tetroxide
P	Plastid
Ph	Phenolics
RA	Resin acids
SC	Secretory cavity
SEM	Scanning electron microscopy

Sh	Sheath cells
SM	Secretory material
SPR	Surface plasmon resonance
TEM	Transmission electron microscopy
UV-vis	Ultraviolet visible spectroscopy
V	Vacuoles
v	Vesicles

CHAPTER 1: INTRODUCTION

1.1. Traditional Medicine in South Africa

"There is a plant for every need on every continent" (Victor and David, 2015).

Traditional herbal medicine or ethnomedicine is defined as a multi-disciplinary complex involving the use of plants and indigenous knowledge to treat illness and disease (Gurib-Fakim, 2006; Qazi and Molvi, 2016). The use of plant material for therapeutic healing occurred approximately 60 000 years ago (Qazi and Molvi, 2016), thus being recognised as one of the oldest forms of health care (Gurib-Fakim, 2006). Although ethnomedicine has played a fundamental role for millennia, it is still an important source of medical treatment in poverty-stricken regions of the world (Meena et al., 2009). The socio-economic status of developing countries prevents many people from accessing modern medical care due to the exorbitant cost of medicine and treatment (Koduru et al., 2007; Qazi and Molvi, 2016). As a result, ethnomedicine is recognised as an inexpensive, reliable and accessible source of health care among rural populations (Meena et al., 2009; Gunjan et al., 2015).

The use of herbal medicine is an important component of the socio-cultural lifestyle of developing African countries (Elujoba et al., 2005; Koduru et al., 2007). The majority of South Africa's population prefer to be treated with traditional herbal medicine or "Muthi" despite the availability of Western medical practices (Makunga et al., 2008; Xego et al., 2016) since it is affordable, easily accessible and effective (Elujoba et al., 2005). Many of these remedies have been tried and tested for hundreds of years and passed on through generations via verbal communication (Gurib-Fakim, 2006; Koduru et al., 2007).

The South African medicinal plant trade is a successful industry supported by 27 million consumers (Petersen et al., 2017). South Africa hosts approximately 30 000 species of higher plants of which 3000 species are traditionally used in herbal remedies (Van Wyk and Prinsloo, 2018) and 350 are regularly traded in the country (Xego et al., 2016). However, medicinal flora faces many threats such as an increase in human population, overharvesting and land degradation (Street and Prinsloo, 2012). This poses a threat on the country's indigenous biodiversity with the increased demand for medicinal plant material (Xego et al., 2016). As a result, the interest in medicinal plants has increased and many species have been pharmacologically screened for their undiscovered therapeutic potential (Street and Prinsloo, 2012; Shakya, 2016). In addition,

scientists have been interested in identifying the structures responsible for pharmacological activity in medicinal flora (Shakya, 2016). Therefore, understanding the pharmacological, phytochemical and micromorphological characteristics of medicinal flora may also implement conservation strategies for threatened plant species throughout South Africa (Petersen et al., 2017).

1.2. Botanical Description of *Heteropyxis natalensis*

Heteropyxis natalensis Harv., commonly known as the "Lavender tree", is a deciduous tree that is indigenous to South Africa (Adesanwo et al., 2009; Henley-Smith et al., 2018). Its distribution ranges from KwaZulu-Natal to Limpopo (Fig. 1.1) (Van Vuuren et al., 2007) whilst thriving in evergreen forests and bushveld regions.

Figure 1.1: *Heteropyxis natalensis* growing alongside a car park at the University of KwaZulu-Natal (Westville Campus). Inset: The distribution of *H. natalensis* in South Africa (Image adapted from University of Connecticut webpage, 2018).

The tree belongs to the Myrtaceae family (Van Wyk, 2011) as it retains many phenotypic traits resembling other species within the family such as simple leaves with secretory cavities/oil glands (Schmid, 1980; Wilson et al., 2001), flowers with twice as many stamens than petals and inferior to semi-inferior ovaries (Conti et al., 1997). *Heteropyxis natalensis* is a tree of approximately 10 metres in height (Braithwaite et al., 2008). The trunk is thin and erect, consisting of many branches with dense foliage (Muchuweti et al., 2006). The leaves are arranged in a spiral, forming a "drooping crown". Mature trees consist of shiny green leaves with a smooth upper surface (Fig. 1.1) whereas the underside is pale green in colour, featuring an abundance of visible pellucid glands. However, fragile red-tinged leaves are an indication of younger trees (Van Vuuren and Viljoen, 2008). Small yellow flowers are in bloom during the summer which intensifies the lavender scent emitted when the leaves are crushed (Chagonda et al., 2000). The scent is sometimes described as camphoraceous (Weyerstahl et al., 1992).

Venda and Zulu communities use various parts of the tree to treat variety of ailments (Van Vuuren and Viljoen, 2008; Adesanwo et al., 2009) such as respiratory disorders, nosebleeds and gingivitis (Muchuweti et al., 2006; Van Vuuren et al., 2007; Henley-Smith et al., 2018). *Heteropyxis natalensis* has numerous socio-economic uses. The leaves are crushed and used in tobacco (Adesanwo et al., 2009) while the bark is used as a form of charcoal and an aphrodisiac (Abdillahi and Van Staden, 2012).

The essential oils of *H. natalensis* are known to contain extremely aromatic compounds (Braithwaite et al., 2008). Previous studies have shown the presence of eucalyptol and limonene as the main constituents of the oils which are responsible for the medicinal properties of the tree (Gundidza et al., 1993; Van Vuuren et al., 2007). These monoterpenes are commonly used in fragrances, foods and the pharmaceutical industry (Gundidza et al., 1993). The presence of these compounds provides a plausible explanation regarding the traditional medicinal use of this species in South Africa (Van Vuuren et al., 2007).

1.3. Rationale of Research Study

The use of medicinal plants as a form of therapeutic healing is a worldwide phenomenon. Ethnomedicine has incorporated centuries worth of indigenous knowledge to treat variety of ailments (Light et al., 2005). Medicinal plants have played a fundamental role with regards to the discovery of novel compounds and drug development due to the presence of secondary metabolites (Ngo et al., 2013; Hosseinzadeh et al., 2015). Previously, methods used to determine

the presence of these phytochemicals were tedious and ineffective. However, in recent times, there has been incredible advances in technology which increased the pace of screening, discovering and analysing novel compounds (Ngo et al., 2013).

Over the years, extensive research has been conducted on the chemical composition and antibacterial activity of the essential oils of *H. natalensis* (Gundidza et al., 1993; Chagonda et al., 2000; Van Vuuren et al., 2007). However, research regarding the micromorphology of foliar secretory structures responsible for the synthesis, accumulation and secretion of exudates has not been investigated. In addition, the antibacterial effect using crude leaf extract and silver nanoparticles (AgNPs) have not been explored. Therefore, this study aims to characterise the foliar structures of the leaves, locate the site of secondary metabolites, determine the phytochemical composition of the leaves, and investigate the antibacterial efficacies and AgNPs of the methanolic extract. Additionally, this study will further validate the traditional medicinal use of *H. natalensis* and determine whether this species can be used in herbal drug development.

1.4. Aims and Objectives

The aims and objectives for each research chapter are outlined as follows:

Chapter 3

Aim: To identify the foliar micromorphology, ultrastructure and histochemical composition of *H. natalensis* leaves.

Objective 3.1: Examine and characterise foliar trichomes using stereomicroscopy, scanning electron microscopy and light microscopy.

Objective 3.2: Identify secretory tissues across three leaf developmental stages (emergent, young and mature) using light microscopy and transmission electron microscopy.

Objective 3.3: Determine the location and nature of secondary metabolites using histochemical assays.

Chapter 4

Aim: To elucidate the secondary metabolites in crude leaf extracts and investigate the chemical profile and antibacterial efficacy of crude methanolic leaf extract of *H. natalensis*.

Objective 4.1: Elucidate the secondary metabolites of crude leaf extracts using preliminary qualitative phytochemical tests.

Objective 4.2: Identify the bioactive compounds using gas chromatography-mass spectrometry and assess the antibacterial activity of crude methanolic extract using various bacterial strains.

Chapter 5

Aim: To examine the synthesis, characterisation and antibacterial activity of AgNPs from crude methanolic leaf extract of *H. natalensis*.

Objective 5.1: Identify and characterise AgNPs using ultraviolet–visible spectroscopy, high resolution transmission electron microscopy, energy dispersive x-ray analysis and fourier-transform infrared spectroscopy.

Objective 5.2: Assess the antibacterial activity of AgNPs using various bacterial strains.

1.5. Outline of Dissertation

This dissertation consists of six chapters.

Chapter 1 presents an overview of traditional medicine in South Africa, provides a detailed botanical description of *H. natalensis*, states the rationale, aims and objectives of the study, provides a summary of the dissertation and a brief outline of the methodology used to conduct the various components of the study.

Chapter 2 consists of an in-depth literature review pertaining to the family, genus, micromorphological characteristics and taxonomic position of *Heteropyxis*. In addition, information on nanotechnology and AgNPs are also presented in this chapter.

Chapter 3 presents a manuscript on the foliar micromorphology of the leaves as well as the histochemical analyses used to identify various secondary metabolites.

Chapter 4 presents a manuscript on preliminary phytochemical analyses performed on crude leaf extracts as well as the chemical composition and antibacterial screening of crude methanolic leaf extract.

Chapter 5 presents a manuscript involving the green synthesis of AgNPs using crude methanolic extract, characterisation, and antibacterial screening of AgNPs.

Chapter 6 provides major findings, the challenges associated with the study and identifies future research possibilities.

1.6. Outline of Methodology

The methodology used in this study is outlined in Figure 1.2.

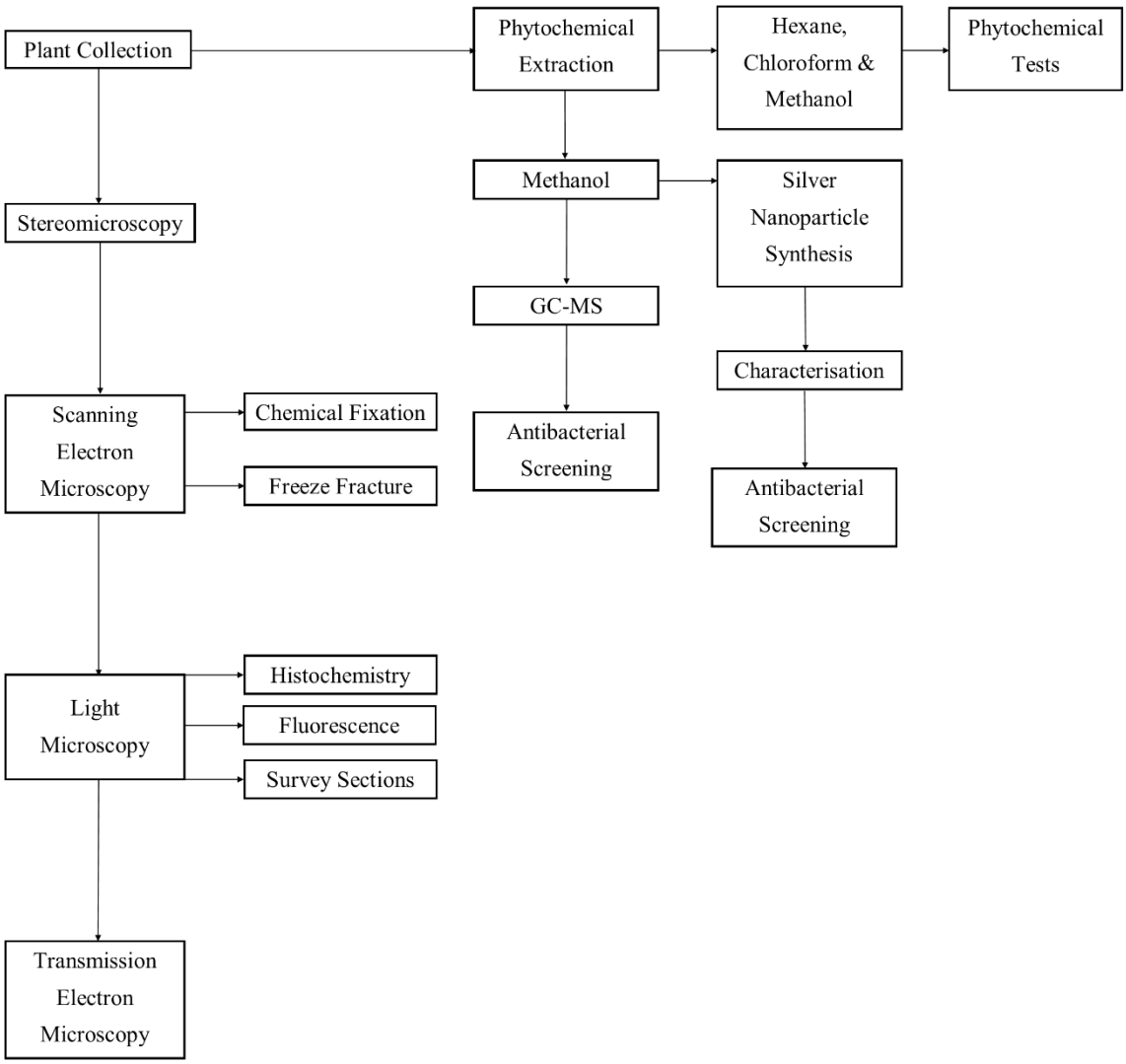

Figure 1.2: An outline of the methodology used in this study

CHAPTER 2: LITERATURE REVIEW

2.1. The Myrtaceae Family

The Myrtales is an extensively researched plant order (Conti et al., 1996). A combination of features separates Myrtales from various angiosperm groups. These features include the presence of vestured pits in the secondary xylem and bicollateral vascular bundles in the primary stem (Conti et al., 1996; Cardoso et al., 2009).

Myrtaceae A.L. Juss (Cardoso et al., 2009) is the ninth largest angiosperm family (Cascaes et al., 2015) in the world comprising of 131 genera and 5,638 species (Berger et al., 2016). It is one of the largest families in Myrtales amongst eight flowering families (Conti et al., 1997). The family's woody trees and shrubs (Donato and de Morretes, 2013) inhabit wet and humid environmental conditions thus being extremely diverse in tropical regions of the southern hemisphere (Fig. 2.1). Distinguishable characteristics of the family include the presence of oil glands within simple leaves, floral parts in multiples of four or five with many stamens, inferior to semi-inferior ovaries, vestured pits in xylem vessels, and internal phloem (Wilson et al., 2001; Grattapaglia et al., 2012).

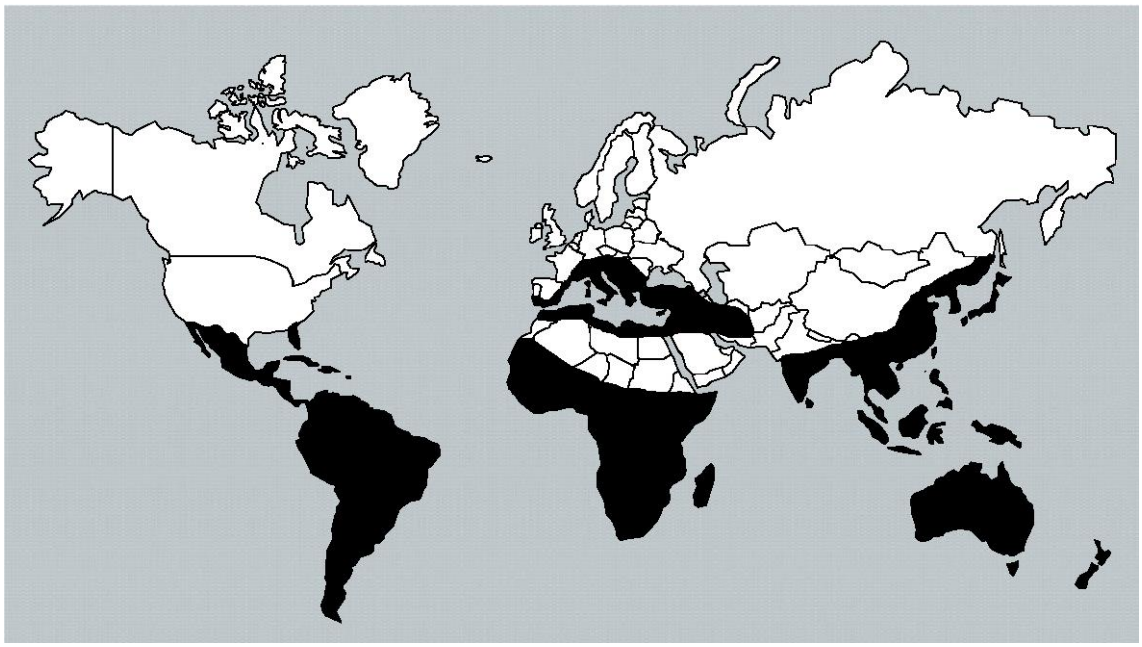

Figure 2.1: World distribution of the Myrtaceae family (Grattapaglia et al., 2012)

In recent decades, the family was divided into two subfamilies; Myrtoideae and Leptospermoideae (Wilson et al., 2001; Barbosa et al., 2013). Species with fleshy fruits and

opposite leaves were placed within Myrtoideae and species with capsular fruits and alternate leaves were placed within Leptospermoideae (Grattapaglia et al., 2012; Barbosa et al., 2013). However, the division was challenged and abandoned by Johnson and Briggs (1984) after a cladistic analysis was performed on morphological and anatomical characteristics (Wilson et al., 2001).

Myrtaceae genera including *Psidium* (guava), *Syzgium* (clove), *Eucalyptus* and *Myrtus* (myrtle) are of economic and ecological importance worldwide (Al-Edany and Al-Saadi, 2012; Cascaes et al., 2015). Myrtaceous species possess high concentrations of terpenes (Barbosa et al., 2013) as well as anticancer, antimalarial and anti-inflammatory properties (Donato and de Morretes, 2013). Essential oils produced by species in this family are often used in the culinary industry (Cascaes et al., 2015) and pharmaceutical trade (Barbosa et al., 2013).

2.2. The Genus *Heteropyxis*

The genus name, *Heteropyxis* is of Greek and Latin origin. In Greek "*Hetero*" means "different" and "*pyxis*" means "container with a lid" in Latin (Van Vuuren and Viljoen, 2008). *Heteropyxis* is a small genus with only three species in southern Africa; *H. canescens* Oliv., *H. dehniae* Suess. and *H. natalensis* Harv. (Van Vuuren et al., 2007). *Heteropyxis natalensis* is frequently used in traditional medicine due to an array of phytomedicinal compounds (Adesanwo et al., 2009). However, the leaves and roots of *H. dehniae* are also of medicinal value and are used to treat headaches and nosebleeds (Sibanda et al., 2004).

Heteropyxis shares many myrtalean features such as oil glands/secretory cavities within the leaves, sunken styles, similar pollen structure and the presence of essential oils (Stern and Brizicky, 1958; Schmid, 1980; Wilson et al., 2001).

2.3. Essential Oils

The occurrence of essential oils is common in the plant kingdom (Bernáth, 2009). They are produced as secondary metabolites by many aromatic plants (Bakkali et al., 2008; Dhifi et al., 2016). The presence of essential oils is partially responsible for the medicinal properties of a plant (Edris, 2007). Essential oils, alternatively known as volatile or ethereal oils are described as "natural, complex compounds characterised by a strong odour" (Bakkali et al., 2008). The properties of the oils vary in different species depending on the complexity of the chemical

compound mixture (Siddique et al., 2015). Essential oils can sometimes contain approximately 20 – 60 chemical compounds at different concentrations. These compounds range from terpenes, aromatic compounds and terpenoids (Bakkali et al., 2008; Akthar et al., 2014). The oils are obtained from the various plant organs by expression, fermentation, enfleurage, extraction or steam distillation (Burt, 2004; Djilani and Dicko, 2012; Tongnuanchan and Benjakul, 2014). The use of aromatic plants to treat illness and disease is well documented (Akthar et al., 2014).

In recent decades, the interest in aromatic plants and essential oil production has increased (Siddique et al., 2015). Approximately 3,000 essential oils have been discovered, of which 300 are used in various applications (Burt, 2004; Bakkali et al., 2008; Akthar et al., 2014). Plant families such as Asteraceae, Lamiaceae, Fabiaceae, Piperaceae, Lauraceae and Myrtaceae comprise of genera and species that are commercially important (Bernáth, 2009) as they produce essential oils via secondary metabolism (Sartoratto et al., 2004; Akthar et al., 2014). These oils are in high demand as they are responsible for the flavour in food (Edris, 2007), fragrance in perfumes (Djilani and Dicko, 2012) and therapeutic properties in pharmaceutical drugs (Bernáth, 2009). Essential oils also have an important role in the natural environment. They act as insect attractants to ensure successful dispersal of pollen and seeds, as well as herbivore repellents to inhibit over-grazing (Bakkali et al., 2008).

Many studies indicated that essential oils possess biological activity (Tongnuanchan and Benjakul, 2014). The oils have been reported to exhibit antiviral (Burt, 2004), antifungal, antibacterial (Dhifi et al., 2016), anti-inflammatory (Bakkali et al., 2008) and anticancer (Edris, 2007) activities due to their chemical constituents (Burt, 2004).

The essential oils of *H. natalensis* were found to exhibit antimicrobial activity. The major compounds present in the oils were 1,8-cineole and limonene (Van Vuuren et al., 2007). The compound 1,8-cineole, also known as eucalyptol is a main component in *Eucalyptus* oil (Sefidkon et al., 2007) as well as tea tree oil (*Melaleuca alternifolia*) (Cox et al., 2001). Eucalyptol is used in cough syrups and inhalants as well as detergents and toiletries (Sefidkon et al., 2007). Limonene is considered as one of the major essential oil components in *Citrus* (Gomes et al., 2014) and is also found in many Lamiaceae species (Gracindo et al., 2006; Takeoka et al., 2010). This compound is often used in culinary and cosmetic industries. It is also used as an expectorant (Amanzadeh et al., 2006). *Heteropyxis natalensis* is traditionally used to treat respiratory disorders and the presence of these compounds provide plausibility for the ethnobotanical utilisation of this species (Van Vuuren et al., 2007).

The chemical composition of essential oils is influenced by the species' genotype as well as the surrounding environment (Sartoratto et al., 2004; Siddique et al., 2015). Different species synthesise and accumulate a variety of compounds at different concentrations either internally or externally. Essential oils are often stored in specialised foliar secretory structures such as glandular trichomes, resin ducts, oil glands or secretory cavities (Akthar et al., 2014).

2.4. Specialised Foliar Secretory Structures

Vascular plants contain an assortment of specialised microstructures varying in morphology and function (Fahn, 1988a). These structures are either secretory or non-secretory in nature (Roshchina, 2003; Wagner et al., 2004). Secretory tissues are defined as unicellular or multicellular structures (Roshchina, 2003) responsible for the synthesis, storage, and secretion of phytochemicals. The mode of secretion depends on the secretory tissues present in the plant (Svoboda and Svoboda, 2000). Secretory tissues are reported to be important anatomical features of a plant family (Jiang et al., 2010; Vargas et al., 2015) and can be found on aerial surfaces of plant organs or within the plant body (Fahn, 1988b; Demarco, 2017). External structures include trichomes, hydathodes and salt glands (Fahn, 1988a; Dassanayake and Larkin, 2017) whereas internal secretory structures consist of laticifers, secretory cavities and resin ducts (Fahn 1988a; Evert, 2006).

The phytochemicals secreted include various classes of primary and secondary metabolites that assist in plant pollination and plant protection. Genetic and environmental conditions also influence the chemical composition of exudates (Svoboda and Svoboda, 2000) which may be composed of oils, resins, latex or mucilage (Evert, 2006; Pickard, 2008).

2.5. Epidermal Vestiture

"Most surfaces of most plants are said to be pubescent, bearing trichomes or hairs" (Wagner, 1991). Trichomes are defined as unicellular or multicellular epidermal projections emerging from aerial tissues of plant organs such as leaves and stems or petals (Levin, 1973; Werker, 2000; Kim et al., 2012). The word "Trichome" is a derivative of the Greek word "Trichos" which translates to "Hair" (Glas et al., 2012). These hair-like structures are sometimes referred to as epidermal protrusions (Werker, 2000) or specialised epidermal cells (Wagner, 1991) and are similar to the hairs found on the human body (Peter and Shanower, 1998). Botanical literature has reported more than 300 types of trichomes varying in size and shape (Wagner, 1991). The location and

function of these microstructures are species-specific (Glas et al., 2012) and provide a protective barrier on the epidermal surface against abiotic and biotic stresses (Xiao et al., 2017).

Trichomes are often categorised as being glandular or non-glandular (Fig. A to C) protuberances based on their morphology and secretory capability (Choi and Kim, 2013; Xiao et al., 2017). Glandular trichomes consist of a glandular head that can synthesise, accumulate and exude secondary metabolites (Werker, 2000; Glas et al., 2012; Santos Tozin et al., 2016) whereas non-glandular trichomes are primarily involved in protecting the plant from environmental threats (Santos Tozin et al., 2016). There are various terms used to describe trichomes based on their exterior structure (Levin, 1973; Wagner, 1991).

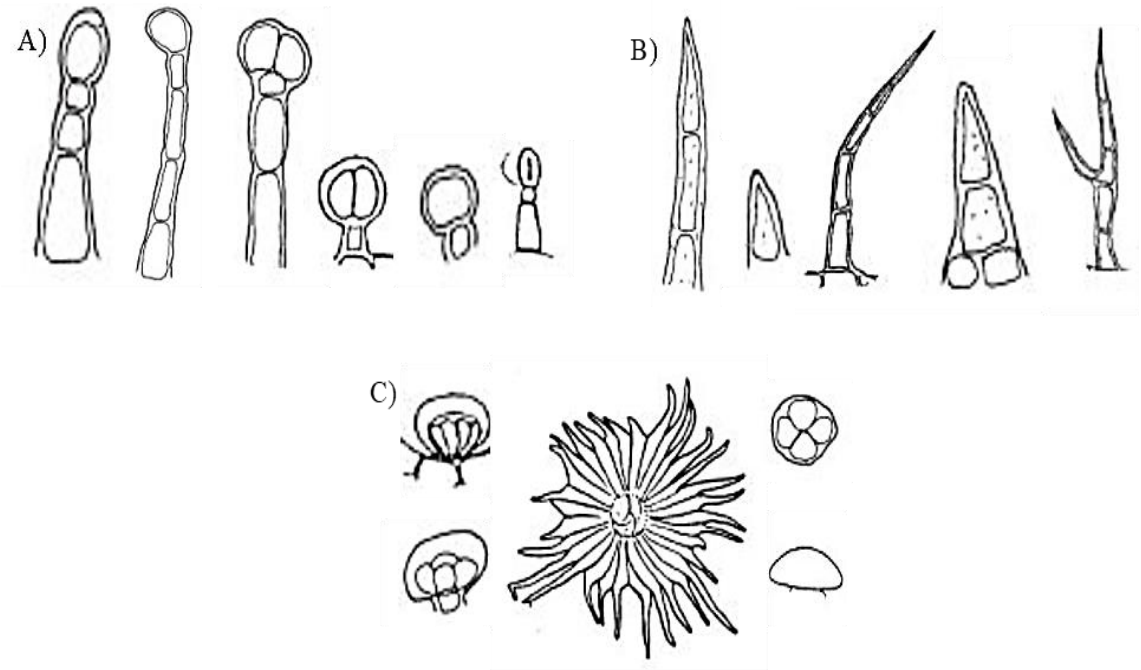

Figure 2.2: Representations of various glandular (A and C) and non-glandular (B) trichomes found on aerial surfaces of vascular plants. (Adapted from Roe, 1971; Payne, 1978; Kaya et al., 2003; Grubešić et al., 2007)

Trichomes are used as diagnostic characters for species identification and classification (Choi and Kim, 2013) and are of great interest to botanists and taxonomists (Payne, 1978). Morphological variation of trichomes allows for evolutionary trends to be evaluated and understood amongst species, genera and families (Kim et al., 2012). Some species contain a wide array of trichomes (Choi and Kim, 2013) whereas certain species are limited to a single trichome type. The latter trend is observed in many myrtaceous species such as *Amomyrtus luma*, *Luma apiculata*,

Myrteola nummularia and *Ugni molinae* where non-glandular trichomes are found on the epidermal surfaces (Retamales and Scharaschkin, 2015).

2.5.1. Non-Glandular Trichomes

Non-glandular or simple trichomes are found in many angiosperm species but are also found in some gymnosperms and bryophytes (Wagner et al., 2004; Glas et al., 2012). These trichomes exhibit remarkable variation in size and shape (Werker, 2000; Santos Tozin et al., 2016). Therefore, they are often classified according to their diverse morphology as seen in various species of *Mentha* (Choi and Kim, 2013). Non-glandular trichomes may be unicellular or multicellular, branched or unbranched structures with blunt or tapering apices ranging from a few microns to many centimeters (Werker, 2000; Glas et al., 2012; Santos Tozin et al., 2016). They are often found in abundance on various plant organs forming a dense indumentum (Werker, 2000). The formation of trichomes occur at any stage of plant development. The cells of non-glandular trichomes are metabolically active during trichome development and eventually senesce or die when the plant reaches maturity (Santos Tozin et al., 2016). In some cases, dead trichomes still remain functional on the epidermal layer of a plant (Wagner et al., 2004).

The morphology of non-glandular trichomes indicate that they are not involved in the production, accumulation and exudation of secondary metabolites due to the absence of a glandular head (Santos Tozin et al., 2016). However, this category of trichomes offer physical protection against extreme environmental stresses as these appendages form a physical barrier on the aerial surface of a plant. Non-glandular trichomes offer protection against extreme temperatures, increased light intensity and extensive water loss (Werker, 2000; Glas et al., 2012; Santos Tozin et al., 2016).

An important function associated with non-glandular trichomes is the defense mechanism they provide against insects depending on the morphology and orientation of the hairs. The dense indumentum hinders the movement of insects on the surface of the plant (Werker, 2000; Glas et al., 2012). Herbivorous arthropods are sometimes impaled on to hooked trichomes as seen on *Phaseolus* leaves (Levin, 1973).

2.6. Internal Secretory Structures

Vascular plants experience two modes of secretion based on the location of their secretory apparatus (Fahn, 1988b). External secretory structures undergo exogenous secretion which

involves the discharge of material on to the plant surface (Svoboda and Svoboda, 2000). However, plant families such as the Euphorbiaceae (Nicole et al., 1986), Myrtaceae (Evert, 2006) and Pinaceae (Arbellay et al., 2014) contain a variety of secretory tissues within the plant body and undergo endogenous secretion. This mode of secretion involves the release of secondary metabolites within the plant (Evert, 2006). Internal secretory structures include mucilage idioblasts, oil glands, resin ducts and secretory cavities (Fahn, 1988b). According to Fahn (2002), secretory tissues are of evolutionary interest and are extremely important for taxonomic purposes (Evert, 2006).

2.6.1. Secretory Cavities

Foliar secretory cavities or internal secretory spaces (Castro and Demarco, 2008) are well documented in the Rutaceae (Bennici and Tani, 2004), Asteraceae (Monteiro et al., 1999), Rubiaceae (Vieira et al., 2001) and Myrtaceae families (Ciccarelli et al., 2003; Kalachanis and Psaras, 2005; Retamales and Scharaschkin, 2015). The presence of subdermal cavities in myrtaceous species is an important familial characteristic (Ciccarelli et al., 2003). A secretory cavity is an isodiametric intercellular space also known as a lumen which is lined with secretory epithelial cells (Fahn, 1988a; Texeira et al., 2000; Castro and Demarco, 2008). These structures are of anatomical importance and are used as a diagnostic tool to identify certain plant families (Vieira et al., 2001). Secretory cavities are interchangeably called oil glands (Evert, 2006) or oil cavities (Fahn, 1988a) and have also been reported as pellucid glands, translucent and pellucid dots (Texeira et al., 2000; Vieira et al., 2001).

The lumen is encircled by many epithelial cell layers involved in the secretory process (Kalachanis and Psaras, 2005) while the outer layers merge into the epithelium as the cavity expands (Fahn, 1988a). A protective sheath is formed by the outermost cell layers of the cavity (Fahn, 1988a). The epithelial cells are responsible for synthesising and secreting a variety of compounds into the intercellular space such as terpenes, phenolics and polysaccharides (Evert, 2006; Castro and Demarco, 2008). Phenolic compounds are often located in cavities of *Eucalyptus* species (Castro and Demarco, 2008).

During early stages of leaf growth secretory cavities begin to develop. However, in mature leaves their appearance tends to decrease (Kalachanis and Psaras, 2005). Schizogenous, lysigenous and schizolysigenous cavities are the three developmental types of secretory cavities present in most vascular plants (Fahn, 1988a; Evert, 2006). Schizogenous cavity development occurs due to cell

separation (Fig. 2.3 A) whereas lysigenous cavities undergo cellular disintegration (Fig. 2.3 B) (Texeria et al., 2000; Ciccarelli et al., 2003). Schizolysigenous cavity formation involves cell separation followed by cellular disintegration which results in cavity enlargement (Texeira et al., 2000; Ciccarelli et al., 2003; Evert, 2006).

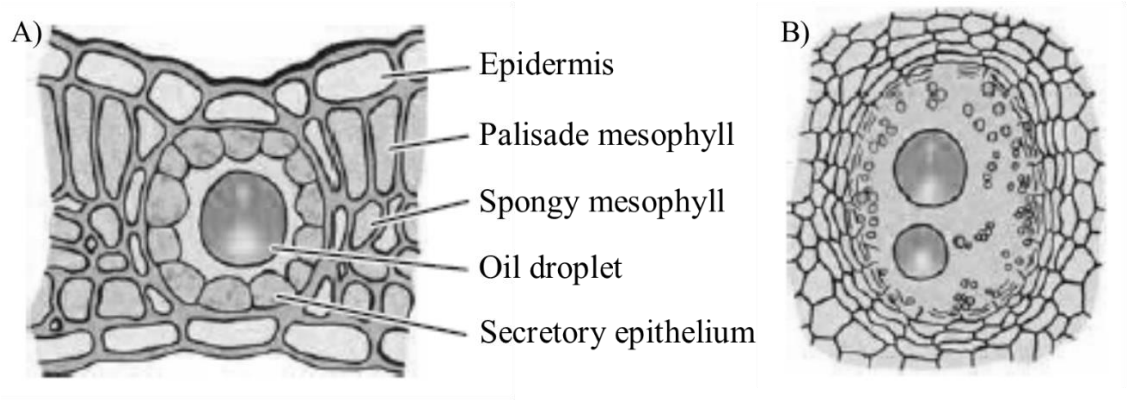

Figure 2.3: Secretory cavities in *Hypericum* and *Citrus* species. A) Schizogenous secretory cavity of *Hypericum perforatum.* B) Lysigenous secretory cavity of *Citrus limon*. (Adapted from Kűck et al., 2009)

The secretory material within the cavity is sometimes released upon mechanical damage as seen in *Myrtus communis* (Kalachanis and Psaras, 2005). Species in the Rutaceae family release their exudates to the epidermal surface via cap cells. The cap cells consist of two to four epidermal cells which are similar to stomatal pores (Kalachanis and Psaras, 2005; Ciccarelli et al., 2008). The secretory content is mainly lipophilic or mucilaginous in nature (Texeira et al., 2000).

2.6.2. Crystal Idioblasts

More than 215 plant families are known to contain calcium oxalate (Molano-Flores, 2001; Konyar et al., 2014; Kartal, 2016). Calcium oxalate is a common biomineral (Franceschi, 2001) found in angiosperms as well as gymnosperms (Ilarslan et al., 2001; Konyar et al., 2014). The presence and accumulation of calcium oxalate crystals occurs in vacuoles of specialised cells called crystal idioblasts (Franceschi, 2001; Nakata, 2003). Calcium oxalate may have negative effects on the plant if the biomineral is excessively accumulated (Konyar et al., 2014). Therefore, crystal idioblasts function primarily as calcium sinks (Nakata, 2003) to reduce, remove or regulate high levels of calcium in the surrounding cells (Franceschi, 2001; Nakata, 2003; Konyar et al., 2014).

The crystals vary in shape, size (Franceschi, 2001; Konyar et al., 2014) and distribution in various organs of the plant such as leaves, flowers, stems and roots (Meric, 2009; Kartal, 2016). These crystal properties may be affected by an array of environmental conditions such as temperature, ion concentration, pressure, light and pH (Meric, 2009; Kartal, 2016). Prisms, druses, raphides, styloids and crystal sand are the terms used to describe the 5 classes of calcium oxalate crystals (Fig. 2.4) (Konyar et al., 2014). Barbosa et al (2013) indicated the presence of idioblasts containing druse crystals in several *Melaleuca* species suggesting druses are common characteristics in the Myrtaceae family. The presence or absence of these various crystals are also important taxonomic characteristics that are often used to elucidate evolutionary relationships among species and families (Konyar et al., 2014). Raphide crystals have previously been used to identify and isolate subfamilies of Rubiaceae (Molano-Flores, 2001).

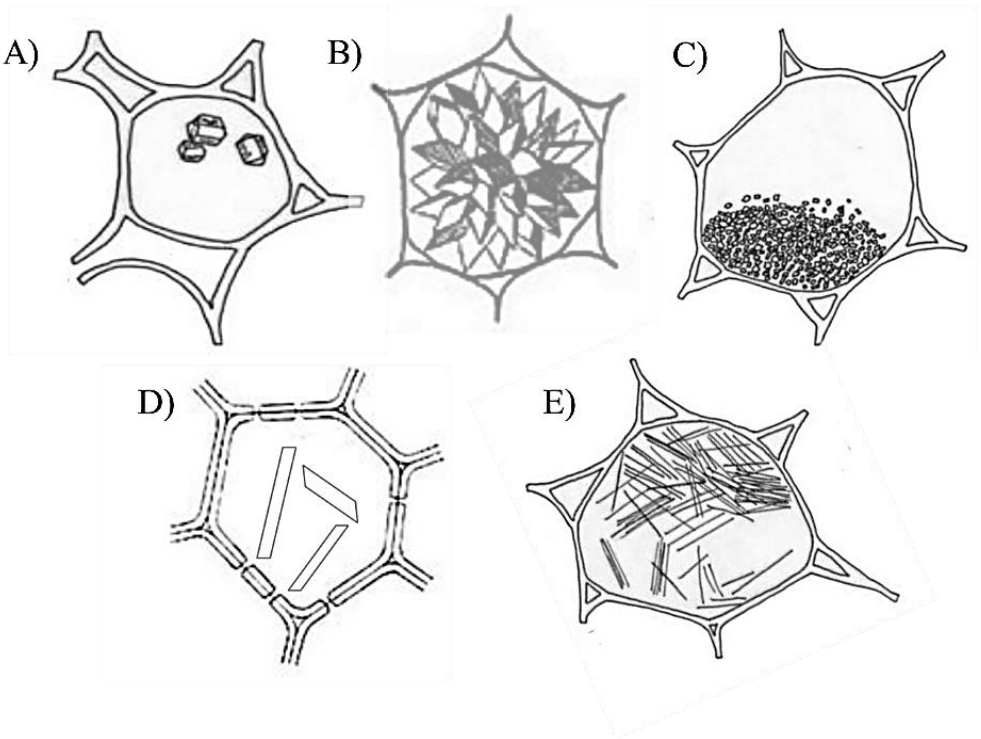

Figure 2.4: Various classes of calcium oxalate crystals found in plant cells; A) Prisms, B) Druses, C) Crystal sand, D) Styloids, E) Raphides (Adapted from Souza et al., 2004; Upton et al., 2016)

The function of the crystals remains unclear (Ilarslan et al., 2001; Kartal, 2016). However, diverse crystal morphology proposes plausible significance (Konyar et al., 2014). It has been reported that the crystals offer structural support to plant tissues as well as protection against grazing herbivores (Nakata, 2003; Kartal, 2016). Additional functions attributed to calcium oxalate

crystals include metal detoxification, calcium homeostasis, light gathering and reflection (Konyar et al., 2014).

2.7. Systematics and Taxonomy

Trichomes, secretory cavities, crystal idioblasts and many other foliar structures are important characteristics in plant taxonomy (Evert, 2006; Kim et al., 2012). These morphological attributes are used as diagnostic tools to identify species that may have been incorrectly placed in genera and families (Vieira et al., 2001; Kim et al., 2012; Konyar et al., 2014). The aforementioned structures are recognised as efficient and successful taxonomic indicators as they have provided extensive information in the field of plant taxonomy and systematics (Wilson et al., 2001; Iroka et al., 2015).

Internal and external features of two *Dahlstedtia* species (*D. pinnata* and *D. pentaphylla*) were investigated to establish the differences between them (Texeira and Gabrielli, 2006). The species are often confused due to their similar floral morphology. Texeira and Gabrielli (2006) studied the inconspicuous features of the species and concluded that the presence of internal secretory cavities was an important diagnostic attribute of *D. pentaphylla* whereas cavities were absent in *D. pinnata*. Additional micromorphological features such as stomatal density and crystal distribution also assisted in separating the species (Texeira and Gabrielli, 2006).

2.7.1. Taxonomic Classification of *Heteropyxis*

Heteropyxis, a unique and controversial genus due to its taxonomic position (Tobe and Raven, 1987) was first recognised by Harvey in 1863 (Stern and Brizicky, 1958) and placed in various families such as Lythraceae, Rhamnaceae, Rutaceae, Myrtaceae and the monogeneric family Heteropyxidaceae (Stern and Brizicky, 1958; Mohammed et al., 2009). Stern and Brizicky (1958) substantiated the placement of *Heteropyxis* in Myrtaceae based on leaf and floral anatomy as well as vegetative and reproductive morphology (Schmid, 1980).

In addition to traditional taxonomic methodologies, DNA barcoding involves nucleic acid sequencing which utilises regions from chloroplast genomes to determine phylogenetic relatedness of plants (Kar et al., 2015). Chloroplast genes such as *matK, trnT-F* and *rbcL* are commonly used to obtain phylogenetic data (Műller et al., 2006). However, *matK* is preferred due

to its fast evolutionary rate and robust analysis of plant phylogenies (Gadek et al., 1996; Műller et al., 2006; Barthet and Hilu, 2007).

Initially the *rbcL* gene was used but it was considered unsuitable to resolve myrtalean lineages (Conti et al., 1996; Gadek et al., 1996). Therefore, Wilson et al (2005) used the *matK* gene to illustrate a phylogeny within Myrtaceae which clearly indicated the placement of *Heteropyxis* (Fig. 2.5). *Heteropyxis* is now placed in the subfamily Psiloxyloideae and basally in Myrtaceae due to its myrtalean similarity as well as DNA barcoding (Wilson et al., 2005; Mohammed et al., 2009).

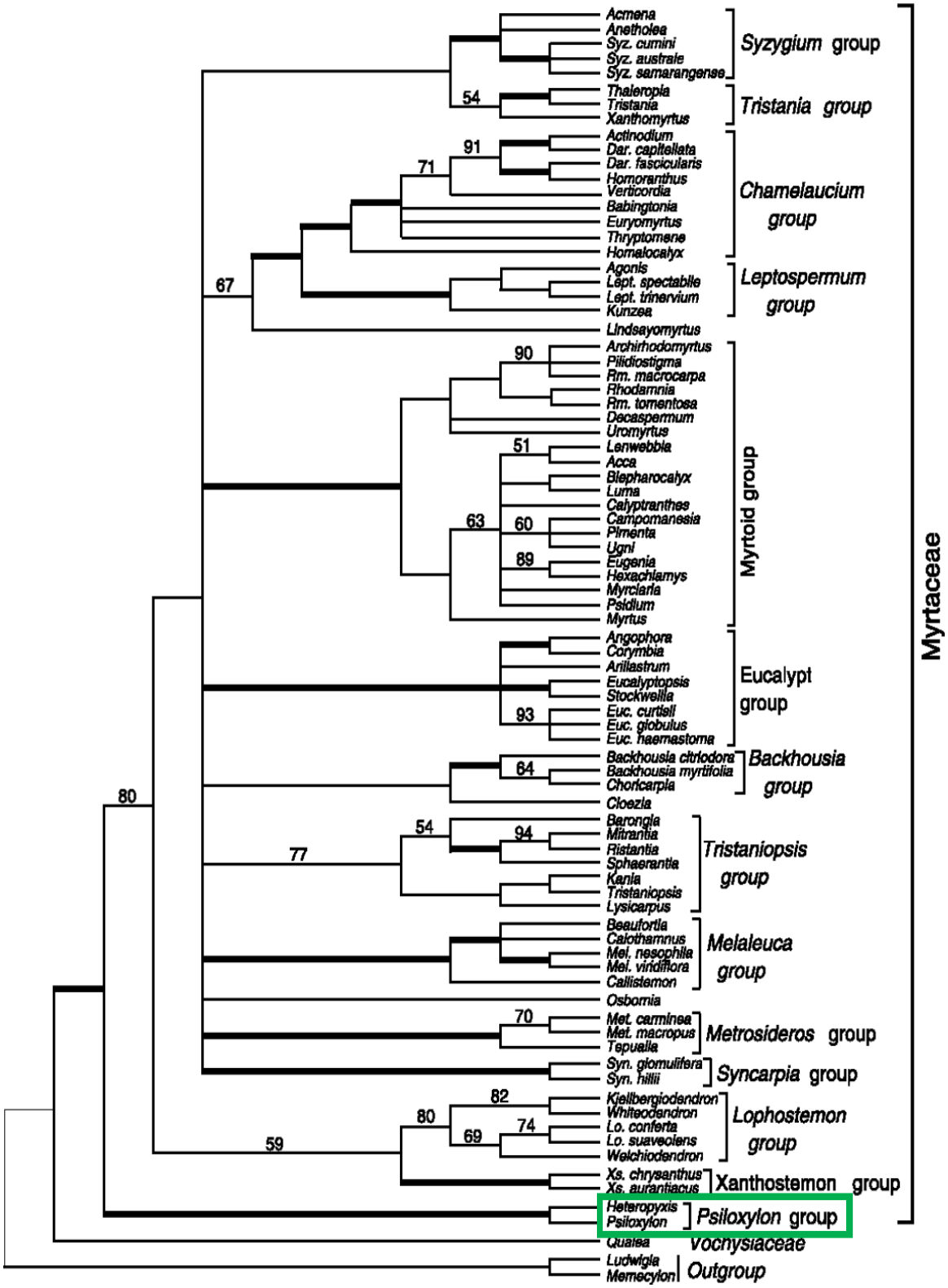

Figure 2.5: Stringent consensus cladogram of 187 927 equally parsimonious trees of 1870 steps (CI = 0.51; RI = 0.70; RC = 0.43) found from experiential searching of *matK* data. Thick branches established at least 95% jackknife support; other values > 50% are displayed above clades (Wilson et al., 2005)

2.8. Nanotechnology

Nanotechnology is an evolving research field and can be defined as a science that includes the synthesis, development and manipulation of nanomaterials (Mondal et al., 2011; Hasan, 2015). The interest in nanotechnology has increased over the years and has been used in many medical procedures such as gene therapy, cancer treatment and drug delivery (Mondal et al., 2011). Metals such as copper, zinc, gold, titanium and silver are used to produce metallic nanomaterials which are commonly known as nanoparticles (Hasan, 2015). Metallic nanoparticles display inimitable optical and chemical properties (Mohammed, 2015; Paosen et al., 2017). Therefore, they are used in the medical field, pharmaceutical industry as well as the agricultural sector (Parveen et al., 2016).

2.8.1. Silver Nanoparticles

Silver nanoparticles (AgNPs) are important constituents in the field of nanotechnology (Mishra and Pani, 2017). AgNPs exhibit unique properties and vary in size and shape (Savithramma et al., 2011; Bose and Chatterjee, 2016). These nanostructures have been deemed successful in numerous applications as they have been used in pathology, wound healing, dentistry and antimicrobial analyses (Nurani et al., 2015; Bose and Chatterjee, 2016).

The production of AgNPs can occur via thermal decomposition, reduction of silver compounds in solution, laser-mediated synthesis and microwave-assisted synthesis (Bose and Chatterjee, 2016). Chemical synthesis often involves hydrazine hydrate, ethylene glycol and sodium borohydride which are extremely toxic. These chemicals produce harmful byproducts which are not safe for the environment (Mishra and Pani, 2017). Therefore, there has been an exponential interest and demand to find a non-toxic alternative (Hasan, 2015; Bose and Chatterjee, 2016). Scientists have resorted to “green synthesis” which can be defined as the synthesis of AgNPs using non-toxic and environmentally friendly biological material (Nurani et al., 2015).

Bacteria, fungi and an array of plants have been used for AgNP synthesis (Hasan, 2015; Paosen et al., 2017). The “green synthesis” approach brings nanotechnology and plant biotechnology together resulting in a risk-free and better-quality system that is suitable for biomedical applications (Rahimi-Nasrabadi et al., 2014; Mohammed, 2015; Parveen et al., 2016). However, the utilisation of plant extracts is preferable as it is inexpensive, less time consuming, non-toxic, eco-friendly and can be easily stored for mass synthesis (Mohammed, 2015; Paosen et al., 2017).

Medicinal plants such as *Azadiracha indica, Carica papaya* (Hasan, 2015) and *Ocimum gratissimum* (Selvamohan et al., 2012) are well known for their antimicrobial activity. Antimicrobial research has been attentive to AgNPs due to their superior antimicrobial potential in comparison to other metals (Hasan, 2015). In addition, AgNPs are non-toxic to human cells while extremely toxic towards bacteria, viruses and various eukaryotic microorganisms (Savithramma et al., 2011; Mohammed, 2015). Myrtaceous species such as *Psidium guajava* and *Eucalyptus camaldulensis* have been utilised for AgNP synthesis based on their medicinal value and antimicrobial activity (Mohammed, 2015; Bose and Chatterjee, 2016).

Lastly, the synthesis of AgNPs could possibly play an important role in plant taxonomy in the future (Mondal et al., 2011). Angiosperm classification can be conducted depending on the species' ability to produce nanoparticles. The morphology, size and concentration of the particles will make it possible to distinguish and identify phylogenetic relationships in different families, genera and species (Mondal et al., 2011).

CHAPTER 3: FOLIAR MICROMORPHOLOGY AND HISTOCHEMICAL ANALYSES OF *Heteropyxis natalensis*

3.1. Abstract

Heteropyxis natalensis is a native South African medicinal tree belonging to the Myrtaceae family. The aim of this study was to identify the foliar micromorphology, ultrastructure and histochemical composition of the leaves. Micromorphological investigations revealed the presence of non-glandular trichomes, schizolysigenous secretory cavities and druse crystals. Ultrastructural and histochemical observations detected the accumulation of secretory material in basal cells of non-glandular trichomes. Histochemical tests revealed the presence of alkaloids, phenolics, lipids, proteins, essential oils, resin acids and trace amounts of unesterified pectins and polysaccharides. The results obtained in this study explain the morphology and function of each familial trait and could possibly benefit future anatomical studies regarding the genus.

Keywords: non-glandular trichomes; micromorphology; schizolysigenous; secretory cavities

3.2. Introduction

Heteropyxis is a unique genus among the Myrtaceae family (Tobe and Raven, 1987) consisting of three species indigenous to southern Africa namely; *H. canescens* Oliv., *H. dehniae* Suess. and *H. natalensis* Harv (Van Vuuren et al., 2007). Because of its therapeutic properties *H. natalensis* has been the focus of medicinal research in the recent past (Gundidza et al., 1993; Van Vuuren et al., 2007). *Heteropyxis natalensis* is a small, deciduous tree (Adesanwo et al., 2009) inhabiting evergreen forests and bushveld regions ranging from KwaZulu-Natal to Limpopo province (Van Vuuren et a., 2007). It is often called the "Lavender tree" (Adesanwo et al., 2009) as the leaves emit a robust lavender scent (Van Vuuren and Viljoen, 2008). The leaves, bark and roots of *H. natalensis* have been used for decades by local Venda and Zulu communities to treat a variety of ailments such as respiratory disorders, oral infections and menorrhagia (Van Vuuren and Viljoen, 2008; Adesanwo et al., 2009; Henley-Smith et al., 2018). It has been reported that the essential oils produced by *H. natalensis* contain eucalyptol and limonene which are partially responsible for its medicinal properties (Gundidza et al., 1993; Van Vuuren et al., 2007). These oils are synthesised and accumulated in specialised foliar structures (Fahn, 1988a).

A variety of specialised foliar structures varying in morphology, location and function are found in vascular plants (Fahn, 1988a). These structures are located on aerial surfaces of the plant or within the plant body (Fahn, 1988a) and could be secretory or non-secretory in nature (Roschina, 2003). Trichomes and secretory cavities are common characteristics in Myrtaceae (Retamales and Scharaschkin, 2015) that vary in type, distribution and location (Xiao et al., 2017). Trichomes are defined as unicellular or multicellular hair-like protrusions emerging from the aerial tissues of leaves, stems and petals (Werker, 2000; Glas et al., 2012). These epidermal appendages vary in size, shape and function (Wagner, 1991, Werker, 2000), and are categorised as glandular or non-glandular structures based on the presence of a glandular head (Choi and Kim, 2013; Xiao et al., 2017). Functionally, glandular trichomes are responsible for the synthesis, accumulation and secretion of secondary metabolites (Werker, 2000; Glas et al., 2012) that assist in pollination (Wagner, 1991), whereas the primary functions of non-glandular trichomes include plant protection, light reflectance and temperature regulation (Wagner, 1991; Santos Tozin et al., 2016).

In addition to trichomes, foliar secretory cavities have been documented in many families such as Rutaceae (Bennici and Tani, 2004), Asteraceae (Monteiro et al., 1999), Rubiaceae (Vieira et al., 2001) as well as Myrtaceae (Kalachanis and Psaras, 2005; Retamales and Scharaschkin, 2015). Secretory cavities or internal secretory spaces are located within the plant body and are lined with

secretory epithelial cells that are responsible for the synthesis and exudation of secondary metabolites into the intercellular space (lumen) of the cavity (Fahn, 1988a; Castro and Demarco, 2008). Secretory cavities are also referred to as oil glands (Evert, 2006), pellucid glands or pellucid dots (Texeira et al., 2000; Vieira et al., 2001). Three types of secretory cavities occur within the plant: schizogenous, lysigenous and schizolysigenous cavities (Fahn, 1988a; Evert, 2006). Schizogenous cavity development involves epithelial cell separation whereas cellular disintegration results in lysigenous cavity formation (Texeira et al., 2000; Cicarelli et al., 2003). Schizolysigenous cavity development involves cell separation followed by cellular disintegration which results in cavity enlargement (Texeira et al., 2000; Evert, 2006).

Although the essential oil composition of *H. natalensis* has been rigorously investigated in previous studies (Gundidza et al., 1993; Van Vuuren et al., 2007). The micromorphology, ultrastructure and location of secondary metabolites have not yet been elucidated. Thus, in order to gain clear insights into the structures responsible for synthesis, accumulation and exudation of secondary metabolites, this study aimed to identify the foliar micromorphology, ultrastructure and histochemical composition of *H. natalensis* leaves.

3.3. Materials and Methods

3.3.1. Plant Collection and Sampling

Heteropyxis natalensis was purchased from Tropical Nursery, Durban and kept in a private residence in Isipingo Hills (29°59'10.8"S 30°55'11.2"E). Fresh, intact leaves were collected from the private residence as well as the University of KwaZulu-Natal, Westville Campus (29°49'01.0"S 30°56'51.2"E) for various microscopy analyses. Three stages of leaf development were sampled i.e. emergent (length < 15 mm), young (15 mm – 40 mm) and mature (length > 40 mm). A voucher specimen (Chetty 01 - 18223) was deposited in the Ward Herbarium at the University of KwaZulu-Natal.

3.3.2. Stereomicroscopy

The foliar indumentum on abaxial and adaxial surfaces of entire leaves was investigated using a Nikon AZ100 stereomicroscope equipped with a Nikon Fiber Illuminator and NIS-Elements D image software. Leaf samples were secured onto glass microscope slides using two-way adhesive tape and surface structures were captured at various magnifications (0.5x, 1x and 4x) with a camera fitted onto the stereomicroscope.

3.3.3. Scanning Electron Microscopy (SEM)

SEM was used to investigate the surface and internal structures of each developmental leaf stage. Two techniques were used for SEM: chemical fixation and freeze fracture.

3.3.3.1. Chemical Fixation

Fresh emergent, young and mature leaves were hand sectioned around the midrib (± 2 mm^2). The samples were primarily fixed in 2.5% glutaraldehyde for 24 h at 4°C. Thereafter, the samples underwent three washes (5 min each) using 0.1 M phosphate buffer (pH 7.2) and were subjected to post fixation at room temperature (24°C) in 0.5% osmium tetroxide (OsO_4) for 3 h. The samples underwent three washes (5 min each) using the phosphate buffer and were dehydrated by exposing them to increasing concentrations of ethanol (25%, 50%, 75% and 100%). Samples were dehydrated twice for 10 min each in 25%, 50% and 75% and twice for 20 min each in 100% ethanol. The dehydrated samples were then critical point dried using a Quorum K850 Critical Point Dryer, mounted onto aluminium stubs using carbon conductive tape and sputter coated in a

Quorum Q150 RES gold coater. The prepared stubs were viewed and imaged using a Leo 1450 SEM at 5 kV and a working distance of 14 – 18 mm.

3.3.3.2. Freeze Fracture

Each developmental stage of fresh leaf material was hand sectioned around the midrib (10 mm^2). The samples were immersed in liquid nitrogen slush for 3 – 5 s and then fractured on large aluminium stubs submerged in liquid nitrogen. The fractured segments were placed in an aluminium sample holder and transferred to an Edwards EPTD3 freeze-dryer for 3 days at -50°C. Dried samples were mounted onto aluminium stubs using carbon cement and sputter coated in a Quorum Q150 RES gold coater. The prepared stubs were viewed and imaged using a Leo SEM 1450 at 5 kV and a working distance of 12 – 16 mm.

3.3.4. Light Microscopy and Transmission Electron Microscopy (TEM)

Fresh emergent, young and mature leaves were hand sectioned around the midrib (± 2 mm^2) and primarily fixed in 2.5% glutaraldehyde for 24 h at 4°C. The samples were subjected to three 5 min washes using 0.1 M phosphate buffer (pH 7.2) and post fixed in 0.5% OsO_4 for 4 h. This was followed by three 5 min washes using the phosphate buffer. The samples were then dehydrated by introducing them to a graded series of acetone (20%, 50%, 75% and 100%). Samples were dehydrated twice for 10 min each in 25%, 50% and 75% and twice for 20 min each in 100% acetone. The acetone was then removed, and propylene oxide solution was added to the samples as well as a graded series of Spurr's resin (25%, 50%, 75% and 100%) (Spurr, 1969). Following this, samples were placed in silicon moulds with 100% Spurr's resin and polymerised over 8 h at 70°C.

3.3.4.1. Survey Sections

To identify a region of interest, survey sections were obtained using a Leica Ultramicrotome EM UC7 (Leica Microsystems, Germany) and glass knives. Resin sections (1 µm) were stained with 1% Toluidine Blue and viewed using a Nikon 80i light microscope. Images were captured using a Nikon DS-Fi1 camera and NIS-Elements D image software.

3.3.4.2. Ultra-Thin Resin Sections

To view the fine structure of the leaf tissue, ultrathin sections (100 – 120 nm) were prepared using a Leica Ultramicrotome EM UC7 and glass knives. Resin sections were picked up on copper grids and stained using lead acetate and uranyl acetate and viewed using a Jeol JEM 1010 TEM.

3.3.5. Histochemistry

Fresh cut segments of young leaves were positioned between two pieces of dental wax. The dental wax containing the leaf segments were placed in an Oxford® vibratome sectioning system. Leaf cross sections (80 – 100 µm) were collected and various histochemical tests were conducted at room temperature (24°C) as per Demarco (2017) with slight modifications. Leaf sections were mounted in distilled water ($_dH_2O$).

3.3.5.1. Phenolics

Phenolic compounds were detected by staining leaf sections with 10% ferric chloride. The sections were stained for 10 – 15 min. The production of deep brown or black deposits indicated the presence of phenolic compounds.

3.3.5.2. Alkaloids

Wagner's reagent was used to determine the presence of alkaloids. Leaf sections were stained for 10 min and an orange – brown colour indicated the presence of alkaloids.

3.3.5.3. Lipids

Fresh sections were stained with Sudan IV to detect the presence of lipid inclusions by staining orange – red. The sections were immersed in the stain for approximately 20 min and thereafter rinsed with 70% ethanol to remove the excess stain.

3.3.5.4. Proteins

Proteins were identified by staining leaf sections in 0.25% Coomassie Blue. Sections were stained for 15 min and differentiated in 7% acetic acid. Sections were then rinsed in $_dH_2O$ and a blue colouration indicated the presence of proteins.

3.3.5.5. Essential Oils and Resin Acids

NADI reagent was used to detect the presence of essential oils and resin acids. Sections were placed in the reagent in 1.5 mL Eppendorf tubes and kept in the dark for 1 h. Thereafter, sections were rinsed with sodium phosphate buffer (0.1 M, pH 7.2) for 2 min. Essential oils stained blue – purple whereas resin acids stained dark red.

3.3.5.6. Polysaccharides and Unesterified Pectins

Sections were immersed in 0.1% Ruthenium Red for 2 min and rinsed twice with $_dH_2O$ to remove the excess stain. A light pink colour indicated the presence of polysaccharides and unesterified pectins.

3.3.6. Fluorescence Microscopy

Fresh leaf material was cut using an Oxford® vibratome sectioning system. Sections of approximately 80 – 100 µm were obtained for fluorescence techniques. Unstained leaf sections were mounted in $_dH_2O$ and imaged using a Nikon 80i light microscope at excitation wavelengths between 330 and 380 nm. Red fluorescence indicated the presence of plastids such as chloroplasts and blue fluorescence indicated the presence of lignified components. In addition, sections were stained with 0.01% Acridine Orange for 5 min. Thereafter the sections were rinsed in $_dH_2O$. A green fluorescence indicated cell viability.

3.4. Results and Discussion

3.4.1. Micromorphology

3.4.1.1. Trichomes

Emergent, young and mature leaves of *H. natalensis* were characterised by unicellular non-glandular trichomes on abaxial and adaxial surfaces (Fig. 3.1 A – F). Vascular plants bear glandular and non-glandular trichomes (Choi and Kim, 2013). However, non-glandular trichomes are frequently found in angiosperms (Glas et al., 2012). This observation appeared to be consistent with other myrtaceous species such as *Amomyrtus luma*, *Luma apiculata* and *Nothomyrcia fernandeziana* (Retamales and Scharaschkin, 2015). Non-glandular trichomes were of varying lengths (Fig. 3.2 A) with tapering stalks and globular bases (Fig. 3.2 B) which was observed in *Ugni molinae* (Retamales et al., 2014).

The density of non-glandular trichomes were observed to differ among developmental stages (Fig. 3.1 A – F). Emergent leaves consisted of a dense indumentum (Fig. 3.1 A and B). According to Retamales and Scharaschkin (2015) a dense indumentum implements a fixed environment on the leaf surface thereby preventing water loss, reducing excessive solar radiation and protecting the leaf from herbivorous insects and pathogens (Choi and Kim, 2013; Santos Tozin et al., 2016).

Mature leaves appeared to consist of fewer trichomes on the abaxial and adaxial surfaces (Fig. 3.1 E and F) in comparison to emergent and young leaves. It has been previously reported that younger leaves have a higher trichome density than mature leaves (Valkama et al., 2004). This is due to irregular epidermal cell division as leaf expansion occurs. Trichome initiation from epidermal cells are therefore limited thus preventing the formation of new trichomes on the leaf surface (Oosthuizen and Coetzee, 1984; Szymanski et al., 2000). A similar pattern was observed by Janošević et al (2016) wherein the leaves of *Salvia aegyptiaca* were investigated.

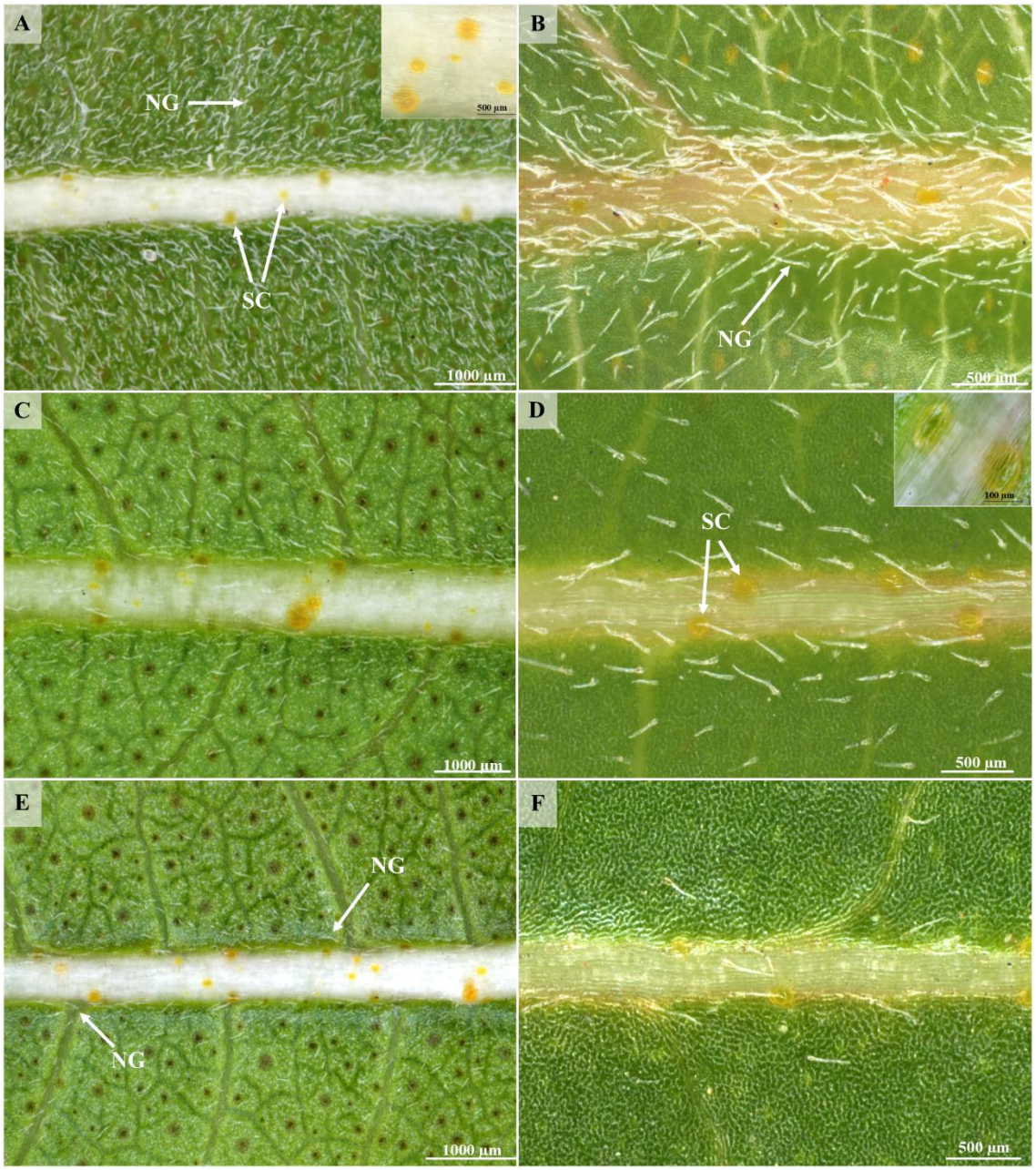

Figure 3.1: Stereomicrographs of emergent, young and mature leaves of *H. natalensis* presenting the overall surface morphology. A) Abaxial surface of an emergent leaf displaying an abundance of non-glandular trichomes and subdermal secretory cavities in the midrib (inset). B) Adaxial surface showing the presence of non-glandular trichomes concentrated on the midrib of an emergent leaf. C) A decrease in abundance of non-glandular trichomes on the abaxial surface of a young leaf. D) Swollen subdermal secretory cavities on the adaxial midrib of a young leaf. E) Abaxial surface of a mature leaf displaying non-glandular trichomes near the midrib. F) Sparsely distributed non-glandular trichomes on the adaxial surface of a mature leaf.

Abbreviations: NG = Non-glandular trichomes, SC = Secretory cavity

Domatia, miniscule structures existing as pockets, pits, pouches or tufts (Nishida et al., 2006), were observed in the vein axils on abaxial surfaces of *H. natalensis* leaves (Fig. 3.2 C). Non-glandular trichomes were observed covering the entrances of pit type-domatia (Fig. 3.2 C). A similar finding was observed in *Legrandia concinna* (Retamales and Scharaschkin, 2015). In Figure 3.2 D, a mite was observed in a domatium. Domatia have been reported to play an ecological role as they provide shelter for mites seeking refuge from herbivorous predators (Pireda et al., 2017). The relationship between mite and domatium is mutualistic as the mites reduce plant damage by feeding on pathogenic fungi on the leaves (Romero et al., 2011; Pireda et al., 2017).

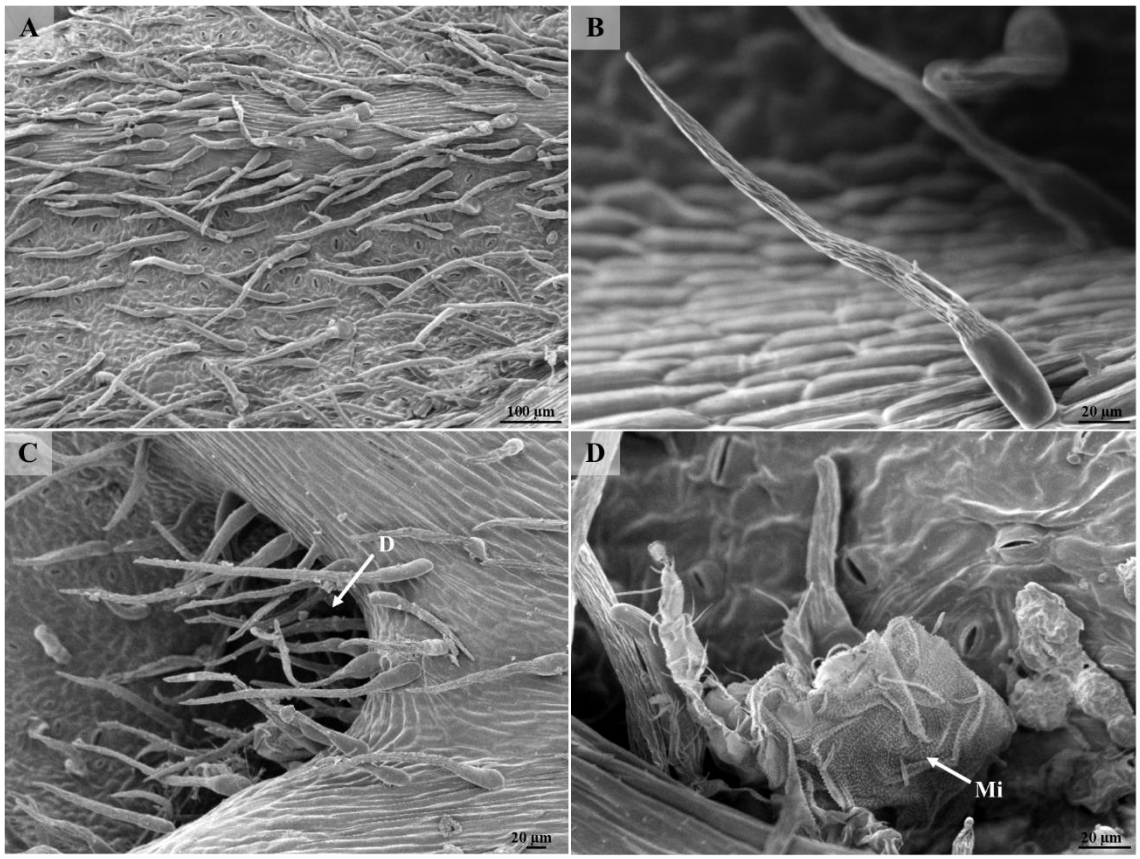

Figure 3.2: SEM micrographs of *H. natalensis*. A) An abundance of non-glandular trichomes parallel to the leaf surface. B) A single non-glandular trichome. C) A pubescent domatium on the abaxial surface of a mature leaf. D) A mite contained within a domatium.
Abbreviations: D = Domatium, Mi = Mite

3.4.1.2. Secretory Cavities

Subdermal secretory cavities were embedded in the midrib of the leaves across all developmental stages (Fig. 3.1 A – F) as well as the lamina of the leaves (Fig. 3.3 A). Secretory cavities are a common characteristic of the Myrtaceae family (Barbosa et al., 2013; Retamales et al., 2014) and were studied in *Melaleuca* species (Barbosa et al., 2013), *Myrtus communis* (Ciccarelli et al., 2008) and *U. molinae* (Retamales et al., 2014).

Schizogenous cavity development is often exhibited in Myrtaceae (Retamales et al., 2014). However, studies conducted on *M. communis* display schizolysigenous cavity development (Ciccarelli et al., 2008). The secretory cavities of *H. natalensis* appear to follow the same arrangement as *M. communis* which involves secretory epithelial cell separation followed by cellular disintegration resulting in a lumen (Fig. 3.3 D). Cavity development has had conflicting views regarding which cavity type occurs within a family (Turner et al., 1998) for the following reasons:

- preparation of plant tissue may be misconstrued for programmed cell death,
- the developmental stage of the cavities could yield false results,
- cavity development could differ in different organs of the same plant
  (Turner et al., 1998; Ciccarelli et al., 2008).

Flattened, elongated secretory cells were observed outlining the periphery of the cavity (Fig. 3.3 C and D). These cells are referred to as sheath cells and provide a protective layer around the cavity (Fahn, 1988a). Secretory epithelial cells were observed lining the lumen of the cavity (Fig. 3.3 D). Secretory epithelia are responsible for synthesising and secreting secretory material into the lumen (Russin et al., 1992; Evert, 2006). The secretory material contains a variety of compounds such as terpenes, phenolics and polysaccharides (Evert, 2006; Castro and Demarco, 2008). Four swollen epidermal cells were observed (Fig. 3.3 B and D). These cells have previously been reported as “Cap cells” (Ciccarelli et al., 2008) and secretory material is released to the external environment via these cells (Kalachanis and Psaras, 2005). A similar observation was reported in *M. communis* (Ciccarelli et al., 2008).

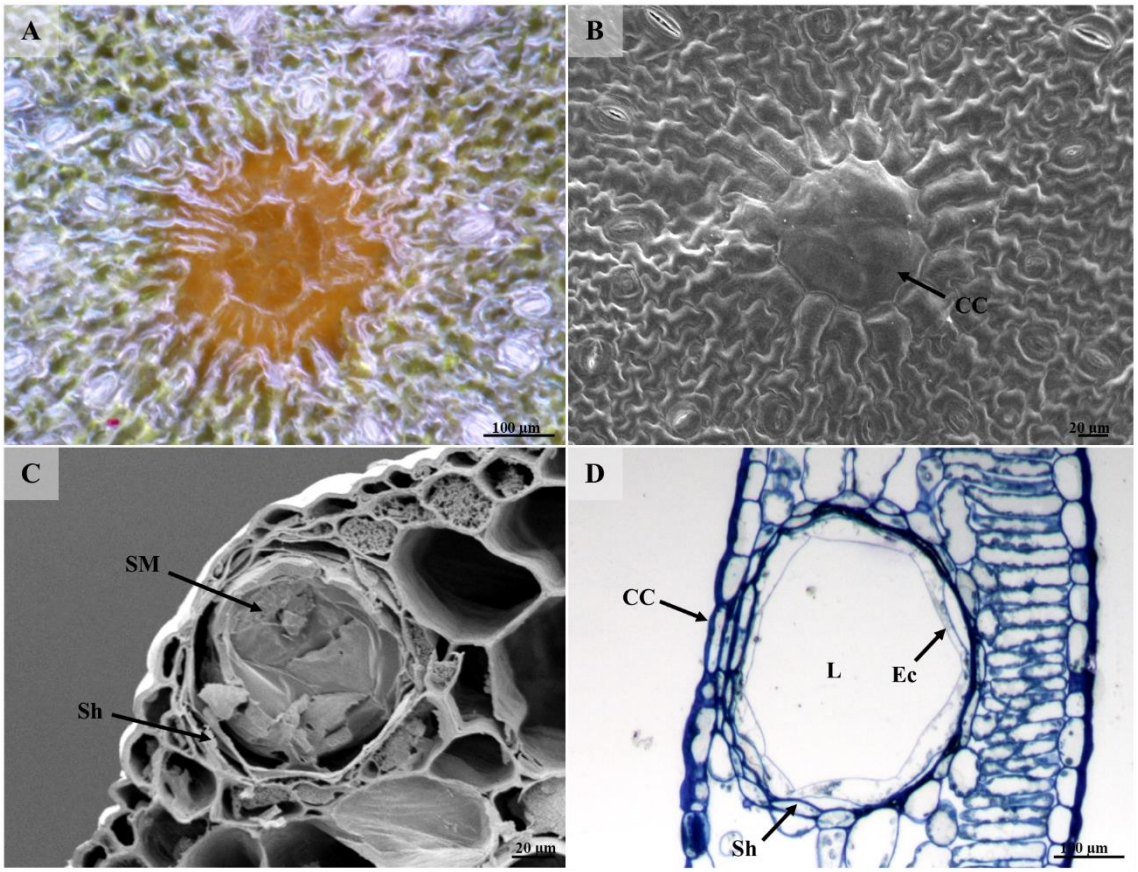

Figure 3.3: Secretory cavities of *H. natalensis*. A) Stereomicrograph of a subdermal secretory cavity surrounded by stomata. B) Electron micrograph displaying swollen cap cells of a subdermal secretory cavity on the lamina. C) Secretory material surrounded by flattened sheath cells. D) A secretory cavity displaying a cross section of cap cells, sheath cells and secretory epithelial cells. Abbreviations: CC = Cap cells, SM = Secretory material, Sh = Sheath cells, L = Lumen, Ec = Secretory epithelial cells, SC = Secretory cavity

3.4.1.3. Druse Crystals

Calcium oxalate crystals were distributed throughout the mesophyll and phloem of the leaves (Fig. 3.4 A). Druse crystals were observed with electron microscopy (Fig. 3.4 B) and were previously found in vegetative and reproductive organs of many myrtaceous genera (Retamales et al., 2014). The function of these crystals remains unclear, but studies have stated that the crystals offer structural support to internal tissues as well as preventing herbivory from occurring (Nakata, 2003; Kartal, 2016). Additional functions attributed to calcium oxalate crystals include detoxification and calcium regulation (Konyar et al., 2014).

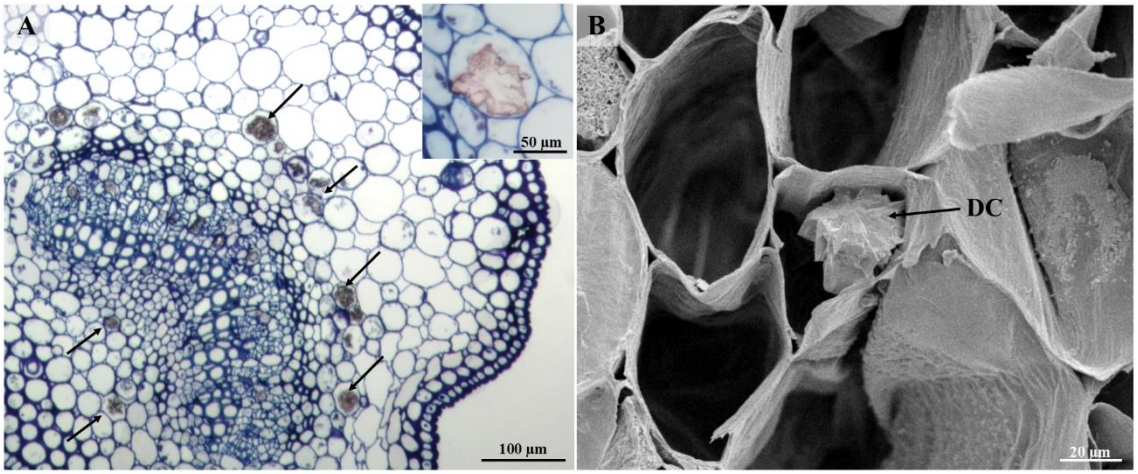

Figure 3.4: Crystals found in *H. natalensis*. A) Cross section of the leaf showing crystals distributed throughout the mesophyll and phloem (arrows). B) A single druse crystal in a mesophyll cell.

Abbreviations: DC = Druse crystal

3.4.2. Ultrastructure

The ultrastructure of a secretory cavity is presented in Figure 3.5 A. Elongated cells containing osmiophilic material in vacuoles (Valkama et al., 2003) were observed surrounding the sheath cells of the cavity which were flattened and had tapered ends. This was observed in cavities of *Citrus* species (Bennici and Tani, 2004). Secretory epithelial cells were irregular in shape and appeared to be disintegrating around the lumen. This reiterates that the secretory cavities of *H. natalensis* appear to be schizolysigenous and similar to the cavities in *M. communis* (Ciccarelli et al., 2008). The cell walls of secretory epithelia were very thin (inset) in comparison to the cell walls of the sheath cells. Thin cell walls of secretory epithelia were observed in *Metrodorea nigra* and allowed for easy access of secretory material into the lumen (Machado et al., 2017). Secretory epithelial cells were observed to contain nuclei, plastids, mitochondria, vesicles, rough endoplasmic reticulum cisternae (RER) and Golgi bodies (Fig. 3.5 B, C and D). Vesicles, Golgi bodies and RER cisternae were observed in Figure 3.5 C. This organelle system was observed in *Leonotis leonorus* and Ascensão and Pais (1998) stated that proteinaceous compounds of the final secretory material are synthesised in the ER and transferred to the Golgi bodies via vesicles. Plastids and mitochondria are primarily involved in the secretory process (Monteiro et al., 1999) hence the presence of these organelles in secretory epithelia (Fig. 3.5 B).

An intact basal cell of a non-glandular trichome is shown in Figure 3.5 E. An abundance of mini vacuoles and mitochondria with osmiophilic granulations were present (Fig. 3.5 F). According to Guo et al (2013), the presence of mitochondria and numerous vacuoles suggests that these organelles are possible sites of terpene and lipid synthesis. Therefore, this suggests that the basal cells of non-glandular trichomes of *H. natalensis* are involved in the synthesis and accumulation of secondary metabolites.

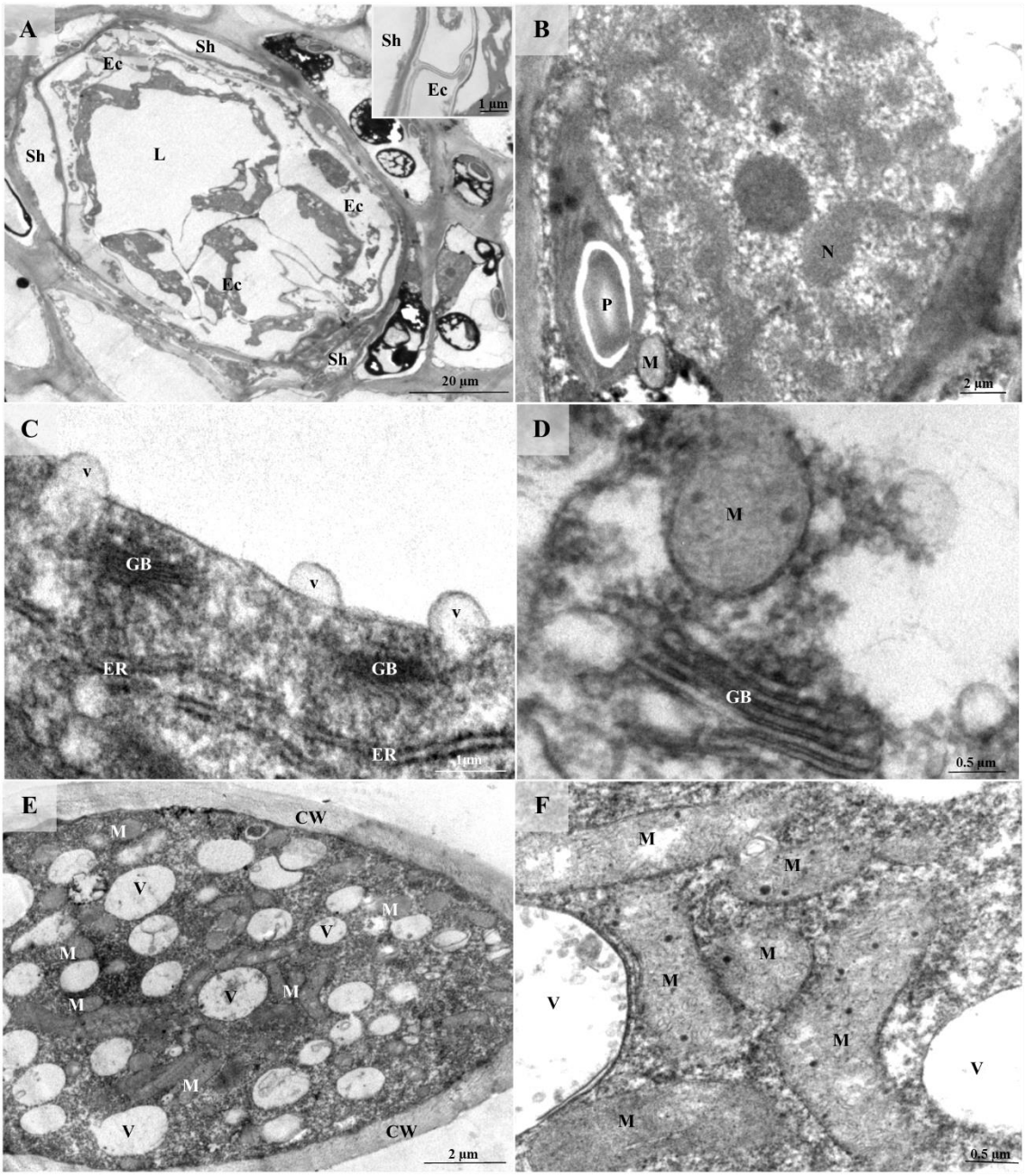

Figure 3.5: TEM micrograph of the leaves of *H. natalensis*. A) General overview of a secretory cavity containing a newly developed lumen, disintegrating secretory epithelial cells with thin cell walls (inset) and flattened elongated sheath cells at the periphery of the cavity. B) A secretory epithelial cell containing a nucleus, a plastid with a starch grain and plastoglobuli, and a mitochondrion. C) Vesicles, RER cisternae and Golgi bodies were present in a secretory epithelial cell. D) A Golgi body and a mitochondrion present in a secretory epithelial cell. E) The basal cell of a non-glandular trichome containing mitochondria and mini vacuoles surrounded by a thick cell wall. F) Globular and elongated mitochondria with osmiophilic granulations were surrounded by mini vacuoles in the basal region of a non-glandular trichome.

Abbreviations: Ec = Epithelial cell, L = Lumen, Sh = Sheath cells, N = Nucleus, P = Plastid, M = Mitochondrion, v = Vesicles, ER = Endoplasmic reticulum, GB = Golgi body, V = Vacuoles, CW = Cell wall

3.4.3. Histochemistry

Secretory cavities and non-glandular trichomes of *H. natalensis* displayed the presence of various secondary metabolites such as phenolics, alkaloids, lipids, proteins, essential oils, resin acids and trace amounts of polysaccharides and unesterified pectins (Fig. 3.6 A – I).

Alkaloids and lipids accumulated in basal cells of non-glandular trichomes (Fig. 3.6 B and E). Traditionally, non-glandular trichomes function as defense mechanisms against herbivorous insects (Santos Tozin et al., 2016). However, research conducted on Lamiaceae and Verbenaceae species observed non-glandular trichomes as sites of secondary metabolite synthesis and accumulation (Santos Tozin et al., 2016). Trace amounts of polysaccharides and unesterified pectins were detected in the stalks of non-glandular trichomes (Fig. 3.6 I). In addition, there appears to be an accumulation of material within the basal cell which was previously observed in Figure 3.5 E and F.

Secretory cavities stained intensely for phenolics (Fig. 3.5 A) and alkaloids (Fig. 3.5 C). Phenolic compounds are associated with several ecological functions and respond to environmental stressors such as increased light conditions as well as mineral deprivation (Veberic, 2016). The presence of alkaloids ensures successful pollination as well as controlled pollinator visitation (Matsuura and Fett-Neto, 2015). These compounds play a role in plant defense by poisoning herbivorous insects upon ingesting leaf material (Santos Tozin et al., 2016).

Lipid bodies were distributed throughout the mesophyll and epidermis (Fig. 3.6 D). This observation was previously reported in *M. nigra* where lipid inclusions were detected in and around secretory cavities (Machado et al., 2017). Essential oils were observed in peripheral cells of the secretory cavity (Fig. 3.6 G). Myrtaceous essential oils are primarily involved in pollinator attraction, defense against herbivory and contributing to plant aroma (Padovan et al., 2014; Zaman et al., 2018).

Proteinaceous material (Fig. 3.6 F) and resin acids (Fig. 3.6 H) were also observed within the leaf tissues. These compounds contribute to plant-environment interactions, plant protection and structural stability (Retamales et al., 2014; Freeman and Beattie, 2008).

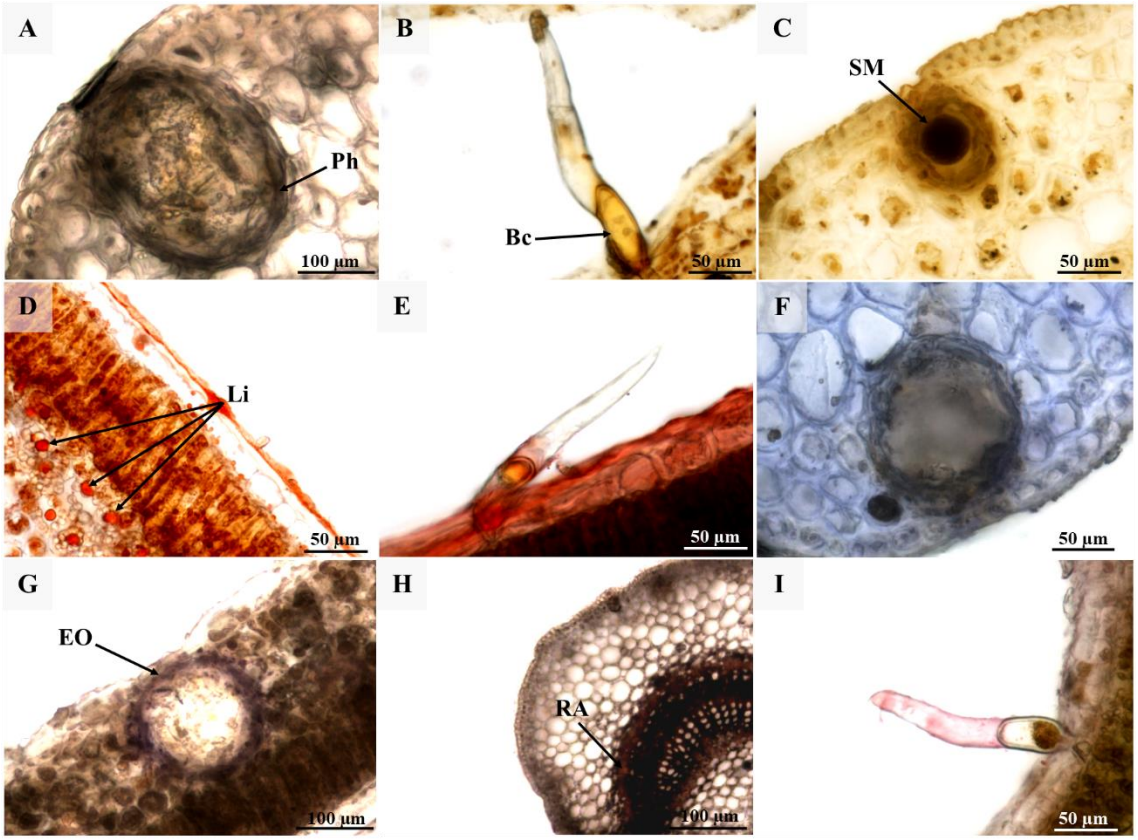

Figure 3.6: Light micrographs of histochemical observations of young *H. natalensis* leaves. A) Secretory cavity stained intensely for phenolics. B) Basal cell of non-glandular trichome stained positively for alkaloids. C) Secretory material within secretory cavity stained intensely for alkaloids. D) Lipids were observed in the epidermis and mesophyll cells. E) Base of non-glandular trichome stained positive for lipids. F) Coomassie Blue stained positively for proteins in secretory epithelial cells. G) NADI reagent stained positive for essential oils. H) Resin acids were observed after staining with NADI reagent. I) Stalk of non-glandular trichome stained positively for polysaccharides and unesterified pectins.

Abbreviations: Ph = Phenolics, Bc = Basal cell, SM = Secretory material, Li = Lipid bodies, EO = Essential oils, RA = Resin acids

3.4.4. Fluorescence Microscopy

Autofluorescence on secretory cavities and non-glandular trichomes was observed. Sheath cells of secretory cavities (Fig. 3.7 A) and the walls of basal cells of non-glandular trichomes (Fig. 3.7 B) emitted a blue fluorescence under UV light indicating the presence of lignified material (Demarco, 2017). Lignin is an important phenolic polymer as it enhances cell wall rigidity and offers cellular support (Liu et al., 2018). A similar observation was made for secretory cavities of *Eucalyptus polybractea* (Goodger et al., 2010) and cells walls of trichomes of *Arabidopsis thaliana* (Kulich et al., 2015). Mesophyll cells shown in Figure 3.7 A and B as well as the contents within the basal cells of non-glandular trichomes emitted a red fluorescence indicative of plastids (Roschina, 2003). Secretory cavities and non-glandular trichomes were preliminarily tested for viability using Acridine Orange (Foglieni et al., 2001). Sheath cells of secretory cavities (Fig. 3.7 C), basal cells and stalks of non-glandular trichomes (Fig. 3.7 D) emitted a green fluorescence indicating cell viability. However, cell viability will be investigated further in future research.

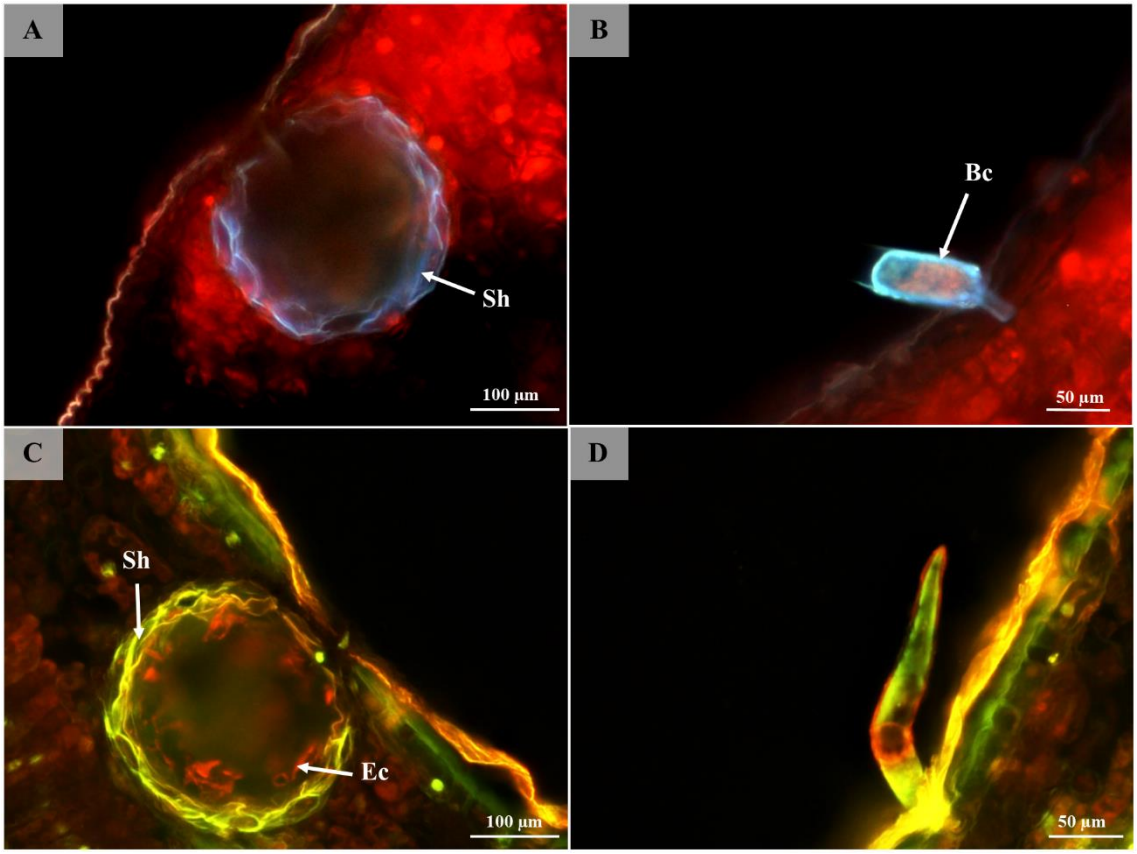

Figure 3.7: Fluorescence micrographs showing autofluorescence and cell viability. A) A secretory cavity exhibiting autofluorescence. B) A basal cell of a non-glandular trichome exhibiting

autofluorescence. C) Sheath cells of a secretory cavity displaying viability. D) A non-glandular trichome displaying viability.
Abbreviations: Bc = Basal cell; Ec = Epithelial cell, Sh = Sheath cells

3.5. Conclusion

In this study, the foliar micromorphology of *H. natalensis* has been identified and characterised for the first time. *Heteropyxis natalensis* shares many myrtalean traits such as non-glandular trichomes, secretory cavities and druse crystals. The secretory cavities within the leaves appear to be schizolysigenous and contain phenolics, alkaloids and essential oils according to histochemical testing. Non-glandular trichomes appear to be synthesising and accumulating secretory material in their basal cells. The results obtained in this study could potentially benefit future anatomical research for *H. canescens* and *H. dehniae*.

CHAPTER 4: PHYTOCHEMICAL ANALYSES AND ANTIBACTERIAL ACTIVITY OF *Heteropyxis natalensis*

4.1. Abstract

Heteropyxis natalensis is a South African medicinal tree that has been utilised by Venda and Zulu communities to treat several health ailments. The aim of this study was to elucidate the secondary metabolites in crude leaf extracts as well as to investigate the chemical profile and antibacterial efficacy of the methanolic leaf extract of *H. natalensis*. Qualitative phytochemical screening confirmed the presence of carbohydrates, alkaloids, phenolics, saponins, sterols, terpenes and fixed fats and oils in crude leaf extracts. Gas chromatography-mass spectrometry identified 119 bioactive chemical compounds in the methanolic leaf extract of which 14 compounds had a peak area greater than 1%. In addition, methanolic extract was subjected to antibacterial screening using the well diffusion method. *Heteropyxis natalensis* exhibited antibacterial efficacy against 5 strains of pathogenic bacteria*: Escherichia coli*, *Staphylococcus aureus*, methicillin-resistant *Staphylococcus aureus*, *Pseudomonas aeruginosa* and *Bacillus subtilis*. The results obtained in this study indicate the presence of naturally occurring bioactive compounds in *H. natalensis* leaves.

Keywords: bioactive compounds; GC-MS; herbal drug; phytochemical; methanolic extract

4.2. Introduction

The utilisation of plant material as a form of medicine is a 60 000-year-old tradition (Qazi and Molvi, 2016) that is still practiced worldwide to treat several health ailments (Meena et al., 2009; Mahomoodally, 2013). Traditional herbal medicine or ethnomedicine forms the backbone of health care in many developing countries plagued by poverty and limitations on modern medical treatment (Koduru et al., 2007; Meena et al., 2009). As a result, ethnomedicine is utilised daily as plant material is inexpensive, moreover, fewer side effects are exhibited (Gunjan et al., 2015; Akinyemi et al., 2018). Herbal medicine is embedded in the socio-cultural lifestyle of third-world African countries (Koduru et al., 2007). Indigenous knowledge on herbal medicine has been formulated through trial and error for hundreds of years and passed on through generations via verbal communication (Gurib-Fakim, 2006; Mahomoodally, 2013).

South Africans rely on herbal medicine as opposed to Western medical treatment since it is affordable, effective and easily accessible (Xego et al., 2016; Akinyemi et al., 2018). Therefore, the South African medicinal plant industry continuously thrives as it is supported by 27 million local consumers (Petersen et al., 2017). However, the indigenous biodiversity of medicinal flora faces several threats such as population increase, overharvesting and land degradation (Street and Prinsloo, 2012) resulting in an increased demand for medicinal plant material (Sen and Samanta, 2014; Xego et al., 2016; Akinyemi et al., 2018). Therefore, medicinal plants are phytochemically screened to determine the bioactive chemical compounds responsible for their therapeutic potential (Savithramma et al., 2011) in order to establish preservation management strategies as well as to prevent the overexploitation of important medicinal flora (Sen and Samanta, 2014; Akinyemi et al., 2018). Additionally, screening of medicinal plants is at the forefront of the medical field as the isolated compounds provide a promising future in novel drug development to treat several human diseases such as cancer, diabetes, cardiovascular disease and hepato-renal disease (Shakya, 2016).

Heteropyxis natalensis (Myrtaceae) is a South African medicinal tree that has been utilised by Venda and Zulu communities (Van Vuuren and Viljoen, 2008; Adesanwo et al., 2009) to treat respiratory ailments, nosebleeds, toothaches, bleeding gums and menorrhagia (Van Vuuren and Viljoen, 2008; Henley-Smith et al., 2018). Van Vuuren et al (2007) reported that the plant is also used as a decongestant and antimicrobial agent. The essential oils of *H. natalensis* have been reported to contain eucalyptol and limonene which are responsible for the species' medicinal characteristics (Gundidza et al., 1993; Van Vuuren et al., 2007). These compounds are used in

fragrances, flavours, detergents, cosmeceuticals and pharmaceuticals (Pesonen et al., 2014; Bhowal and Gopal, 2015).

The chemical composition and antimicrobial activity of the essential oils of *H. natalensis* have been explored in previous studies (Gundidza et al., 1993; Van Vuuren et al., 2007) but phytochemical and antibacterial investigations of crude leaf extracts have not been determined. Therefore, this study aimed to elucidate the secondary metabolites in crude leaf extracts and investigate the chemical profile and antibacterial efficacy of crude methanolic leaf extract of *H. natalensis*.

4.3. Materials and Methods

4.3.1. Preparation of Crude Leaf Extract

Fresh leaves of *H. natalensis* were collected from the University of KwaZulu-Natal, Westville Campus (29°49'01.0"S 30°56'51.2"E) and were air dried at 24°C for 6 weeks. Dried leaves were ground into a fine powder using a domestic spice mill (Kenwood Ltd, United Kingdom) and crude extracts were prepared by continuous extraction using a soxhlet apparatus.

Approximately 10 g of powdered material was added to 100 mL of hexane (organic solvent) in a round bottom flask. The powder and solvent mixture was boiled for three sessions (3 h each) and filtered after each session using Whatman No. 1 filter paper. This process was repeated using chloroform and methanol solvents. The resulting filtrates were stored in mason jars at room temperature (24°C) and used for phytochemical analyses.

4.3.2. Phytochemical Analyses

Preliminary phytochemical tests were conducted on each crude extract with a few modifications to determine the presence of the following secondary metabolites:

4.3.2.1. Carbohydrates

Two drops of Molisch reagent (solution of alcoholic α-naphthol) was added to 2 mL of extract and mixed. Concentrated sulphuric acid (H_2SO_4) (2 mL) was carefully added to the solution. The presence of red – violet rings in the middle of the solution indicated the presence of carbohydrates (Vimalkumar et al., 2014).

4.3.2.2. Alkaloids

Wagner's reagent (1 mL) was added to 2 mL of extract. The formation of a red – brown precipitate indicated the presence of alkaloids (Vimalkumar et al., 2014).

4.3.2.3. Phenolics

Two drops of 5% ferric chloride was added to 2 mL of extract. Dark green – black precipitate indicated a positive test for phenolic compounds (Mishra et al., 2014).

4.3.2.4. Saponins

Two mL of extract was diluted with 5 mL of distilled water ($_dH_2O$) and shaken vigorously by hand for 10 min. The persistence of a foam layer for 10 min above the mixture indicated the presence of saponins (Dhanesekaran et al., 2014).

4.3.2.5. Sterols

Chloroform (2 mL) and 2 mL of concentrated H_2SO_4 was added to 2 mL of extract and shaken carefully for 2 min. Sterols were present if the chloroform layer was red and the acid layer was fluorescent green (Sheel et al., 2014).

4.3.2.6. Terpenes

Chloroform (2 mL) was added to 5 mL of extract. Concentrated H_2SO_4 (3 mL) was carefully added down the side of the test tube. Red – brown rings indicated a positive test for terpenes (Ismail et al., 2016).

4.3.2.7. Fixed Fats and Oils

A drop of extract was placed on Whatman No. 1 filter paper and the appearance of an oily residue tested positive for fixed fats and oils in the extract (Mishra et al., 2014).

4.3.3. Gas Chromatography-Mass Spectrometry (GC-MS)

Powdered leaf material (± 2.5 g) was added to 50 mL of methanol in a round bottom flask. The powder and solvent mixture was boiled for 2 h followed by a 1 h session. Thereafter, the filtrates were filtered using Whatman No. 1 filter paper and stored in a mason jar at 24°C.

The filtrate was analysed using GC-MS (QP-2010 Ultra Shimadzu, Japan) with an Rx-5SilMS fused silica capillary column of length 30 m (0.25 µm internal diameter and 0.1 µm film thickness). Helium was used as the carrier gas with a flow rate of 0.96 $mL.min^{-1}$ and a total flow of 4.9 $mL.min^{-1}$, along with a linear velocity of 36.7 $cm.s^{-1}$ at a purge flow of 3.0 $mL.min^{-1}$. The injection port temperature was set at 250°C. The oven was set to an initial temperature of 50°C and was maintained at this temperature for 1 min. The temperature then increased to 310°C at a rate of $5°C.min^{-1}$ and was maintained at that temperature for a further 10 min. The MS was taken at 70 eV with a mass range of 50 to 800 $m.z^{-1}$. Chemical compounds present in the crude

methanolic extract of *H. natalensis* were identified using NIST Chemistry WebBook (2018) and expressed as percentages based on peak area.

4.3.4. Antibacterial Assay

Additional crude methanolic extract in section 4.3.3 was dried and preserved at 4°C for the antibacterial assay.

Preliminary screening of antibacterial activity of crude methanolic extract was determined using the agar well diffusion method described by Saif et al (2017) against two strains of gram-negative bacteria: *Escherichia coli* (ATCC 25218) and *Pseudomonas aeruginosa* (ATCC 27853) and three gram-positive bacterial strains: *Staphylococcus aureus* (ATCC 25923), methicillin-resistant *Staphylococcus aureus* (MRSA) (Clinical type) and *Bacillus subtilis*. Bacterial strains were grown for 18 h in Nutrient Broth (Biolab, South Africa) in a 37°C incubator on a shaker and were then standardised by adjusting the turbidity of the samples according to a 0.5 McFarland standard by suspending the bacteria in sterile $_dH_2O$.

The medium was prepared by mixing 38 g Mueller Hinton agar (MHA) in 1 L of $_dH_2O$. The medium was then boiled for 1 min and autoclaved at 121°C for 20 min. After reaching room temperature (24°C), the medium was carefully poured into sterile petri dishes and left to solidify under a sterile environment. Each bacterial strain was evenly swabbed onto MHA plates and left to dry. Thereafter, wells were aseptically punched using a sterile cork borer (5 mm in diameter). One gram of dried methanolic extract was resuspended in 1 mL of methanol and 90 µl of the stock solution (1 $mg.mL^{-1}$) was pipetted into each well. Petri dishes were then transferred to incubators of various temperatures to allow the extract to diffuse through the MHA and inhibition zones were observed after 18 h.

4.4. Results and Discussion

Qualitative phytochemical screening of *H. natalensis* leaves revealed the presence of several classes of secondary metabolites in hexane, chloroform and methanol extracts (Table 4.1). These compounds provide protection against plant damage and disease, deter herbivorous insects as well as withstand harsh environmental conditions (Saxena et al., 2013; Ahmed et al., 2017). In addition to plant defense, the phytochemicals presented in Table 4.1 play an important role in combatting many human ailments (Wink, 2015; Pakkirisamy et al., 2017). It has been reported that the medicinal potential of a plant is directly proportional to the occurrence of biologically active chemical compounds within the species (Saxena et al., 2013; Pakkirisamy et al., 2017).

Alkaloids, terpenes and phenolics exhibit several pharmacological activities such as anticancer, anti-inflammatory, antiulcer and antibacterial activities (Saxena et al., 2013; Shakya, 2016; Aziz and Banerjee, 2018). Medicinal plants containing saponins and sterols display anticancer and antimicrobial properties (Shakya, 2016; Kumar et al., 2018). These compounds were also present in the leaf extracts of other myrtaceous species such as *Syzygium cumini* and *Eugenia uniflora* (Fathima and Pandian, 2015; Aziz and Banerjee, 2018; Kumar et al., 2018). In addition to the medicinal properties, these compounds are also responsible for flavour, colour and aroma in food, perfumes and cosmetics (Saxena et al., 2013).

Table 4.1: Qualitative phytochemical screening of crude leaf extracts of *H. natalensis*

Phytochemical Compounds	Hexane	Chloroform	Methanol
Carbohydrates	+	+	+
Alkaloids	+	++	+
Phenolics	-	-	++
Saponins	+	+	-
Sterols	+	+	+
Terpenes	+	+	+
Fixed Fats and Oils	+	+	+

- = Absent, + = Present, ++ = Intense reaction

The chemical compounds in the methanolic extract of *H. natalensis* were identified by GC-MS analysis and represented in Figure 4.1. The extract revealed the presence of 119 bioactive compounds (Appendix A: Table A 1). However, among the 119 compounds, 14 of them are reported in Table 4.2 as their peak area was greater than 1%. Compounds with a peak area less

than 1% were considered as low-level compounds (Pakkirisamy et al., 2017). The main chemical compounds present in *H. natalensis* were squalene (13.57%) and 1,2,3-benzenetriol (22.53%) which were also identified in the following myrtaceous species: *Syzygium jambos* (Sharma et al., 2013) and *Eugenia flocossa* (Kala et al., 2012), respectively. These naturally occurring bioactive compounds in these plants are primarily responsible for their medicinal properties.

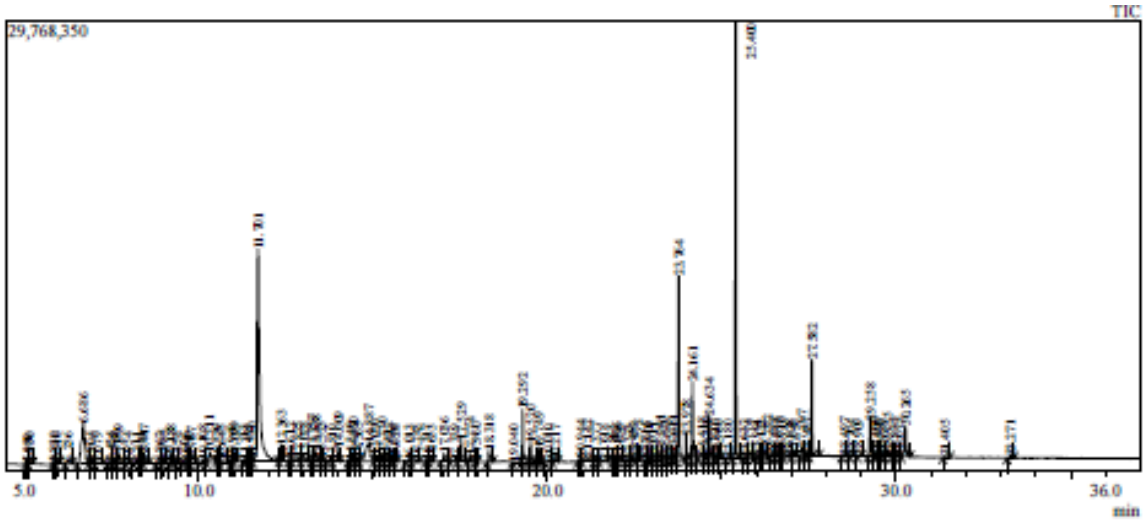

Figure 4.1: GC-MS chromatogram of methanolic extract of *H. natalensis* leaves

The synthesis of squalene occurs in plants and animals and is also a precursor for sterol synthesis (Lozano-Grande et al., 2018). Squalene is an independent oxygen carrier that carries oxygen to various cell membranes in the body experiencing limited levels of oxygen (Gűneş, 2013). The pharmacological properties of squalene include antitumor and antioxidant activity (Gűneş, 2013; Lozano-Grande et al., 2018) which was highlighted in Table 4.3.

The leaf paste of *E. flocossa* is used to treat rheumatic pain (Kala et al., 2012). The anti-inflammatory properties of *E. floccosa* leaf extract could be attributed to 1,2,3-benzenetriol (26.72%), the main constituent compound. However, according to Table 4.3 and Kala et al (2012), 1,2,3-benzenetriol does not exhibit the aforementioned pharmacological property. This indicates that a variety of chemical compounds within the plant may work additively or synergistically to bring about a greater effect than an individual compound which may catalyse the healing process (Mahomoodally, 2013). Therefore, the compounds present in *H. natalensis* are working as a cohesive system to treat ailments such as respiratory disorders, menorrhagia and gingivitis (Van Vuuren and Viljoen, 2008; Henley-Smith et al., 2018).

Table 4.2: Phytochemical compounds with a peak area % > 1 in the methanolic extract of *H. natalensis* detected by GC-MS

No.	Compound	CAS	RT (min)	Area %	Mol Formula	Mol Weight
6	Eucalyptol	470-82-6	6.686	5.41	$C_{10}H_{18}O$	154
24	Hydroquinone	123-31-9	10.311	1.17	$C_6H_6O_2$	110
32	1,2,3-Benzenetriol	87-66-1	11.701	22.53	$C_6H_6O_3$	126
38	2-Isopropenyl-4a,8-dimethyl-1,2,3,4,4a,5,6,7-octahydronaphthalene	0-00-0	13.338	1.06	$C_{15}H_{24}$	204
45	1α,2β,3α,5β -Cyclohexanetetrol	53585-08-3	14.887	3.92	$C_6H_{12}O_4$	148
62	9-Octadecen-1-ol, (Z)-	143-28-2	19.292	1.93	$C_{18}H_{36}O$	268
84	(S)-5,7-dihydroxy-6,8-dimethyl flavanone	56297-79-1	23.764	7.81	$C_{17}H_{16}O_4$	284
85	2,2,4-Trimethyl-6-(1-oxo-3-phenylprop-2-enyl)-cyclohexane-1,3,5-trione	0-00-0	23.978	1.25	$C_{18}H_{18}O_4$	298
86	5,7-Dimethoxyflavanone	1036-72-2	24.161	3.82	$C_{17}H_{16}O_4$	284
89	Benzaldehyde, (diphenylmethylene) hydrazine	13118-38-2	24.634	2.21	$C_{20}H_{16}N_2$	284
93	Squalene	111-02-4	25.400	13.57	$C_{30}H_{50}$	410
106	Vitamin E	59-02-9	27.582	3.67	$C_{29}H_{50}O_2$	430
110	β-Sitosterol	83-46-5	29.258	2.17	$C_{29}H_{50}O$	414
117	α-Amyrin	638-95-9	30.265	2.21	$C_{30}H_{50}O$	426

CAS = Unique numerical identified assigned by the Chemical Abstracts Service, RT = Retention time

Table 4.3: Pharmacological properties associated with the chemical compounds with a peak area % > 1 in the methanolic extract of *H. natalensis*

No.	Compound	Properties
6	Eucalyptol	Anti-inflammatory, antioxidant, antiseptic, antimicrobial (Juergens, 2014)
24	Hydroquinone	Anti-oxidant, neuroprotective, immunomodulatory, anti-inflammatory (Byeon et al., 2018)
32	1,2,3-Benzenetriol	Antioxidant, antiseptic, antibacterial, antidermatitic (Kala et al., 2012)
38	2-Isopropenyl-4a,8-dimethyl-1,2,3,4,4a,5,6,7-octahydronaphthalene	Antifungal (Wang et al., 2011)
45	1α,2β,3α,5β-Cyclohexanetetrol	Antioxidant, antimicrobial, anti-inflammatory (Ravikumar et al., 2012)
62	9-Octadecen-1-ol, (Z)-	No activity reported (Karthikeyan et al., 2016)
84	(S)-5,7-dihydroxy-6,8-dimethyl flavanone	Antimalarial (Bero et al., 2009)
85	2,2,4-Trimethyl-6-(1-oxo-3-phenylprop-2-enyl)-cyclohexane-1,3,5-trione	Antimicrobial (Bonilla et al., 2005)
86	5,7-Dimethoxyflavanone	Anti-inflammatory (Panthong et al., 1989)
89	Benzaldehyde, (diphenylmethylene) hydrazine	Anti-bacterial, antifungal, antitumor (Arulkumaran et al., 2017)
93	Squalene	Antibacterial, antioxidant, immunostimulant, antitumor (Karthikeyan et al., 2016)
106	Vitamin E	Antioxidant, anticancer, anti-inflammatory (Rizvi et al., 2014)
110	β-Sitosterol	Antimicrobial, antidiabetic, anti-inflammatory, anticancer (Bin Sayeed et al., 2016)
117	α-Amyrin	Anti-inflammatory (Okoye et al., 2014)

The antibacterial efficacy of *H. natalensis* against 5 bacterial strains is summarised in Table 4.4. The methanolic extract exhibited varying degrees of inhibition against *E. coli*, *P. aeruginosa*, *S. aureus*, MRSA and *B. subtilis*. The highest degree of inhibition was exhibited against MRSA. This strain is known to cause pneumonia, meningitis, urinary tract infections and nosocomial contamination (Heyman et al., 2009).

The smallest zone of inhibition was exhibited against *B. subtilis*. This suggests that the strain was less sensitive compared to the other microorganisms used in this study. Liliwirianis et al (2011) highlighted that a small inhibition zone is attributed to their ability to form endospores (resting stage), thus allowing them to remain viable and more resistant over time.

According to the results presented in Table 4.4, the leaves of *H. natalensis* can be used as effective antibacterial agents in the treatment of gastrointestinal, skin, respiratory and nosocomial ailments as the phytochemicals present in the leaves (Table 4.1 and 4.2) exhibit various pharmacological properties (Table 4.3). These results confirm previous findings by Gowri and Vasantha (2010) wherein the methanolic extract of the leaves of *S. cumini* were investigated.

Table 4.4: Preliminary screening of antibacterial activity of methanolic extract of *H. natalensis*

Bacterial Strain	Zone of Inhibition (mm)[a]
E. coli	9
S. aureus	8
P. aeruginosa	8
MRSA	11
B. subtilis	7

[a] = inhibition zone including the cork borer (5 mm) diameter

4.5. Conclusion

The results obtained in this study provides substantial information for the utilisation of the leaves of *H. natalensis* as traditional medicine. Several phytochemical classes and compounds were elucidated along with their pharmacological activity. In addition, preliminary antibacterial screening of the methanolic extract against various strains of bacteria suggests the leaves of *H. natalensis* possess bioactive compounds that could be used as antibacterial agents. The results presented in this study could potentially benefit future research regarding the development of herbal drugs.

CHAPTER 5: SYNTHESIS, CHARACTERISATION AND ANTIBACTERIAL ACTIVITY OF SILVER NANOPARTICLES OF *Heteropyxis natalensis*

5.1. Abstract

The biosynthesis of metallic nanoparticles utilising plant material is favoured in many medical applications such as gene therapy, cancer treatment and drug delivery, due to its cost effective and environmentally friendly nature. Silver is considered an ideal metal for nanoparticle synthesis due to its profound antimicrobial properties. Additionally, silver nanoparticles (AgNPs) are sought after by many industries including medical, pharmaceutical, textile and food industries. The aim of this study was to synthesise and characterise AgNPs from methanolic leaf extract of *H. natalensis*, a native South African medicinal tree. The synthesised particles were characterised by ultraviolet visible spectroscopy (UV-vis), energy dispersive X-ray spectroscopy (EDX), high resolution transmission electron microscopy (HRTEM) and fourier transform infrared spectroscopy (FTIR). A colour change of the reaction solution from yellow to brown preliminarily confirmed the presence of AgNPs and UV-vis spectroscopy observed a single absorbance peak at 422 nm which was indicative of AgNPs. EDX revealed the presence of elemental silver in the sample and HRTEM identified spherical AgNPs ranging from 5 – 60 nm. FTIR identified hydroxyls, alkynes, alkenes, alkanes, esters and alkyl halides as possible capping agents of silver ions (Ag^{+}) into AgNPs. In addition, AgNPs exhibited antibacterial efficacy against 5 strains of pathogenic bacteria*: Escherichia coli*, *Staphylococcus aureus*, methicillin-resistant *Staphylococcus aureus*, *Pseudomonas aeruginosa* and *Bacillus subtilis*. Lastly, the results obtained in this study could potentially benefit future research in nanomedical-driven fields.

Keywords: AgNPs; synthesis; nanoparticles; antibacterial efficacy; characterisation

5.2. Introduction

Nanotechnology is a research field that is currently evolving (Hasan, 2015) at an exponential rate with the aim of revolutionising the medical world (Saidi, 2018). This field of study involves the synthesis, development and manipulation of nanomaterials ranging from 0 – 100 nm (Mondal et al., 2011; Mohammed, 2015). Over the years, nanotechnology has been introduced into various medical applications such as gene therapy, cancer treatment and drug delivery (Mondal et al., 2011; Jyoti et al., 2016). Metals such as copper, zinc, gold, titanium and silver are used to produce nanoparticles (Hasan, 2015; Parveen et al., 2016). The synthesis of metal nanoparticles has gained significant importance due to their inimitable optical, electronic, magnetic, chemical and antimicrobial characteristics (Anandalakshmi et al., 2016). Therefore, metallic nanoparticles present advantageous opportunities in different industries including the medical, pharmaceutical, and textile industries (Parveen et al., 2016).

Silver is considered an ideal metal for the synthesis of nanoparticles (Zargar et al., 2011). Additionally, silver nanoparticles (AgNPs) are at the forefront of nanotechnology and are sought after for several applications based on their unique structural properties (Zargar et al., 2011; Mishra and Pani, 2017). AgNPs have been successfully exploited in the following industries: pathology, medicine, textile, food and pharmaceutical industries (Mishra and Chauhan, 2015; Bose and Chatterjee, 2016). The synthesis of nanoparticles can occur via chemical, physical, biological and hybrid methods (Jyoti et al., 2016). However, chemical and physical methods are considered toxic and non-ecofriendly (Mishra and Pani, 2017). Scientists are currently relying on safer alternatives such as "green synthesis" which is defined as the synthesis of AgNPs using non-toxic, environmentally friendly biological material (Dubey et al., 2009; Zargar et al., 2011; Mishra and Pani, 2017). This approach brings nanotechnology and plant biotechnology together resulting in a risk-free and better-quality system that is suitable for biomedical applications (Mohammed, 2015; Parveen et al., 2016).

Plants have previously been used to synthesise AgNPs as it is inexpensive, efficient, safer and environmentally friendly (Paosen et al., 2017). The phytochemicals present in plant extracts serve as perfect reducing and capping agents during synthesis (Bose and Chatterjee, 2016). Medicinal plants are known for their antimicrobial properties against bacteria, fungi and viruses (Paosen et al., 2017) Antimicrobial research has focused on AgNPs due to their antimicrobial potential and were reported to be efficient antibacterial agents (Zargar et al., 2011; Hasan, 2015).

Heteropyxis natalensis (Myrtaceae) is a small, deciduous tree inhabiting evergreen forests and bushveld regions ranging from KwaZulu-Natal to Limpopo province (Van Vuuren et al., 2007; Adesanwo et al., 2009). The leaves, bark and roots of *H. natalensis* have previously been reported to exhibit medicinal properties. Venda and Zulu communities utilise *H. natalensis* to treat several ailments such as respiratory disorders, nosebleeds and gingivitis (Van Vuuren and Viljoen, 2008; Adesanwo et al., 2009; Henley-Smith et al., 2018). To the author's knowledge, there are no reports available on silver nanosynthesis on this species. Therefore, this study aimed to examine the synthesis, characterisation and antibacterial efficacy of AgNPs from crude methanolic leaf extract of *H. natalensis*.

5.3. Materials and Methods

5.3.1. Preparation of Crude Leaf Extract

Fresh leaves of *H. natalensis* were collected from the University of KwaZulu-Natal, Westville Campus (29°49'01.0"S 30°56'51.2"E) and were air dried at 24°C for 6 weeks. Dried leaves were ground into a fine powder using a domestic spice mill (Kenwood Ltd, UK) and the crude extract was prepared by continuous extraction using a soxhlet apparatus.

Powdered leaf material (± 2.5 g) was added to 50 mL of methanol in a round bottom flask. The powder and solvent mixture was boiled for 2 h followed by a 1 h session. Thereafter, the filtrates were filtered using Whatman No. 1 filter paper and stored in a mason jar at room temperature (24°C).

5.3.2. Silver Nanosynthesis

The biosynthesis of AgNPs was conducted according to a method described by Sudha et al (2017) with a few modifications. Methanolic extract (1 mL) was added to 19 mL of a 1 mM aqueous silver nitrate ($AgNO_3$) solution. The $AgNO_3$ and methanolic extract solution was mixed in a conical flask and incubated in a water bath at 60°C for 30 min. A colour change from yellow to brown indicated the formation of AgNPs.

Thereafter, the solution was centrifuged using an Eppendorf Centrifuge 5415R (Merck, SA) at 16 000 rpm for 5 min. After removing the supernatant, deionised water ($_{di}H_2O$) was added to the Eppendorf tube and centrifuged. The centrifugation process was repeated thrice. The resultant pellet was then suspended in 10 ml of $_{di}H_2O$, vortexed and further used for characterisation.

5.3.3. Characterisation

5.3.3.1. Ultraviolet Visible Spectroscopy (UV-vis)

The presence of AgNPs was confirmed by UV-vis spectroscopy. The absorbance spectrum was recorded using a UV-1800 Shimadzu Spectrophotometer (Japan) at an absorbance wavelength of 300 – 600 nm.

5.3.3.2. Energy Dispersive X-Ray Spectroscopy (EDX)

A drop of synthesised AgNPs was placed directly onto an aluminium stub and was left to dry for 24 h. The stub was then sputter coated in a Polaron SC500 Sputtercoater. EDX microanalysis was conducted using an Ultra Plus Field Emission Gun Scanning Electron microscope (FEGSEM) (Carl Zeiss, Germany) and AzTec Analysis Software (Oxford Instruments, UK) to determine the presence of elemental silver in the sample.

5.3.3.3. High Resolution Transmission Electron Microscopy (HRTEM)

A drop of sonicated synthesised AgNPs were placed on copper grids and left to dry for 20 min. The overall micromorphology (shape and size) of AgNPs was observed using an HRTEM JEOL 2100 and particle size was determined using iTEM software (Soft Imaging System GmBH, Münster, Germany).

5.3.3.4. Fourier Transform Infrared Spectroscopy (FTIR)

FTIR was conducted on AgNPs using a Perkin Elmer Spectrum 100 Spectrophotometer (USA) at a wavelength of 4000 – 400 cm^{-1}.

5.3.4. Antibacterial Screening

Preliminary screening of antibacterial activity of AgNPs was determined using the agar well diffusion method described by Saif et al (2017) against two strains of gram-negative bacteria: *Escherichia coli* (ATCC 25218) and *Pseudomonas aeruginosa* (ATCC 27853) and three gram-positive bacterial strains: *Staphylococcus aureus* (ATCC 25923), methicillin-resistant *Staphylococcus aureus* (MRSA) (Clinical type) and *Bacillus subtilis*. Bacterial strains were grown for 18 h in Nutrient Broth (Biolab, South Africa) in a 37°C incubator on a shaker and were then standardised by adjusting the turbidity of the samples according to a 0.5 McFarland standard by suspending the bacteria in sterile distilled water ($_dH_2O$).

The medium was prepared by mixing 38 g Mueller Hinton agar (MHA) in 1 L of $_dH_2O$. The medium was then boiled for 1 min and autoclaved at 121°C for 20 min. After reaching room temperature (24°C), the medium was carefully poured into sterile petri dishes and left to solidify under a sterile environment. Each bacterial strain was evenly swabbed onto MHA plates and left to dry. Wells were aseptically punched using a sterile cork borer (5 mm in diameter). Thereafter,

90 µl of the AgNP stock solution (1 $mg.mL^{-1}$) was pipetted into each well. Petri dishes were then transferred to incubators of various temperatures to allow the solution to diffuse through the MHA and inhibition zones were observed after 18 h.

5.4. Results and Discussion

In the present study, the formation of AgNPs was observed based on a gradual colour change in the reaction vessel from yellow to dark brown over 30 min (Fig. 5.1). The biosynthesis of AgNPs is often confirmed by a colour change of the reaction solution (Dubey et al., 2010; Swamy et al., 2015) as a consequence of the surface plasmon resonance (SPR) (Rout et al., 2012; Vijayakumar et al., 2013) indicative of the reduction of silver ions (Ag^+). Sudha et al (2017) suggests that the reduction of Ag^+ may be attributed to the chemical components present in the leaf extract.

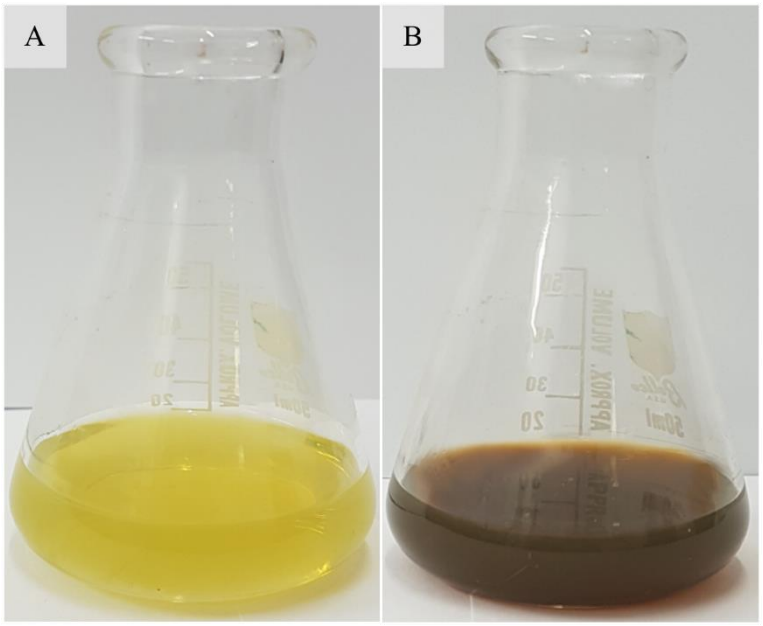

Figure 5.1: Silver nanoparticle synthesis from methanolic leaf extract of *H. natalensis*. A) Before incubation and synthesis of AgNPs. B) After incubation and synthesis of AgNPs

In addition, the synthesis of AgNPs was further confirmed by UV-vis spectroscopy to determine the progression of the reduction of Ag^+ (Shaik et al., 2018). In Figure 5.2, a single absorbance peak was observed at 422 nm which was indicative of SPR of AgNPs (Anandalakshmi et al., 2016). Absorbance peaks observed between a wavelength of 410 and 450 nm may possibly be attributed to the presence of spherical nanoparticles (Zaheer, 2012; Jyoti et al., 2016). Similar absorbance peaks were observed in a study conducted by Paosen et al (2017) on several myrtaceous species including *Xanthostemon chrysanthus* (424 nm) and *Callistemon lanceolatus* (420 nm).

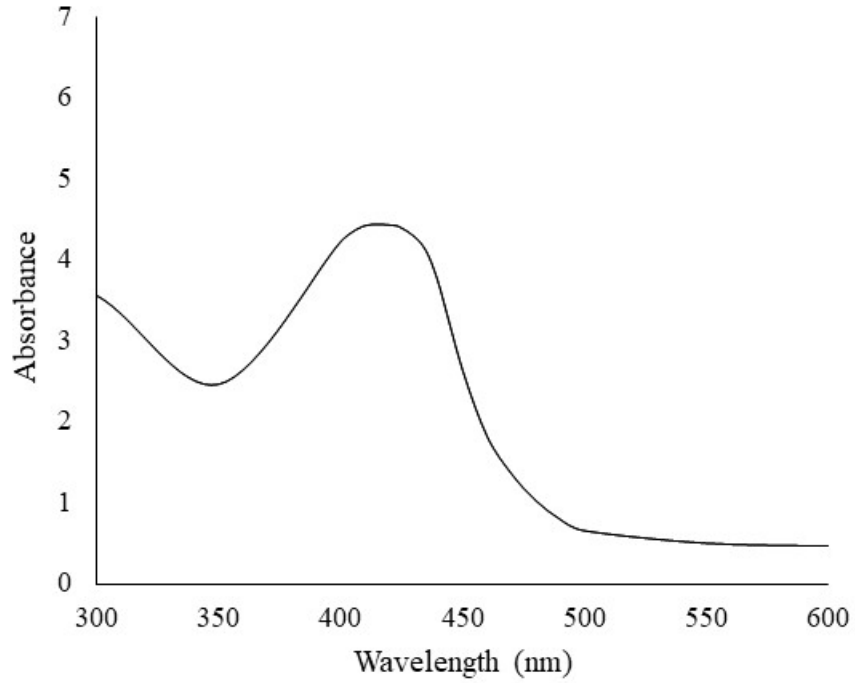

Figure 5.2: UV-vis spectra of synthesised AgNPs of *H. natalensis* methanolic leaf extract

The elemental composition of synthesised AgNPs was investigated by EDX. The EDX spectrum revealed a peak at 3 keV displaying elemental silver (60.5%) in Figure 5.3. Silver nanocrystals often have an optical absorption peak at 3 keV as a result of SPR (Jyoti et al., 2016). This indicates the reduction of Ag^{+} into elemental silver and authenticates the synthesis of AgNPs (Dubey et al., 2010; Jyoti et al., 2016). Additional elements were present in the 0 – 0.5 keV range which denotes the optical absorption of carbon (22.81%) and oxygen (16.03%) (Shaik et al., 2018), and a peak at 2.5 keV which signifies the absorption of chlorine (0.30%). The presence of these elements suggests that they have emanated from *H. natalensis* leaf extract and act as capping agents for AgNPs (Paosen et al., 2017; Sudha et al., 2017; Shaik et al., 2018). These results confirm previous findings by Pourmortazavi et al (2014) wherein the EDX spectrum revealed the presence of elemental silver and additional elements after synthesising AgNPs using *Eucalyptus oleosa* leaf extract.

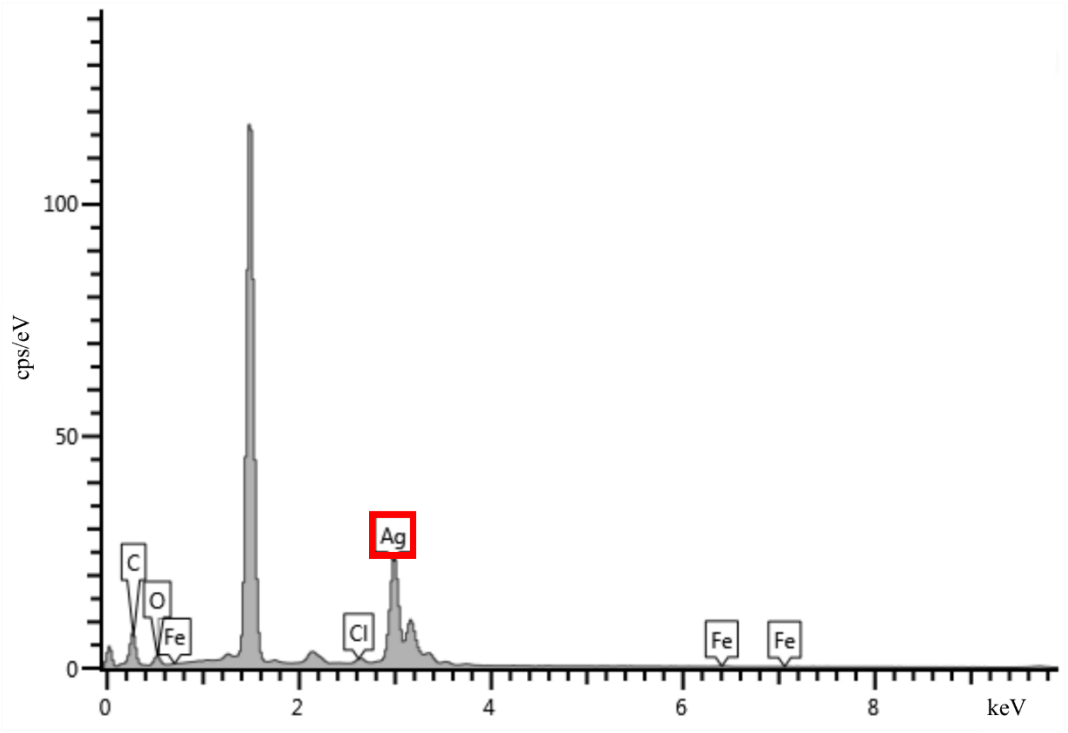

Figure 5.3: EDX analysis of synthesised AgNPs of *H. natalensis* methanolic leaf extract

The morphology and particle size distribution of synthesised AgNPs are shown in Figure 5.4 A and B, respectively. The structural morphology of synthesised particles appears to be spherical in nature with an average size of 23.38 nm in diameter. The morphology of nanoparticles primarily rely on the reducing efficacy of the reducing agents present in the leaf extract (Zaheer, 2012). The size of particles were between 5 – 60 nm. However, many particles were observed in the 10 – 20 nm range which justifies the single absorbance peak at 422 nm seen in Figure 5.2. AgNPs were well dispersed after sonication and displayed crystalline characteristics as shown by distinct lattice fringes (inset). According to the histogram in Figure 5.4 B, the AgNPs are not uniform in size; however, the particles are below 100 nm which are favourable in textile, food and medical fields (Mishra and Chauhan, 2015). The shape and size of AgNPs are similar to the particles synthesised in a study by Paosen et al (2017) on several myrtaceous species.

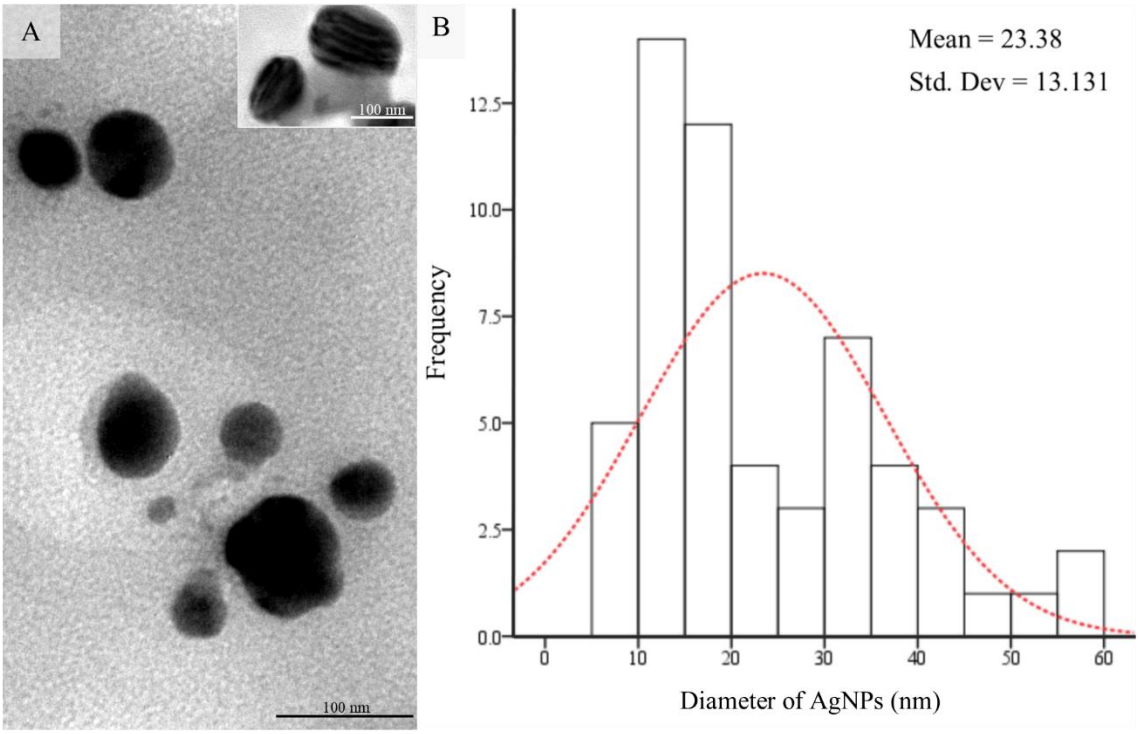

Figure 5.4: Particle size distribution of AgNPs of *H. natalensis*. A) Electron micrograph of synthesised spherical AgNPs and distinct lattice fringes (inset). B) Histogram representing the range of particles according to diameter size

The functional groups of AgNPs were detected using FTIR spectroscopy between a scan range of 4000 – 400 cm^{-1}. The functional groups that were identified in the sample are recorded in Table 5.1 according to the absorption bands (peaks) in the FTIR spectrum in Figure 5.5. Hydroxyls, alkynes, alkenes, alkanes, esters and alkyl halides were identified in the sample. The presence of these functional groups indicate that they belong to secondary metabolites such as alkaloids, terpenes and phenolics (Paosen et al., 2017) present in the leaf extract of *H. natalensis*. In addition, these functional groups are responsible for the reduction, stabilisation and capping of Ag^{+} into AgNPs (Jyoti et al., 2016; Sekhar et al., 2018).

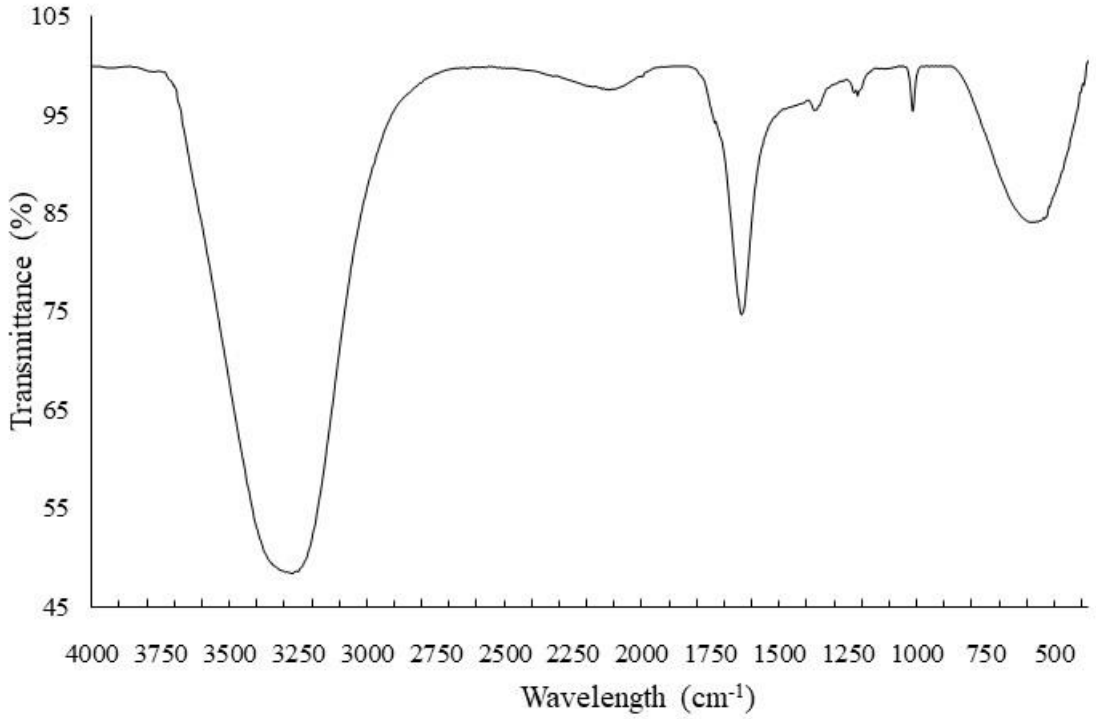

Figure 5.5: FTIR spectra of synthesised AgNPs of *H. natalensis*

Hydroxyl, alkene, alkane and ester functional groups were also identified in synthesised AgNPs of *Syzygium campanulatum* and *Eucalyptus citriodora* (Paosen et al., 2017). A broad hydroxyl peak (3270.82 cm^{-1}) was detected in the FTIR spectrum of *Eucalyptus corymbia* (Sila et al., 2014) which was similar to the peak identified in the current study (3268.08 cm^{-1}). Sila et al (2014) suggested that this functional group is mainly involved in the synthesis of AgNPs in comparison to other functional groups in the sample.

Table 5.1: FTIR peak values, functional groups and vibrations of AgNPs of *H. natalensis*

Absorption Peak (cm^{-1})	Functional Group	Type of Vibration
3268.08	O – H	Stretch
2118.83	C ≡ C	Stretch
1638.42	C = C	Stretch
1374.95	C – H	Bending
1217.16	C – O	Stretch
1016.61	C – O	Stretch
575.93	C – Br	Stretch

The antibacterial activity of synthesised AgNPs of *H. natalensis* is summarised in Table 5.2. The zones of inhibition varied against *E.coli*, *P. aeruginosa*, *S. aureus*, MRSA and *B. subtilis.*

Antibacterial activity against *P. aeruginosa* exhibited the highest zone of inhibition. *Pseudomonas aeruginosa* is an opportunistic bacterial strain (Singh et al., 2014) and often causes infections in immunocompromised postoperative patients suffering with cancer, burn wounds and cystic fibrosis (Salomoni et al., 2017). This bacterium also causes pneumonia, bacteremia and gastrointestinal infections (Salomoni et al., 2017).

The smallest zone of inhibition was exhibited against *B. subtilis* indicating that this strain was less sensitive to the AgNPs compared to other strains used in this study. According to Liliwirianis et al (2011), a small inhibition zone signifies the ability of the bacteria to form endospores (resting stage). This enables the bacteria to remain viable and more resistant over time.

Elemental silver has been used for centuries due to its reputable antimicrobial properties (Dipankar and Murugan, 2012; Ahmed et al., 2016). Therefore, synthesised AgNPs have been utilised in medicine, food storage, pharmaceuticals and several environmental sectors (Ahmed et al., 2016). The antibacterial effect is possibly attributed to the size of AgNPs (Jyoti et al., 2016). As seen in Figure 5.4 B, the synthesised AgNPs are relatively small in size however, these particles have a large surface area (Dipankar and Murugan, 2012; Jyoti et al., 2016) that allows AgNPs to have better contact and interaction with the bacterium (Jyoti et al., 2016). As a result, AgNPs attach to the surface of the bacterial membrane resulting in structural changes which eventually leads to cell death (Yugandhar and Savithramma, 2015; Paosen et al., 2017).

The results presented in Table 5.2 suggest that the synthesized AgNPs of *H. natalensis* can be used as effective antibacterial agents in the treatment of several ailments including gastrointestinal, skin, respiratory and nosocomial ailments. These results confirm previous findings by Sila et al (2014) and Yugandhur and Savithramma (2015) wherein myrtaceous AgNPs exhibited antibacterial activity against similar bacterial strains.

Table 5.2: Preliminary screening of antibacterial activity of AgNPs of *H. natalensis*

Bacterial Strain	Zone of Inhibition (mm)[a]
E. coli	8
S. aureus	8
P. aeruginosa	12
MRSA	8
B. subtilis	7

[a] = inhibition zone including the cork borer (5 mm) diameter

5.5. Conclusion

In the current investigation, an effective "green approach" for the synthesis of AgNPs using methanolic leaf extract of *H. natalensis* was demonstrated. A colour change of the reaction solution from yellow to brown as a result of SPR indicated the reduction of Ag^{+} and the formation of AgNPs. Synthesised particles were below 100 nm and spherical in shape. Additionally, preliminary screening of AgNPs against various strains of bacteria highlighted the efficiency of these particles as antibacterial agents. Lastly, the results obtained in this study could potentially add beneficial information to future research in nanomedical-driven fields that utilise medicinal flora.

CHAPTER 6: CONCLUSIONS AND RECOMMENDATIONS FOR FURTHER RESEARCH

6.1. Major Findings

Micromorphological investigations on *Heteropyxis natalensis* have not been reported in literature. Therefore, **Chapter 3** identified non-glandular trichomes, secretory cavities and druse crystals on the leaves of *H. natalensis*. Histochemical tests detected alkaloids, phenolics, lipids, proteins, essential oils, resin acids and trace amounts of unesterified pectins and polysaccharides. These secondary metabolites are involved in pollinator attraction, defense against herbivory and plant aroma. The results obtained in this chapter could assist future anatomical studies regarding the genus as well as understanding the taxonomic position of *H. natalensis* in Myrtaceae.

Scientific literature on the essential oil composition of *H. natalensis* has been rigorously investigated in previous studies. Therefore, **Chapter 4** confirmed the presence of carbohydrates, alkaloids, phenolics, saponins, sterols, terpenes and fixed fats and oils in crude leaf extracts. A total of 119 bioactive compounds were detected in the crude methanolic leaf extract which are responsible for the plant's medicinal potential. Additionally, *H. natalensis* methanolic leaf extract exhibited antibacterial activity against five pathogenic strains of bacteria. This indicates that *H. natalensis* could be exploited for future research regarding the development of herbal drugs due to the presence of bioactive compounds.

Chapter 5 introduced a "green approach" for the synthesis of silver nanoparticles (AgNPs) from methanolic leaf extract of *H. natalensis* and silver nitrate ($AgNO_3$). The reaction solution underwent a gradual colour change from yellow to brown indicating the reduction of silver ions (Ag^+) and the formation of AgNPs. Further characterisation identified spherical particles below 100 nm in size, as well as the functional groups responsible for the capping of Ag^+. Lastly, *H. natalensis* exhibited antibacterial activity against five pathogenic strains of bacteria suggesting that synthesised AgNPs could possibly benefit nanomedical-driven fields.

6.2. Aim and Objectives

The overall aim of this research project was to identify the micromorphology of *H. natalensis* using several microscopy techniques, and preliminarily investigate the medicinal potential using various phytochemical analyses, AgNP characterisation protocols and antibacterial assays.

6.3. Challenges

A major challenge in this study was optimising standard operating protocols for electron microscopy that would be suitable for *H. natalensis* leaves.

6.4. Future Perspectives

Based on the current study, there are numerous possibilities for future research.

a) With regards to microscopy, secretory cavity development can be investigated which will provide updated systematic evidence for the taxonomic position of *H. natalensis*.

b) Antibacterial activity of crude leaf extracts and AgNPs can be further studied by investigating their minimum inhibitory concentrations.

c) A comparative study among leaves, bark and roots of *H. natalensis* can be conducted to compare the micromorphology of foliar structures and the chemical composition of bioactive compounds among the plant organs.

d) Phytochemical analyses can be elaborated on by isolating individual compounds and investigating their antimicrobial potential.

e) A variety of $AgNO_3$ and plant extract ratios could be investigated to determine whether different ratios would produce a higher yield of smaller AgNPs and test them against several bacterial strains.

6.5. Final Comments and Summary Conclusions

The current study provided information on the micromorphology, ultrastructure, chemical composition, synthesis of AgNPs and antibacterial activity of *H. natalensis*. According to the

results obtained in this study, the phytochemical compounds present in the leaves justify the traditional use of this species. In conclusion, the leaves of *H. natalensis* have beneficial medicinal potential as a precursor in drug development.

REFERENCES

Abdillahi, H.S., Van Staden, J., 2012. South African plants and male reproductive healthcare: conception and contraception. Journal of Ethnopharmacology 143, 475 – 480.

Adesanwo, J.K., Shode, F.O., Aiyelaagbe, O., Oyede, R.T., Baijnath, H., 2009. Isolation and characterization of a new chalcone from the leaves of *Heteropyxis natalensis*. International Journal of Medicine and Medical Sciences 1, 23 – 32.

Ahmed, E., Arshad, M., Khan, M.Z., 2017. Secondary metabolites and their multidimensional prospective in plant life. Journal of Pharmacognosy and Phytochemistry 6, 205 – 214.

Ahmed, S., Ahmad, M., Swami, B.L., Ikram, S., 2016. Green synthesis of silver nanoparticles using *Azadirachta indica* aqueous leaf extract. Journal of Radiation Research and Applied Sciences 9, 1 – 7.

Akinyemi, O., Oyewole, S.O., Jimoh, K.A., 2018. Medicinal plants and sustainable human health: A review. Horticulture International Journal 2, 194 – 195.

Akthar, M.S., Degaga, B., Azam, T., 2014. Antimicrobial activity of essential oils extracted from medicinal plants against the pathogenic microorganisms: a review. Biological Sciences and Pharmaceutical Research 2, 1 – 7.

Al-Edany, T.Y., Al-Saadi, S.A.M., 2012. Taxonomic significance of anatomical characters in some species of the family Myrtaceae. American Journal of Plant Sciences 3, 572 – 581.

Amanzadeh, Y., Ashrafi, M., Mohammadi, F., 2006. New elaborated technique for isolation and purification of limonene from orange oil. Iranian Journal of Pharmaceutical Sciences 2, 87 – 90.

Anandalakshmi, K., Venugobal, J., Ramasamy, V., 2016. Characterization of silver nanoparticles by green synthesis method using *Pedalium murex* leaf extract and their antibacterial activity. Applied Nanoscience 6, 399 – 408.

Arbellay, E., Stoffel, M., Sutherland, E.K., Smith, K.T., Falk, D.A., 2014. Resin duct size and density as ecophysiological traits in fire scars of *Pseudotsuga menziesii* and *Larix occidentalis*. Annals of Botany 114, 973 – 980.

Arulkumaran, R., Manikandan, V., Christuraj, P., Thirunarayanan, G., 2017. Synthesis and spectral correlation studies of some substituted (E)-1-Benzylidene-2-(diphenylmethylene) hydrazines. World Scientific News 62, 93 – 110.

Ascensão, L., Pais, M.S., 1998. The leaf capitate trichomes of *Leonotis leonurus*: histochemistry, ultrastructure and secretion. Annals of Botany 81, 263 – 271.

Aziz, A., Banerjee, S., 2018. Phytochemical Screening and Antibacterial Activity study of *Syzygium cumini* (Myrtaceae) Seed Extracts. PharmaTutor 6, 70 – 73.

Bakkali, F., Averbeck, S., Averbeck, D., Idaomar, M., 2008. Biological effects of essential oils–a review. Food and Chemical Toxicology 46, 446 – 475.

Barbosa, L.C.A., Silva, C.J., Teixeira, R.R., Meira, R.M.S.A., Pinheiro, A.L., 2013. Chemistry and biological activities of essential oils from *Melaleuca* L. species. Agriculturae Conspectus Scientificus 78, 11 – 23.

Barthet, M.M., Hilu, K.W., 2007. Expression of *matK*: functional and evolutionary implications. American Journal of Botany 94, 1402 – 1412.

Bennici, A., Tani, C., 2004. Anatomical and ultrastructural study of the secretory cavity development of *Citrus sinensis* and *Citrus limon*: evaluation of schizolysigenous ontogeny. Flora-Morphology, Distribution, Functional Ecology of Plants 199, 464 – 475.

Berger, B.A., Kriebel, R., Spalink, D., Sytsma, K.J., 2016. Divergence times, historical biogeography, and shifts in speciation rates of Myrtales. Molecular Phylogenetics and Evolution 95, 116 – 136.

Bernáth, J., 2009. Aromatic plants. Cultivated Plants, Primarily as Food Sources 2, 329 – 352.

Bero, J., Frédérich, M., Quetin-Leclercq, J., 2009. Antimalarial compounds isolated from plants used in traditional medicine. Journal of Pharmacy and Pharmacology 61, 1401 – 1433.

Bhowal, M. and Gopal, M., 2015. Eucalyptol: safety and pharmacological profile. Journal of Pharmaceutical Sciences 5, 125 – 131.

Bin Sayeed, M.S., Karim, S.M.R., Sharmin, T., Morshed, M.M., 2016. Critical analysis on characterization, systemic effect, and therapeutic potential of beta-sitosterol: a plant-derived orphan phytosterol. Medicines 3, 1 – 25.

Bonilla, A., Duque, C., Garzón, C., Takaishi, Y., Yamaguchi, K., Hara, N., Fujimoto, Y., 2005. Champanones, yellow pigments from the seeds of champa (*Campomanesia lineatifolia*). Phytochemistry 66, 1736 – 1740.

Bose, D., Chatterjee, S., 2016. Biogenic synthesis of silver nanoparticles using guava (*Psidium guajava*) leaf extract and its antibacterial activity against *Pseudomonas aeruginosa*. Applied Nanoscience 6, 895 – 901.

Braithwaite, M., Van Vuuren, S.F., Viljoen, A.M., 2008. Validation of smoke inhalation therapy to treat microbial infections. Journal of Ethnopharmacology 119, 501 – 506.

Burt, S., 2004. Essential oils: their antibacterial properties and potential applications in foods - a review. International Journal of Food Microbiology 94, 223 – 253.

Byeon, S.E., Yi, Y.S., Lee, J., Yang, W.S., Kim, J.H., Kim, J., Hong, S., Kim, J.H., Cho, J.Y., 2018. Hydroquinone Exhibits In Vitro and In Vivo Anti-Cancer Activity in Cancer Cells and Mice. International Journal of Molecular Sciences 19, 1 – 13.

Cardoso, C.M.V., Proença, S.L., Sajo, M.G., 2009. Foliar anatomy of the subfamily Myrtoideae (Myrtaceae). Australian Journal of Botany 57, 148 – 161.

Cascaes, M., Guilhon, G., Andrade, E., Zoghbi, M., Santos, L., 2015. Constituents and pharmacological activities of *Myrcia* (Myrtaceae): a review of an aromatic and medicinal group of plants. International Journal of Molecular Sciences 16, 23881 – 23904.

Castro, M.D., Demarco, D., 2008. Phenolic compounds produced by secretory structures in plants: a brief review. Natural Product Communications 3, 1273 – 1274.

Chagonda, L.S., Makanda, C.D., Chalchat, J.C., 2000. Essential oils of cultivated *Heteropyxis natalensis* (Harv.) and cultivated *Heteromorpha trifoliata* (Wendl.) Eckl. & Zey. from Zimbabwe. Journal of Essential Oil Research 12, 317 – 321.

Choi, J.S., Kim, E.S., 2013. Structural Features of Glandular and Non-glandular Trichomes in Three Species of *Mentha*. Applied Microscopy 43, 47 – 53.

Ciccarelli, D., Garbari, F., Pagni, A.M., 2008. The flower of *Myrtus communis* (Myrtaceae): Secretory structures, unicellular papillae, and their ecological role. Flora-Morphology, Distribution, Functional Ecology of Plants 203, 85 – 93.

Ciccarelli, D., Pagni, A.M., Andreucci, A.C., 2003. Ontogeny of secretory cavities in vegetative parts of *Myrtus communis* L. (Myrtaceae): an example of schizolysigenous development. Israel Journal of Plant Sciences 51, 193 – 198.

Conti, E., Litt, A., Sytsma, K.J., 1996. Circumscription of Myrtales and their relationships to other rosids: evidence from *rbcL* sequence data. American Journal of Botany 83, 221 – 233.

Conti, E., Litt, A., Wilson, P.G., Graham, S.A., Briggs, B.G., Johnson, L.A.S., Sytsma, K.J., 1997. Interfamilial relationships in Myrtales: molecular phylogeny and patterns of morphological evolution. Systematic Botany 22, 629 – 647.

Cox, S.D., Mann, C.M., Markham, J.L., 2001. Interactions between components of the essential oil of *Melaleuca alternifolia*. Journal of Applied Microbiology 91, 492 – 497.

Dassanayake, M., Larkin, J.C., 2017. Making plants break a sweat: the structure, function, and evolution of plant salt glands. Frontiers in Plant Science 8, 1 – 20.

Demarco, D., 2017. Histochemical analysis of plant secretory structures, in: Pellicciari, C., Biggiogera (Eds.), Histochemistry of Single Molecules. Humana Press., New York, pp. 313 – 330.

Dhanasekaran, M., Abraham, G.C., Mohan, S., 2014. Preliminary phytochemical and histochemical investigation on *Kigelia pinnata* DC. International Journal of Pharma Sciences and Research 5, 413 – 419.

Dhifi, W., Bellili, S., Jazi, S., Bahloul, N., Mnif, W., 2016. Essential oils' chemical characterization and investigation of some biological activities: a critical review. Medicines 3, 1 – 16.

Dipankar, C., Murugan, S., 2012. The green synthesis, characterization and evaluation of the biological activities of silver nanoparticles synthesized from *Iresine herbstii* leaf aqueous extracts. Colloids and Surfaces B: Biointerfaces 98, 112 – 119.

Djilani, A., Dicko, A., 2012. The therapeutic benefits of essential oils. Nutrition, Well-being and Health, 155 – 173.

Donato, A.M., Morretes, B.L.D., 2013. *Plinia edulis* - leaf architecture and scanning electron micrographs. Revista Brasileira de Farmacognosia 23, 410 – 418.

Dubey, M., Bhadauria, S., Kushwah, B.S., 2009. Green synthesis of nanosilver particles from extract of *Eucalyptus hybrida* (Safeda) leaf. Digest Journal of Nanomaterials and Biostructures 4, 537 – 543.

Dubey, S.P., Lahtinen, M., Sillanpää, M., 2010. Green synthesis and characterizations of silver and gold nanoparticles using leaf extract of *Rosa rugosa*. Colloids and Surfaces A: Physicochemical and Engineering Aspects 364, 34 – 41.

Edris, A.E., 2007. Pharmaceutical and therapeutic potentials of essential oils and their individual volatile constituents: a review. Phytotherapy Research 21, 308 – 323.

Elujoba, A.A., Odeleye, O.M., Ogunyemi, C.M., 2005. Traditional medicine development for medical and dental primary health care delivery system in Africa. African Journal of Traditional, Complementary and Alternative Medicines 2, 46 – 61.

Evert, R.F., Eichhorn, S.E., 2006. Internal secretory structures. Esau's Plant Anatomy 3, 473 – 501.

Fahn, A., 1988a. Tansley Review No. 14. Secretory tissues in vascular plants. New Phytol 108, 229 – 257.

Fahn, A., 1988b. Secretory tissues and factors influencing their development. Phyton 28, 13 – 26.

Fahn, A., 2002. Functions and location of secretory tissues in plants and their possible evolutionary trends. Israel Journal of Plant Sciences 50, 59 – 64.

Fathima, S.B.N., Pandian, R., 2015. Qualitative and quantitative analysis of medicinal tree's belonging to Myrtaceae family. International Journal of Advances in Science Engineering and Technology 6, 132 – 137.

Foglieni, C., Meoni, C., Davalli, A.M., 2001. Fluorescent dyes for cell viability: an application on prefixed conditions. Histochemistry and Cell Biology 115, 223 – 229.

Franceschi, V., 2001. Calcium oxalate in plants. Trends in Plant Science 6, 331.

Freeman, B.C., Beattie, G.A., 2008. An overview of plant defenses against pathogens and herbivores. The Plant Health Instructor 50, 443 – 450.

Gadek, P.A., Wilson, P.G., Quinn, C.J., 1996. Phylogenetic reconstruction in Myrtaceae using *matK*, with particular reference to the position of *Psiloxylon* and *Heteropyxis*. Australian Systematic Botany 9, 283 – 290.

Glas, J., Schimmel, B., Alba, J., Escobar-Bravo, R., Schuurink, R., Kant, M., 2012. Plant glandular trichomes as targets for breeding or engineering of resistance to herbivores. International Journal of Molecular Sciences 13, 17077 – 17103.

Gomes, M.S., Cardoso, M.D.G., Soares, M.J., Batista, L.R., Machado, S.M., Andrade, M.A., de Azeredo, C.M., Resende, J.M.V., Rodrigues, L., 2014. Use of essential oils of the genus *Citrus* as biocidal agents. African Journal of Plant Sciences 5, 299 – 305.

Goodger, J.Q., Heskes, A.M., Mitchell, M.C., King, D.J., Neilson, E.H., Woodrow, I.E., 2010. Isolation of intact sub-dermal secretory cavities from *Eucalyptus*. Plant Methods 6, 1 – 10.

Gowri, S.S., Vasantha, K., 2010. Phytochemical screening and antibacterial activity of *Syzygium cumini* (L.) (Myrtaceae) leaves extracts. International Journal of PharmTech Research 2, 1569 – 1573.

Gracindo, L.A.M.B., Grisi, M.C.M., Silva, D.B., Alves, R.B.N., Bizzo, H.R., Vieira, R.F., 2006. Chemical characterization of mint (*Mentha* spp.) germplasm at Federal District, Brazil. Revista Brasileira de Plantas Medicinais 8, 5 – 9.

Grattapaglia, D., Vaillancourt, R.E., Shepherd, M., Thumma, B.R., Foley, W., Külheim, C., Potts, B.M., Myburg, A.A., 2012. Progress in Myrtaceae genetics and genomics: *Eucalyptus* as the pivotal genus. Tree Genetics and Genomes 8, 463 – 508.

Grubešić, R.J., Vladimir-Knežević, S., Kremer, D., Kalodera, Z., Vuković, J., 2007. Trichome micromorphology in *Teucrium* (Lamiaceae) species growing in Croatia. Biologia 62, 148 – 156.

Gundidza, M., Deans, S.G., Kennedy, A.I., Mavi, S., Waterman, P.G., Gray, A.I., 1993. The essential oil from *Heteropyxis natalensis* Harv: its antimicrobial activities and phytoconstituents. Journal of the Science of Food and Agriculture 63, 361 – 364.

Günes, F.E., 2013. Medical use of squalene as a natural antioxidant. Clinical and Experimental Health Sciences 3, 220 – 228.

Gunjan, M., Naing, T.W., Saini, R.S., Ahmad, A., Naidu, J.R., Kumar, I., 2015. Marketing trends & future prospects of herbal medicine in the treatment of various disease. World Journal of Pharmaceutical Research 4, 132 – 155.

Guo, J., Yuan, Y., Liu, Z., Zhu, J., 2013. Development and structure of internal glands and external glandular trichomes in *Pogostemon cablin*. PloS one 8, 1 – 12.

Gurib-Fakim, A., 2006. Medicinal plants: traditions of yesterday and drugs of tomorrow. Molecular Aspects of Medicine 27, 1 – 93.

Hasan, S., 2015. A review on nanoparticles: their synthesis and types. Research Journal of Recent Sciences 4, 1 – 3.

Henley-Smith, C.J., Botha, F.S., Hussein, A.A., Nkomo, M., Meyer, D., Lall, N., 2018. Biological activities of *Heteropyxis natalensis* against micro-organisms involved in oral infections. Frontiers in Pharmacology 9, 1 – 9.

Heyman, H.M., Hussein, A.A., Meyer, J.J.M., Lall, N., 2009. Antibacterial activity of South African medicinal plants against methicillin resistant *Staphylococcus aureus*. Pharmaceutical Biology 47, 67 – 71.

Hosseinzadeh, S., Jafarikukhdan, A., Hosseini, A., Armand, R., 2015. The application of medicinal plants in traditional and modern medicine: a review of *Thymus vulgaris*. International Journal of Clinical Medicine 6, 635 – 642.

Ilarslan, H., Palmer, R.G., Horner, H.T., 2001. Calcium oxalate crystals in developing seeds of soybean. Annals of Botany 88, 243 – 257.

Iroka, C.F., Okeke, C.U., Okereke, C.N., 2015. Systematic implications of trichomes in the species of *Stachytarpheta* found in Awka, Nigeria. Asian Journal of Plant Science and Research 5, 30 – 34.

Ismail, A.M., Mohamed, E.A., Marghany, M.R., Abdel-Motaal, F.F., Abdel-Farid, I.B., El-Sayed, M.A., 2016. Preliminary phytochemical screening, plant growth inhibition and antimicrobial activity studies of *Faidherbia albida* legume extracts. Journal of the Saudi Society of Agricultural Sciences 15, 112 – 117.

Janošević, D., Budimir, S., Alimpić, A., Marin, P., Al Sheef, N., Giweli, A., Duletić-Laušević, S., 2016. Micromorphology and histochemistry of leaf trichomes of *Salvia aegyptiaca* (Lamiaceae). Archives of Biological Sciences 68, 291 – 301.

Jiang, B., Peng, Q.F., Shen, Z.G., Möller, M., Pi, E.X., Lu, H.F., 2010. Taxonomic treatments of *Camellia* (Theaceae) species with secretory structures based on integrated leaf characters. Plant Systematics and Evolution 290, 1 – 20.

Johnson, L.A.S., Briggs, B.G., 1984. Myrtales and Myrtaceae - a phylogenetic analysis. Annals of the Missouri Botanical Garden, 700 – 756.

Juergens, U.R., 2014. Anti-inflammatory properties of the monoterpene 1.8-cineole: current evidence for co-medication in inflammatory airway diseases. Drug Research 64, 638 – 646.

Jyoti, K., Baunthiyal, M., Singh, A., 2016. Characterization of silver nanoparticles synthesized using *Urtica dioica* Linn. leaves and their synergistic effects with antibiotics. Journal of Radiation Research and Applied Sciences 9, 217 – 227.

Kala, S.M.J., Tresina Soris, P., Mohan, V.R., 2012. GC-MS determination of bioactive components of *Eugenia floccosa* Bedd (Myrtaceae). International Journal of Pharma and Bio Sciences 3, 277 – 282.

Kalachanis, D., Psaras, G.K., 2005. Structure and development of the secretory cavities of *Myrtus communis* leaves. Biologia Plantarum 49, 105 – 110.

Kar, P., Goyal, A., Sen, A., 2015. *Maturase K* gene in plant DNA barcoding and phylogenetics, in: Ali, M.A., Gabor, G., Al-Hemaid, F. (Eds.), Plant DNA Barcoding. Lambert Academic Publishing., Germany, pp. 75 – 86.

Kartal, C., 2016. Calcium oxalate crystals in some species of the Tribe Cardueae (Asteraceae). Botanical Sciences 94, 107 – 119.

Karthikeyan, V., Baskaran, A., Rajasekaran, C.S., 2016. Gas Chromatography-Mass Spectrometry (GC-MS) Analysis of Ethanolic Extracts of *Barleria acuminata* Nees. International Journal of Pharmacological Research 6, 55 – 61.

Kaya, A., Demirci, B., Başer, K.H.C., Van Staden, J., 2003. Glandular trichomes and essential oils of *Salvia glutinosa* L. South African Journal of Botany 69, 422 – 427.

Kim, H.J., Seo, E.Y., Kim, J.H., Cheong, H.J., Kang, B.C., Choi, D.I., 2012. Morphological classification of trichomes associated with possible biotic stress resistance in the genus *Capsicum*. The Plant Pathology Journal 28, 107 – 113.

Koduru, S., Grierson, D.S., Afolayan, A.J., 2007. Ethnobotanical information of medicinal plants used for treatment of cancer in the Eastern Cape Province, South Africa. Current Science 92, 906 – 908.

Konyar, S.T., Öztürk, N., Dane, F., 2014. Occurrence, types and distribution of calcium oxalate crystals in leaves and stems of some species of poisonous plants. Botanical Studies 55, 1 – 9.

Kück, U., Wolff, G., Rathke, H.J., 2009. Botanisches Grundpraktikum. Springer, Berlin.

Kulich, I., Vojtíková, Z., Glanc, M., Ortmannová, J., Rasmann, S., Žárský, V., 2015. Cell wall maturation of *Arabidopsis* trichomes is dependent on exocyst subunit EXO70H4 and involves callose deposition. Plant Physiology 168, 120 -131.

Kumar, T.T., Salique, S.M., Ilyas, M.H.M., Thajuddin, N., Panneerselvam, A., Padusha, M.K.S.A., Jahangir, H.S., 2018. Phytochemical Screening and Antimicrobial Studies in Leaf Extracts of *Indigofera aspalathoides* (Vahl.). Pharmacognosy Journal 10, 1208 – 1215.

Levin, D.A., 1973. The role of trichomes in plant defense. The Quarterly Review of Biology 48, 3 – 15.

Light, M.E., Sparg, S.G., Stafford, G.I., Van Staden, J., 2005. Riding the wave: South Africa's contribution to ethnopharmacological research over the last 25 years. Journal of Ethnopharmacology 100, 127 – 130.

Liliwirianis, N., Zain, W.Z.W.M., Kassim, J., Karim, S.A., 2011. Antimicrobial activity of plant extracts against *Bacillus subtilis*, *Staphylococcus aureus* and *Escherichia coli*. Journal of Chemistry 8, 282 – 284.

Liu, Q., Luo, L., Zheng, L., 2018. Lignins: biosynthesis and biological functions in plants. International Journal of Molecular Sciences 19, 1 – 16.

Lozano-Grande, M.A., Gorinstein, S., Espitia-Rangel, E., Dávila-Ortiz, G., Martínez-Ayala, A.L., 2018. Plant Sources, Extraction Methods, and Uses of Squalene. International Journal of Agronomy 2018, 1 – 13.

Machado, S.R., Canaveze, Y., Rodrigues, T.M., 2017. Structure and functioning of oil cavities in the shoot apex of *Metrodorea nigra* A. St.-Hil. (Rutaceae). Protoplasma 254, 1661 – 1674.

Mahomoodally, M.F., 2013. Traditional medicines in Africa: an appraisal of ten potent African medicinal plants. Evidence-Based Complementary and Alternative Medicine 2013, 1 – 14.

Makunga, N.P., Philander, L.E., Smith, M., 2008. Current perspectives on an emerging formal natural products sector in South Africa. Journal of Ethnopharmacology 119, 365 – 375.

Matsuura, H.N., Fett-Neto, A.G., 2015. Plant Alkaloids: Main Features, Toxicity, and Mechanisms of Action, in: Gopalakrishnakone, P., Carlini, C., Ligabue-Braun, R. (Eds.), Plant Toxins. Springer., Dordrecht, pp. 1 – 15.

Meena, A.K., Bansal, P., Kumar, S., 2009. Plants-herbal wealth as a potential source of ayurvedic drugs. Asian Journal of Traditional Medicines 4, 152 – 170.

Meric, C., 2009. Calcium oxalate crystals in some species of the tribe Inuleae (Asteraceae). Acta Biologica Cracoviensia Series Botanica 51, 105 – 110.

Mishra, M., Chauhan, P., 2015. Nanosilver and its medical implications. Journal of Nanomedicine Research 2, 1 – 10.

Mishra, P., Jamdar, P., Desai, S., Patel, D., Meshram, D., 2014. Phytochemical analysis and assessment of in vitro antibacterial activity of *Tinospora cordifolia*. International Journal of Current Microbiology and Applied Sciences 3, 224 – 234.

Mishra, P.M., Pani, K.B., 2017. Biomimetic synthesis of silver nanoparticles and evaluation of their catalytic activity towards degradation of methyl orange. Materials Research Express 4, 1 – 23.

Mohammed, A.E., 2015. Green synthesis, antimicrobial and cytotoxic effects of silver nanoparticles mediated by *Eucalyptus camaldulensis* leaf extract. Asian Pacific Journal of Tropical Biomedicine 5, 382 – 386.

Mohammed, A.M., Coombes, P.H., Crouch, N.R., Mulholland, D.A., 2009. Non-volatile isolates of two *Heteropyxis* species: a first chemotaxonomic assessment of subfamily Psiloxyloideae (Myrtaceae). Biochemical Systematics and Ecology 37, 241 – 243.

Molano-Flores, B., 2001. Herbivory and calcium concentrations affect calcium oxalate crystal formation in leaves of *Sida* (Malvaceae). Annals of Botany 88, 387 – 391.

Mondal, A.K., Mondal, S., Samanta, S., Mallick, S., 2011. Synthesis of Ecofriendly Silver Nanoparticle from Plant Latex used as an Important Taxonomic Tool for Phylogenetic Interrelationship. Advances in Bioresearch 2, 122 – 133.

Monteiro, W.R., Fahn, A., Caldeira, W., Castro, M.D.M., 1999. Ultrastructural observations on the foliar secretory cavities of *Porophyllum lanceolatum* DC. (Asteraceae). Flora 194, 113 – 126.

Muchuweti, M., Nyamukonda, L., Chagonda, L.S., Ndhlala, A.R., Mupure, C., Benhura, M., 2006. Total phenolic content and antioxidant activity in selected medicinal plants of Zimbabwe. International Journal of Food Science and Technology 41, 33 – 38.

Müller, K.F., Borsch, T., Hilu, K.W., 2006. Phylogenetic utility of rapidly evolving DNA at high taxonomical levels: contrasting *matK*, *trnT-F*, and *rbcL* in basal angiosperms. Molecular Phylogenetics and Evolution 41, 99 – 117.

Nakata, P.A., 2003. Advances in our understanding of calcium oxalate crystal formation and function in plants. Plant Science 164, 901 – 909.

National Institute of Standars and Technology., 2018. NIST Chemistry WebBook, https://webbook.nist.gov/chemistry/. Accessed: 11 October 2018.

Ngo, L.T., Okogun, J.I., Folk, W.R., 2013. 21st century natural product research and drug development and traditional medicines. Natural Product Reports 30, 584 – 592.

Nicole, M., Geiger, J.P., Nandris, D., 1986. Ultrastructure of laticifers modifications in *Hevea brasiliensis* infected with root rot fungi. Journal of Phytopathology 116, 259 – 268.

Nishida, S., Tsukaya, H., Nagamasu, H., Nozaki, M., 2006. A comparative study on the anatomy and development of different shapes of domatia in *Cinnamomum camphora* (Lauraceae). Annals of Botany 97, 601 – 610.

Nurani, S.J., Saha, C.K., Khan, M.A.R., Sunny, S.M.H., 2015. Silver Nanoparticles Synthesis, Properties, Applications and Future Perspectives: A Short Review. IOSR Journal of Electrical and Electronics Engineering 10, 117 – 126.

Okoye, N.N., Ajaghaku, D.L., Okeke, H.N., Ilodigwe, E.E., Nworu, C.S., Okoye, F.B.C., 2014. beta-Amyrin and alpha-amyrin acetate isolated from the stem bark of *Alstonia boonei* display profound anti-inflammatory activity. Pharmaceutical Biology 52, 1478 – 1486.

Oosthuizen, L.M., Coetzee, J., 1984. Trichome initiation during leaf growth in *Pelargonium scabrum*. South African Journal of Botany 3, 50 – 54.

Padovan, A., Keszei, A., Külheim, C., Foley, W.J., 2014. The evolution of foliar terpene diversity in Myrtaceae. Phytochemistry Reviews 13, 695 – 716.

Pakkirisamy, M., Kalakandan, S.K., Ravichandran, K., 2017. Phytochemical Screening, GC-MS, FT-IR Analysis of Methanolic Extract of *Curcuma caesia* Roxb (Black Turmeric). Pharmacognosy Journal 9, 952 – 956.

Panthong, A., Tassaneeyakul, W., Kanjanapothi, D., Tantiwachwuttikul, P., Reutrakul, V., 1989. Anti-inflammatory activity of 5, 7-dimethoxyflavone. Planta Medica 55, 133 – 136.

Paosen, S., Saising, J., Septama, A.W., Voravuthikunchai, S.P., 2017. Green synthesis of silver nanoparticles using plants from Myrtaceae family and characterization of their antibacterial activity. Materials Letters 209, 201 – 206.

Parveen, K., Banse, V., Ledwani, L., 2016, April. Green synthesis of nanoparticles: Their advantages and disadvantages. AIP Conference Proceedings 1724, 1 – 8.

Payne, W.W., 1978. A glossary of plant hair terminology. Brittonia 30, 239 – 255.

Pesonen, M., Suomela, S., Kuuliala, O., Henriks-Eckerman, M.L., Aalto-Korte, K., 2014. Occupational contact dermatitis caused by D-limonene. Contact Dermatitis 71, 273 – 279.

Peter, A.J., Shanower, T.G., 1998. Plant glandular trichomes. Resonance 3, 41 – 45.

Petersen, L., Reid, A.M., Moll, E.J., Hockings, M.T., 2017. Perspectives of wild medicine harvesters from Cape Town, South Africa. South African Journal of Science 113, 1 – 8.

Pickard, W.F., 2008. Laticifers and secretory ducts: two other tube systems in plants. New Phytologist 177, 877 – 888.

Pireda, S., Marques, J.D.B.C., Rabelo, G.R., Da Cunha, M., 2017. Structural analysis and developmental stages of domatia of *Schinus terebinthifolius* Raddi (Anacardiaceae). Brazilian Journal of Botany 40, 1041 – 1048.

Pourmortazavi, S.M., Taghdiri, M., Makari, V., Rahimi-Nasrabadi, M., 2014. Procedure optimization for green synthesis of silver nanoparticles by aqueous extract of *Eucalyptus oleosa*. Spectrochimica Acta Part A: Molecular and Biomolecular Spectroscopy 136, 1249 – 1254.

Qazi, M.A., Molvi, M.K., 2016. Herbal medicine: A comprehensive review. International Journal of Pharmaceutical Research 8, 1 – 5.

Rahimi-Nasrabadi, M., Pourmortazavi, S.M., Shandiz, S.A.S., Ahmadi, F., Batooli, H., 2014. Green synthesis of silver nanoparticles using *Eucalyptus leucoxylon* leaves extract and evaluating the antioxidant activities of extract. Natural Product Research 28, 1964 – 1969.

Ravikumar, V.R., Gopal, V., Sudha, T., 2012. Analysis of phytochemical constituents of stem bark extracts of *Zanthoxylum tetraspermum* Wight & Arn. Research Journal of Pharmaceutical, Biological and Chemical Sciences 3, 391 – 402.

Retamales, H.A., Scharaschkin, T., 2015. Comparative leaf anatomy and micromorphology of the Chilean Myrtaceae: Taxonomic and ecological implications. Flora-Morphology, Distribution, Functional Ecology of Plants 217, 138 – 154.

Retamales, H.A., Scherson, R., Scharaschkin, T., 2014. Foliar micromorphology and anatomy of *Ugni molinae* Turcz. (Myrtaceae), with particular reference to schizogenous secretory cavities. Revista chilena de historia natural 87, 1 – 7.

Rizvi, S., Raza, S.T., Ahmed, F., Ahmad, A., Abbas, S., Mahdi, F., 2014. The role of vitamin E in human health and some diseases. Sultan Qaboos University Medical Journal 14, 157 – 165.

Roe, K.E., 1971. Terminology of hairs in the genus *Solanum*. Taxon 20, 501 – 508.

Romero, G.Q., Daud, R.D., Salomão, A.T., Martins, L.F., Feres, R.J.F., Benson, W.W., 2011. Mites and leaf domatia: no evidence of mutualism in *Coffea arabica* plants. Biota Neotropica 11, 27 – 34.

Roshchina, V.V., 2003. Autofluorescence of plant secreting cells as a biosensor and bioindicator reaction. Journal of Fluorescence 13, 403 – 420.

Rout, Y., Behera, S., Ojha, A.K., Nayak, P.L., 2012. Green synthesis of silver nanoparticles using *Ocimum sanctum* (Tulashi) and study of their antibacterial and antifungal activities. Journal of Microbiology and Antimicrobials 4, 103 – 109.

Russin, W.A., Uchytil, T.F., Durbin, R.D., 1992. Isolation of structurally intact secretory cavities from leaves of African marigold, *Tagetes erecta* L.(Asteraceae). Plant Science 85, 115 – 119.

Saidi, T., 2018. Perceived risks and benefits of nanomedicine: a case study of an anti-tuberculosis drug. Global Health Innovation 1, 1 – 7.

Saif, M.M.S., Al-Fakih, A.A., Hassan, M.A.M., 2017. Antibacterial activity of selected plant (Aqueous and methanolic) extracts against some pathogenic bacteria. Journal of Pharmacognosy and Phytochemistry 6, 1929 – 1935.

Salomoni, R., Léo, P., Montemor, A.F., Rinaldi, B.G., Rodrigues, M.F.A., 2017. Antibacterial effect of silver nanoparticles in *Pseudomonas aeruginosa*. Nanotechnology, Science and Applications 10, 115 – 121.

Santos Tozin, L.R.D., de Melo Silva, S.C., Rodrigues, T.M., 2016. Non-glandular trichomes in Lamiaceae and Verbenaceae species: morphological and histochemical features indicate more than physical protection. New Zealand Journal of Botany 54, 446 – 457.

Sartoratto, A., Machado, A.L.M., Delarmelina, C., Figueira, G.M., Duarte, M.C.T., Rehder, V.L.G., 2004. Composition and antimicrobial activity of essential oils from aromatic plants used in Brazil. Brazilian Journal of Microbiology 35, 275 – 280.

Savithramma, N., Rao, M.L., Suhrulatha, D., 2011. Screening of medicinal plants for secondary metabolites. Middle-East Journal of Scientific Research 8, 579 – 584.

Saxena, M., Saxena, J., Nema, R., Singh, D., Gupta, A., 2013. Phytochemistry of medicinal plants. Journal of Pharmacognosy and Phytochemistry 1, 168 – 182.

Schmid, R., 1980. Comparative anatomy and morphology of *Psiloxylon* and *Heteropyxis*, and the subfamilial and tribal classification of Myrtaceae. Taxon 29, 559 – 595.

Sefidkon, F., Assareh, M.H., Abravesh, Z., Barazandeh, M.M., 2007. Chemical composition of the essential oils of four cultivated Eucalyptus species in Iran as medicinal plants (*E. microtheca*, *E. spathulata*, *E. largiflorens* and *E. torquata*). Iranian Journal of Pharmaceutical Research 6, 135 – 140.

Sekhar, E.C., Rao, K.K., Rao, K.M.S., Alisha, S.B., 2018. A Simple Biosynthesis of Silver Nanoparticles from *Syzygium cumini* Stem Bark Aqueous Extract and their Spectrochemical and Antimicrobial Studies. Journal of Applied Pharmaceutical Science 8, 073 – 079.

Selvamohan, T., Ramadas, V., Kishore, S.S.S., 2012. Antimicrobial activity of selected medicinal plants against some selected human pathogenic bacteria. Advances in Applied Science Research 3, 3374 – 3381.

Sen, T., Samanta, S.K., 2014. Medicinal plants, human health, and biodiversity: a broad review, in: Mukherjee, J. (Ed.), Biotechnological Applications of Biodiversity. Springer., Berlin Heidelberg, pp. 59 – 110.

Shaik, M.R., Khan, M., Kuniyil, M., Al-Warthan, A., Alkhathlan, H.Z., Siddiqui, M.R.H., Shaik, J.P., Ahamed, A., Mahmood, A., Khan, M., Adil, S.F., 2018. Plant-Extract-Assisted Green Synthesis of Silver Nanoparticles Using *Origanum vulgare* L. Extract and Their Microbicidal Activities. Sustainability 10, 1 – 14.

Shakya, A.K., 2016. Medicinal plants: future source of new drugs. International Journal of Herbal Medicine 4, 59 – 64.

Sharma, R., Kishore, N., Hussein, A., Lall, N., 2013. Antibacterial and anti-inflammatory effects of *Syzygium jambos* L.(Alston) and isolated compounds on acne vulgaris. BMC Complementary and Alternative Medicine 13, 1 – 10.

Sheel, R., Nisha, K., Kumar, J., 2014. Preliminary phytochemical screening of methanolic extract of *Clerodendron infortunatum*. IOSR Journal of Applied Chemistry 7, 10 – 13.

Sibanda, S., Chigwada, G., Poole, M., Gwebu, E.T., Noletto, J.A., Schmidt, J.M., Rea, A.I., Setzer, W.N., 2004. Composition and bioactivity of the leaf essential oil of *Heteropyxis dehniae* from Zimbabwe. Journal of Ethnopharmacology 92, 107 – 111.

Siddique, S., Perveen, Z., Nawaz, S., Shahzad, K., Ali, Z., 2015. Chemical composition and antimicrobial activities of essential oils of six species from family Myrtaceae. Journal of Essential Oil Bearing Plants 18, 950 – 956.

Sila, J.M., Kiio, I., Mwaura, F.B., Michira, I., Abongo, D., Iwuoha, E., Kamau, G.N., 2014. Green synthesis of silver nanoparticles using *Eucalyptus corymbia* extract and antimicrobial applications. Internation Journal of BioChemiPhysics 22, 21 – 30.

Singh, K., Panghal, M., Kadyan, S., Chaudhary, U., Yadav, J.P., 2014. Antibacterial activity of synthesized silver nanoparticles from *Tinospora cordifolia* against multi drug resistant strains of *Pseudomonas aeruginosa* isolated from burn patients. Journal of Nanomedicine and Nanotechnology 5, 1 – 6.

Souza, L.A., Moscheta, I.S., Oliveira, J.H.G., 2004. Comparative morphology and anatomy of the leaf and stem of *Peperomia dahlstedtii* C. DC., *Ottonia martiana* Miq. and *Piper diospyrifolium* Kunth (Piperaceae). Gayana Botanica 61, 6 – 17.

Spurr, A.R., 1969. A low-viscosity epoxy resin embedding medium for electron microscopy. Journal of Ultrastructural Research 26, 31 – 43.

Stern, W.L., Brizicky, G.K., 1958. The comparative anatomy and taxonomy of *Heteropyxis.* Bulletin of the Torrey Botanical Club 85, 111 – 123.

Street, R.A., Prinsloo, G., 2012. Commercially important medicinal plants of South Africa: a review. Journal of Chemistry 2013, 1 – 16.

Sudha, A., Jeyakanthan, J., Srinivasan, P., 2017. Green synthesis of silver nanoparticles using *Lippia nodiflora* aerial extract and evaluation of their antioxidant, antibacterial and cytotoxic effects. Resource-Efficient Technologies 3, 506 – 515.

Svoboda, K.P., Svoboda, T.G., Syred, A.D., 2000. Secretory structures of aromatic and medicinal plants, in: Microscopix Publications, British Library Cataloguing-in-Publication Data., U.K, pp. 3 – 30.

Swamy, M.K., Sudipta, K.M., Jayanta, K., Balasubramanya, S., 2015. The green synthesis, characterization, and evaluation of the biological activities of silver nanoparticles synthesized from *Leptadenia reticulata* leaf extract. Applied Nanoscience 5, 73 – 81.

Szymanski, D.B., Lloyd, A.M., Marks, M.D., 2000. Progress in the molecular genetic analysis of trichome initiation and morphogenesis in *Arabidopsis*. Trends in Plant Science 5, 214 – 219.

Takeoka, G.R., Hobbs, C., Park, B.S., 2010. Volatile constituents of the aerial parts of *Salvia apiana* Jepson. Journal of Essential Oil Research 22, 241 – 244.

Teixeira, S.D.P., Castro, M.D.M., Tozzi, A.D.A., 2000. Secretory cavities and pellucid dots in leaflets of *Lonchocarpus* (Leguminosae, Papilionoideae, Millettieae). Plant Systematics and Evolution 221, 61 – 68.

Teixeira, S.D.P., Gabrielli, A.C., 2006. Taxonomic value of foliar characters in *Dahlstedtia* Malme: Leguminosae, Papilionoideae, Millettieae. Acta Botanica Brasilica 20, 395 – 403.

Tobe, H., Raven, P.H., 1987. Embryology and systematic position of *Heteropyxis* (Myrtales). American Journal of Botany 74, 197 – 208.

Tongnuanchan, P., Benjakul, S., 2014. Essential oils: extraction, bioactivities, and their uses for food preservation. Journal of Food Science 79, 1231 – 1249.

Turner, G.W., Berry, A.M., Gifford, E.M., 1998. Schizogenous secretory cavities of *Citrus limon* (L.) Burm. F. and a reevaluation of the lysigenous gland concept. International Journal of Plant Sciences 159, 75 – 88.

University of Connecticut., 2018. *Heteropyxis natalensis* Harv. in Biodiversity Education & Research Greenhouses. http://florawww.eeb.uconn.edu/198700171.html. Accessed: 12 November 2018.

Upton, R., Graff, A., Jolliffe, G., Länger, R., Williamson, E., 2016. Structures of the Primary Plant Body and Basic Anatomy, in: Upton, R., Graff, A., Jolliffe, G., Länger, R., Williamson, E. (Eds.), American Herbal Pharmacopoeia: Botanical Pharmacognosy-Microscopic Characterization of Botanical Medicines. CRC Press., New York, pp. 113.

Valkama, E., Salminen, J.P., Koricheva, J., Pihlaja, K., 2003. Comparative analysis of leaf trichome structure and composition of epicuticular flavonoids in Finnish birch species. Annals of Botany 91, 643 – 655.

Valkama, E., Salminen, J.P., Koricheva, J., Pihlaja, K., 2004. Changes in leaf trichomes and epicuticular flavonoids during leaf development in three birch taxa. Annals of Botany 94, 233 – 242.

Van Vuuren, S., Viljoen, A., 2008. Indigenous South African Medicinal Plants: part 10: *Heteropyxis natalensis* ('Lavender tree'): medicinal plants. SA Pharmaceutical Journal 75, 46.

Van Vuuren, S.F., Viljoen, A.M., Özek, T., Demirci, B., Başer, K.H.C., 2007. Seasonal and geographical variation of *Heteropyxis natalensis* essential oil and the effect thereof on the antimicrobial activity. South African Journal of Botany 73, 441 – 448.

Van Wyk, A.S., Prinsloo, G., 2018. Medicinal plant harvesting, sustainability and cultivation in South Africa. Biological Conservation 227, 335 – 342.

Van Wyk, B.E., 2011. The potential of South African plants in the development of new food and beverage products. South African Journal of Botany 77, 857 – 868.

Vargas, W.D., Sartori, A.L., Dias, E.S., 2015. Novelties in secretory structures and anatomy of *Rhynchosia* (Fabaceae). Anais da Academia Brasileira de Ciências 87, 83 – 87.

Veberic, R., 2016. The impact of production technology on plant phenolics. Horticulturae 2, 1 – 8.

Victor, O.O., David, S.M., 2015. GC-MS Analysis of phyto-components from the Leaves of *Senna alata* L. Journal of Plant Sciences 3, 133 – 136.

Vieira, R.C., Delprete, P.G., Leitão, G.G., Leitão, S.G., 2001. Anatomical and chemical analyses of leaf secretory cavities of *Rustia formosa* (Rubiaceae). American Journal of Botany 88, 2151 – 2156.

Vijayakumar, M., Priya, K., Nancy, F.T., Noorlidah, A., Ahmed, A.B.A., 2013. Biosynthesis, characterization and anti-bacterial effect of plant-mediated silver nanoparticles using *Artemisia nilagirica*. Industrial Crops and Products 41, 235 – 240.

Vimalkumar, C.S., Hosagaudar, V.B., Suja, S.R., Vilash, V., Krishnakumar, N.M., Latha, P.G., 2014. Comparative preliminary phytochemical analysis of ethanolic extracts of leaves of *Olea dioica* Roxb., infected with the rust fungus *Zaghouania oleae* (EJ Butler) Cummins and non-infected plants. Journal of Pharmacognosy and Phytochemistry 3, 69 – 72.

Wagner, G.J., 1991. Secreting glandular trichomes: more than just hairs. Plant Physiology 96, 675 – 679.

Wagner, G.J., Wang, E., Shepherd, R.W., 2004. New approaches for studying and exploiting an old protuberance, the plant trichome. Annals of Botany 93, 3 – 11.

Wang, J., Li, J., Li, S., Freitag, C., Morrell, J.J., 2011. Antifungal activities of *Cunninghamia lanceolata* heartwood extractives. BioResources 6, 606 – 614.

Werker, E., 2000. Trichome diversity and development. Advances in Botanical Research 31, 1 – 35.

Weyerstahl, P., Christiansen, C., Gundidza, M., Mavi, S., 1992. Constituents of the essential oil of *Heteropyxis natalensis*. Journal of Essential Oil Research 4, 439 – 445.

Wilson, P.G., O'Brien, M.M., Heslewood, M.M., Quinn, C.J., 2005. Relationships within Myrtaceae sensu lato based on a *matK* phylogeny. Plant Systematics and Evolution 251, 3 – 19.

Wilson, P.G., O'Brien, M.M., Gadek, P.A., Quinn, C.J., 2001. Myrtaceae revisited: a reassessment of infrafamilial groups. American Journal of Botany 88, 2013 – 2025.

Wink, M., 2015. Modes of action of herbal medicines and plant secondary metabolites. Medicines 2, 251 – 286.

Xego, S., Kambizi, L. Nchu, F., 2016. Threatened medicinal plants of South Africa: Case of the family Hyacinthaceae. African Journal of traditional, Complementary and Alternative Medicines 13, 169 – 180.

Xiao, K., Mao, X., Lin, Y., Xu, H., Zhu, Y., Cai, Q., Xie, H., Zhang, J., 2017. Trichome, a functional diversity phenotype in Plant. Molecular Biology 6, 1 – 6.

Yugandhar, P., Savithramma, N., 2015. Biosynthesis, characterization and antimicrobial studies of green synthesized silver nanoparticles from fruit extract of *Syzygium alternifolium* (Wt.) Walp. an endemic, endangered medicinal tree taxon. Applied Nanoscience 6, 223 – 233.

Zaheer, Z., 2012. Silver nanoparticles to self-assembled films: green synthesis and characterization. Colloids and surfaces B: Biointerfaces 90, 48 – 52.

Zaman, F.Q., Al-Hakimi, A.S., Khamis, S., Ruhaizin, F.F., Zaidi, S.M., 2018. Anatomy and histochemistry of structures producing aroma in leaves of *Sygyzium aromaticum* (L.) Merr. and *Clausena excavata* Burm. f. Pertanika Journal of Tropical Agricultural Science 41, 225 – 240.

Zargar, M., Hamid, A.A., Bakar, F.A., Shamsudin, M.N., Shameli, K., Jahanshiri, F., Farahani, F., 2011. Green synthesis and antibacterial effect of silver nanoparticles using *Vitex negundo* L. Molecules 16, 6667 – 6676.

APPENDIX A

Table A 1: 119 phytochemical compounds identified in methanolic leaf extract of *H. natalensis* by GC-MS

No.	Compound	CAS	RT (min)	Area %	Mol Formula	Mol Weight
1	β-Ocimene	13877-91-3	5.080	0.02	$C_{10}H_{16}$	136
2	α-Pinene	80-56-8	5.150	0.13	$C_{10}H_{16}$	136
3	β-Pinene	127-91-3	5.830	0.23	$C_{10}H_{16}$	136
4	2,4-Dihydroxy-2,5-dimethyl-3(2H)-furan-3-one	10230-62-3	5.916	0.21	$C_6H_8O_4$	144
5	Cyclohexane, 1-methylene-4-(1-methylethenyl)-	499-97-8	6.236	0.32	$C_{10}H_{16}$	136
6	Eucalyptol	470-82-6	6.686	5.41	$C_{10}H_{18}O$	154
7	Formamide, N-(1,3,3-trimethyl-2-norbornyl)-	6622-69-1	6.904	0.06	$C_{11}H_{19}NO$	181
8	Cyclopentene, 3-isopropenyl-5,5-dimethyl-	0-00-0	7.079	0.15	$C_{10}H_{16}$	136
9	Thymine	65-71-4	7.454	0.18	$C_5H_6N_2O_2$	126
10	(R,S)-2-Propyl-5-oxohexanal / 5-oxo-2-propylhexanal	0-00-0	7.568	0.34	$C_9H_{16}O_2$	156
11	Linalool	78-70-6	7.699	0.73	$C_{10}H_{18}O$	154
12	14-Chloro-1-tetradecanol	73937-05-0	7.954	0.08	$C_{14}H_{29}ClO$	248
13	Propanoic acid, 2-(methoxyimino)-, methyl ester	53907-93-0	8.211	0.08	$C_5H_9NO_3$	131
14	2-Cyclohexen-1-one, 4-hydroxy-	30182-12-8	8.341	0.16	$C_6H_8O_2$	112
15	4H-Pyran-4-one, 2,3-dihydro-3,5-dihydroxy-6-methyl-	28564-83-2	8.417	0.63	$C_6H_8O_4$	144
16	5-Hepten-2-ol, 6-methyl-	1569-60-4	8.862	0.10	$C_8H_{16}O$	128
17	Terpinen-4-ol	562-74-3	8.985	0.17	$C_{10}H_{18}O$	154

18	L-α-Terpineol	10482-56-1	9.188	0.44	$C_{10}H_{18}O$	154
19	Cyclohexanone, 4,4-dimethoxy-	56180-50-8	9.358	0.05	$C_8H_{14}O_3$	158
20	Dodec-5-yn-6-one	66552-60-1	9.606	0.12	$C_{12}H_{20}O$	180
21	Butanamide, 2-hydroxy-N,3,3-trimethyl-	87919-98-0	9.710	0.11	$C_7H_{15}NO_2$	145
22	5-Hydroxymethylfurfural	67-47-0	9.787	0.65	$C_6H_6O_3$	126
23	4-Pyrimidinol, 5-methoxy-	695-87-4	10.108	0.13	$C_5H_6N_2O_2$	126
24	Hydroquinone	123-31-9	10.311	1.17	$C_6H_6O_2$	110
25	1,4-Cyclohexanedicarbohydrazide	27327-67-9	10.539	0.05	$C_8H_{16}N_4O_2$	200
26	Cyclohexanamine, N-butylidene-	1197-52-0	10.645	0.16	$C_{10}H_{19}N$	153
27	1-[N-Aziridyl]-2-methyl-2-propanethiol	0-00-0	10.960	0.12	$C_6H_{13}NS$	133
28	1,6-Anhydro-3,4-dideoxy-.beta.-D-manno-hexapyranose	39682-49-0	11.029	0.26	$C_6H_{10}O_3$	130
29	1,2-Cyclohexanediol, 1-methyl-4-(1-methylethenyl)-	1946-00-5	11.313	0.05	$C_{10}H_{18}O_2$	170
30	2-Octene, 1-bromo-1,1,2-trifluoro-	74810-71-2	11.425	0.15	$C_8H_{12}BrF_3$	244
31	Curan-17-oic acid, 19,20-dihydroxy-, methyl ester	2111-90-2	11.530	0.25	$C_{20}H_{26}N_2O_4$	358
32	1,2,3-Benzenetriol	87-66-1	11.701	22.53	$C_6H_6O_3$	126
33	Caryophyllene	87-44-5	12.363	0.52	$C_{15}H_{24}$	204
34	Aromandendrene	489-39-4	12.621	0.11	$C_{15}H_{24}$	204
35	1,4,7,-Cycloundecatriene, 1,5,9,9-tetramethyl-, Z,Z,Z-	0-00-0	12.825	0.34	$C_{15}H_{24}$	204
36	Guaia-1(10),11-diene	0-00-0	13.028	0.23	$C_{15}H_{24}$	204
37	Bicyclo[5.3.0]decane, 2-methylene-5-(1-methylvinyl)-8-methyl-	0-00-0	13.257	0.37	$C_{15}H_{24}$	204
38	2-Isopropenyl-4a,8-dimethyl-1,2,3,4,4a,5,6,7-octahydronaphthalene	0-00-0	13.338	1.06	$C_{15}H_{24}$	204
39	Germacrene D	23986-74-5	13.535	0.36	$C_{15}H_{24}$	204

40	Germacrene D	23986-74-5	13.810	0.12	$C_{15}H_{24}$	204
41	1,6,10-Dodecatrien-3-ol, 3,7,11-trimethyl-, (E)-	40716-66-3	14.009	0.52	$C_{15}H_{26}O$	222
42	(-)-Spathulenol	77171-55-2	14.340	0.10	$C_{15}H_{24}O$	220
43	Caryophyllene oxide	1139-30-6	14.420	0.47	$C_{15}H_{24}O$	220
44	Isoledene	0-00-0	14.565	0.29	$C_{15}H_{24}$	204
45	1α,2β,3α,5β-Cyclohexanetetrol	53585-08-3	14.887	3.92	$C_6H_{12}O_4$	148
46	Tetracyclo[6.3.2.0(2,5).0(1,8)]tridecan-9-ol, 4,4-dimethyl-	0-00-0	15.050	0.68	$C_{15}H_{24}O$	220
47	Isoaromadendrene epoxide	0-00-0	15.250	0.51	$C_{15}H_{24}O$	220
48	Ledene oxide-(II)	0-00-0	15.412	0.16	$C_{15}H_{24}O$	220
49	Isosteviol methyl ester	0-00-0	15.546	0.02	$C_{21}H_{32}O_3$	332
50	Hexanoic acid, 3,5-difluorophenyl ester	0-00-0	15.628	0.04	$C_{12}H_{14}F_2O_2$	228
51	1-Heptatriacotanol	105794-58-9	16.013	0.16	$C_{37}H_{76}O$	536
52	Tetradecanoic acid	544-3-8	16.243	0.14	$C_{14}H_{28}O_2$	228
53	3,7-Dimethyl-8-(phenylthio)octa-2,6-dien-1-ol	0-00-0	16.517	0.04	$C_{16}H_{22}OS$	262
54	2,6,8-Trimethylbicyclo[4.2.0]oct-2-ene-1,8-d	0-00-0	16.653	0.06	$C_{11}H_{18}O_2$	182
55	Globulol	51371-47-2	17.036	0.54	$C_{15}H_{26}O$	222
56	Phthalic acid, 1-tert-butoxyprop-2-yl isobutyl ester	0-00-0	17.339	0.10	$C_{19}H_{28}O_5$	336
57	n-Heptadecanol-1	1454-85-9	17.529	0.85	$C_{17}H_{36}O$	256
58	4,4,8-Trimethyltricyclo[6.3.1.0(1,5)]dodecane-2,9-diol	0-00-0	17.774	0.38	$C_{15}H_{26}O_2$	238
59	Hexadecanoic acid, methyl ester	112-39-0	17.960	0.10	$C_{17}H_{34}O_2$	270
60	Pentadecanoic acid	7132-64-1	18.318	0.56	$C_{16}H_{32}O_2$	256
61	4-(2,4-Dimethylcyclohexyl)butan-2-one	29230-18-0	19.040	0.09	$C_{12}H_{22}O$	182

62	9-Octadecen-1-ol, (Z)-	143-28-2	19.292	1.93	$C_{18}H_{36}O$	268
63	n-Nonadecanol-1	1454-84-8	19.520	0.92	$C_{19}H_{40}O$	284
64	Phytol	150-86-7	19.749	0.51	$C_{20}H_{40}O$	296
65	12-Hydroxy-14-methyl-oxa-cyclotetradec-6-en-2-one	77761-61-6	20.010	0.18	$C_{14}H_{24}O_3$	240
66	Octadecanoic acid	57-11-4	20.217	0.09	$C_{18}H_{36}O_2$	284
67	Tributyl acetylcitrate	77-90-7	20.944	0.20	$C_{20}H_{34}O_8$	402
68	9,12,15-Octadecatrienoic acid, 2-(acetyloxy)-1-[(acetyloxy)methyl]ethyl ester, (Z,Z,Z)-	55320-01-9	21.142	0.62	$C_{25}H_{40}O_6$	436
69	Oxiraneoctanoic acid, 3-octyl-, methyl ester,	2566-91-8	21.377	0.18	$C_{19}H_{36}O_3$	312
70	Z-5-Methyl-6-heneicosen-11-one	0-00-0	21.618	0.15	$C_{22}H_{42}O$	322
71	5-Heptyl-4-methyldihydro-2(3H)-furanone, trans	148806-10-4	21.865	0.03	$C_{12}H_{22}O_2$	198
72	13-Docosenamide, (Z)-	112-84-5	21.976	0.15	$C_{22}H_{43}NO$	337
73	Ethyl iso-allocholate	0-00-0	22.050	0.11	$C_{26}H_{44}O_5$	436
74	2-Oxabicyclo[2.2.2]octan-6-ol, 1,3,3-trimethyl-	18679-48-6	22.323	0.23	$C_{10}H_{18}O_2$	170
75	2-Propen-1-one, 1-(2,6-dihydroxy-4-methoxyphenyl)-3-phenyl-, (E)-	18956-15-5	22.452	0.24	$C_{16}H_{14}O_4$	270
76	Ethyl stearate, 9,12-diepoxy	0-00-0	22.572	0.16	$C_{20}H_{36}O_4$	340
77	Ethyl iso-allocholate	0-00-0	22.814	0.07	$C_{26}H_{44}O_5$	436
78	Methyl 9-heptadecenoate or 9-17:1	0-00-0	22.900	0.13	$C_{18}H_{34}O_2$	282
79	13-Tetradecen-1-ol acetate	56221-91-1	23.011	0.22	C16H30O2	254
80	4H-1-Benzopyran-4-one, 2,3-dihydro-5,7-dimethoxy-2-phenyl-	1036-72-2	23.241	0.76	$C_{17}H_{16}O_4$	284
81	Bis(tridecyl) phthalate	119-06-2	23.320	0.52	$C_{34}H_{58}O_4$	530

82	2-Propen-1-one, 1-(2,6-dihydroxy-4-methoxyphenyl)-3-phenyl-, (E)-	18956-15-5	23.528	0.430.43	$C_{16}H_{14}O_4$	270
83	2-Propen-1-one, 1-(2,6-dihydroxy-4-methoxyphenyl)-3-phenyl-, (E)-	18956-15-5	23.611	0.48	$C_{16}H_{14}O_4$	270
84	(S)-5,7-dihydroxy-6,8-dimethylflavanone	56297-79-1	23.764	7.81	$C_{17}H_{16}O_4$	284
85	2,2,4-Trimethyl-6-(1-oxo-3-phenylprop-2-enyl)-cyclohexane-1,3,5-trione	0-00-0	23.978	1.25	$C_{18}H_{18}O_4$	298
86	5,7-Dimethoxyflavanone	1036-72-2	24.161	3.82	$C_{17}H_{16}O_4$	284
87	Methyl abietate isomer	24563-92-6	24.418	0.94	$C_{21}H_{32}O_2$	316
88	2-Methylhexacosane	1561-02-0	24.560	0.72	$C_{27}H_{56}$	380
89	Benzaldehyde (diphenylmethylene) hydrazine	13118-38-2	24.634	2.21	$C_{20}H_{16}N_2$	284
90	2,3-Dihydro-5-hydroxy-6,8,8-trimethyl-2-phenyl-4H-1-benzopyran-4,7(8H)-dione	0-00-0	24.810	0.22	$C_{18}H_{18}O_4$	298
91	1,4-Benzenedicarboxylic acid, bis(2-ethylhexyl) ester	6422-86-2	24.900	0.13	$C_{24}H_{38}O_4$	390
92	8-Methyl-6-nonenamide	0-00-0	25.180	0.12	$C_{10}H_{19}NO$	169
93	Squalene	111-02-4	25.400	13.57	$C_{30}H_{50}$	410
94	1-Pyrrolidinebutanoic acid, 2-[(1,1-dimethylethoxy)carbonyl]-α-nitro-, 2,6-bis(1,1-dimethylethyl)-4-methoxyphenyl ester, [S-(R*,R*)]-	124201-86-1	25.632	0.10	$C_{28}H_{44}N_2O_7$	520
95	Fumaric acid, nonyl propargyl ester	0-00-0	25.774	0.12	$C_{16}H_{24}O_4$	280
96	13-Tetradecen-1-ol acetate	56221-91-1	25.991	0.21	$C_{16}H_{32}O_2$	254
97	(E,E,E)-3,7,11,15-Tetramethylhexadeca-1,3,6,10,14-pentaene	77898-97-6	26.122	0.14	$C_{20}H_{32}$	272
98	Decyl oleate	3687-46-5	26.292	0.33	$C_{28}H_{54}O_2$	422
99	Cyclohexanepropanol, α,2,2,6-tetramethyl-	4361-23-3	26.488	0.30	$C_{13}H_{26}O$	198

100	Oxirane, 2,2-dimethyl-3-(3,7,12,16,20-pentamethyl-3,7,11,15,19-heneicosapentaenyl)-, (all-E)-	7200-26-2	26.633	0.33	$C_{30}H_{50}O$	426
101	1,6,10,14,18,22-Tetracosahexaen-3-ol, 2,6,10,15,19,23-hexamethyl-, (all-E)-	54159-46-5	26.710	0.16	$C_{30}H_{50}O$	426
102	β-Tocopherol	148-03-8	26.928	0.19	$C_{28}H_{48}O_2$	416
103	γ-Tocopherol	7616-22-0	27.043	0.12	$C_{28}H_{48}O_2$	416
104	Cholesta-4,6-dien-3-ol, (3β)-	14214-69-8	27.297	0.77	$C_{27}H_{44}O$	384
105	3,4-Dimethoxybenzaldehyde oxime	2169-98-4	27.437	0.24	$C_9H_{11}NO_3$	181
106	Vitamin E	59-02-9	27.582	3.67	$C_{29}H_{50}O_2$	430
107	Ergost-5-en-3-ol, (3β)-	4651-51-8	28.497	0.11	$C_{28}H_{48}O$	400
108	28-Hydroxylup-20(29)-ene-3,21-dione	13952-73-3	28.704	0.04	$C_{30}H_{46}O_3$	454
109	Nonadecyl heptafluorobutyrate	0-00-0	28.909	0.09	$C_{23}H_{39}F_7O_2$	480
110	β-Sitosterol	83-46-5	29.258	2.17	$C_{29}H_{50}O$	414
111	Hexadecanoic acid, tetradecyl ester	4536-26-9	29.400	0.15	$C_{30}H_{60}O_2$	452
112	3- β -d-Ribofuranosylpyrazolo[4,3-d]pyrimidin-5,7-4H,6H-dione	52492-53-2	29.470	0.12	$C_{10}H_{12}N_4O_6$	284
113	9,19-Cyclo-27-norlanostan-25-one, 3-(acetyloxy)-24-methyl-, (3 β,24R)-	83110-15-0	29.639	0.09	$C_{32}H_{52}O_3$	484
114	β-Amyrone	638-97-1	29.755	0.47	$C_{30}H_{48}O$	424
115	Acetic acid, 3-hydroxy-7-isopropenyl-1,4a-dimethyl-2,3,4,4a,5,6,7,8-octahydronaphthalen-2-yl ester	0-00-0	29.935	0.12	$C_{17}H_{26}O_3$	278
116	9,19-Cycloergost-24(28)-en-3-ol, 4,14-dimethyl-, acetate, (3β,4α,5α)-	10376-42-8	30.073	0.21	$C_{32}H_{52}O_2$	468
117	α-Amyrin	638-95-9	30.265	2.21	$C_{30}H_{50}O$	426
118	E-9-Octadecen-1-ol acetate	2195-92-8	31.405	0.18	$C_{20}H_{38}O_2$	310
119	1,4-Methanoazulene, 7-bromodecahydro-4,8,8-trimethyl-9-methylene-	24503-54-6	33.271	0.21	$C_{15}H_{24}$	204